

Geophysical anomalous zones were detected in addition to the above mineral showings.

Significant low resistivity anomalies were identified at 400 m north of Er-sizlerdere and 1 km south of Ipsinler by CSAMT random point measurements. Array CSAMT measurements were carried out in addition to the original plan, and notable low anomalies were analyzed at both localities. Both anomalies were detected in the talus deposits with tall limestone cliffs in the back.

FE values by IP electrical prospecting lie within the background of 0.5 - 1.0 %. Both anomalies are considered to be caused by groundwater.

The anomalies at, the western end of Lines A and B, east-southeast of Yunusköy, and east of Mt. Koramanyayla, appear to have wide distribution. The first two occur in sediments and the latter in serpentinite. There are no mineral showings in the area and these are not considered to be promising.

3-4-3 Resistivity structure and Geological structure

High measured resistivity is interpreted to be caused by serpentinite and basalt from comparison of both resistivity and geological distribution, and the result of laboratory tests. Also it is considered that the distribution of high resistivity are generally coincident with the occurrence of basalt. The high resistivity extends in the NW-SE to NNW-SSE direction and the discontinuity line of the resistivity also extend in the same direction. This direction is harmonious with the trend of the geologic structure of the zone.

It is difficult to identify rocks by resistivity values, but it would most probably be possible to distinguish igneous rocks and sedimentary rocks.

3-4-4 CSAMT survey

The two low resistivity zones located at the middle-deeper parts under the southeastern part of Aşıköy and the eastern part of Bakibaba Deposit, disappeared after interpretation by two-dimensional analysis. The reason for the disappearance is the difference of methods between one-dimensional and two-dimensional analysis.

The one-dimensional structure is prepared by analyzing each station by the minimum error between the theoretical values of the horizontal multi-layer structure model and the observed values. The other hand, the two-dimensional structure is prepared by analyzing the whole area (or several stations) calculated by the minimum error between theoretical and observed values. The areal extent for calculation and size of cells are carefully considered so that small size anomalies of one or two stations would not be neglected.

The application of one-dimensional analysis is difficult or impossible in

areas with steep dip, and thus the results of two-dimensional analysis is much more reliable than the one-dimensional method.

The above two low anomaly zones are important because these zones are continuous and related to ore deposits or mineral showings. More detailed two-dimensional reanalysis should be considered for the future exploration.

The emphasis of the present survey was in the area adjoining the operating Kure Mine and urban areas. Therefore, noises from ore dressing mill, power transmission cables, ropeways, and other mine facilities were large impediment for geophysical measurements. The result was insufficient measurement points and lines in some of the high potential zones such as Kızılsu Deposit, and Ersizler Stream Prospect. Also the eastern side of the Route 39 where CSAMT array line was established, the noise from three power transmission cables was strong and antenna for measuring the magnetic field could not be set at the center of the array as in normal practice. Also in some cases the strong filtering was necessary in order to eliminate the disturbances in the resistivity curve. Thus the accuracy of the analysis of the above zones are not as high as for other parts of the area.

Many low resistivity anomalies were detected at 50-100m depth southeast of the Aşıköy Orebody. Considering the fact that the orebody (40-80m wide) confirmed by drilling near the Toykondü Orebody could not be detected from the surface, it is necessary to expand the frequency into high regions for acquiring information of shallow subsurface zones. The present technology enables the use of frequencies up to 8,000Hz and thus it would be possible to explore zones up to 20-30m depth.

3-4-5 IP survey

The reason for the inability to detect the shallow, 50m, anomalies of Line DD is considered to be the long electrode interval of $a = 100m$, IP with 25-50m electrode interval would be more appropriate for such shallow depth.

CHAPTER 4 Drilling Survey (Second Phase)

4-1 Outline of Drilling

Geological and geophysical surveys were conducted in the first phase. The extensional localities of the Aşıköy and Bakıbaba ore deposits and the Zemberekler mineralized zone were extracted as targets for future exploration. Drilling survey of four holes totalling 1003.55 m were done this phase to clarify the conditions of subsurface copper mineralization in the south of the Aşıköy ore deposit and in the north of the Zemberekler mineralized zone.

Details of each hole are summarized in Table 2-3.

The drilling locations and geologic cross sections along the drill holes are shown in Figures 2-11 and 2-12 respectively.

Table 2-3 Coordinates of Drill Holes and Hole Length

Hole No.	Locality	Coordinates		Elevation	Inclination	Drilled Length
MJTK-1	South of Aşıköy	30,536N	57,633E	1,095m	-90°	401.00m
MJTK-4	East of Bakıbaba	31,082N	58,912E	1,060m	-90°	200.30m
MJTK-6	East of Aşıköy	30,658N	57,944E	1,181m	-90°	150.80m
MJTK-7	Southeast of Aşıköy	30,088N	58,028E	1,128m	-90°	251.45m

4-2 Drilling Method and Equipment

(1) Method

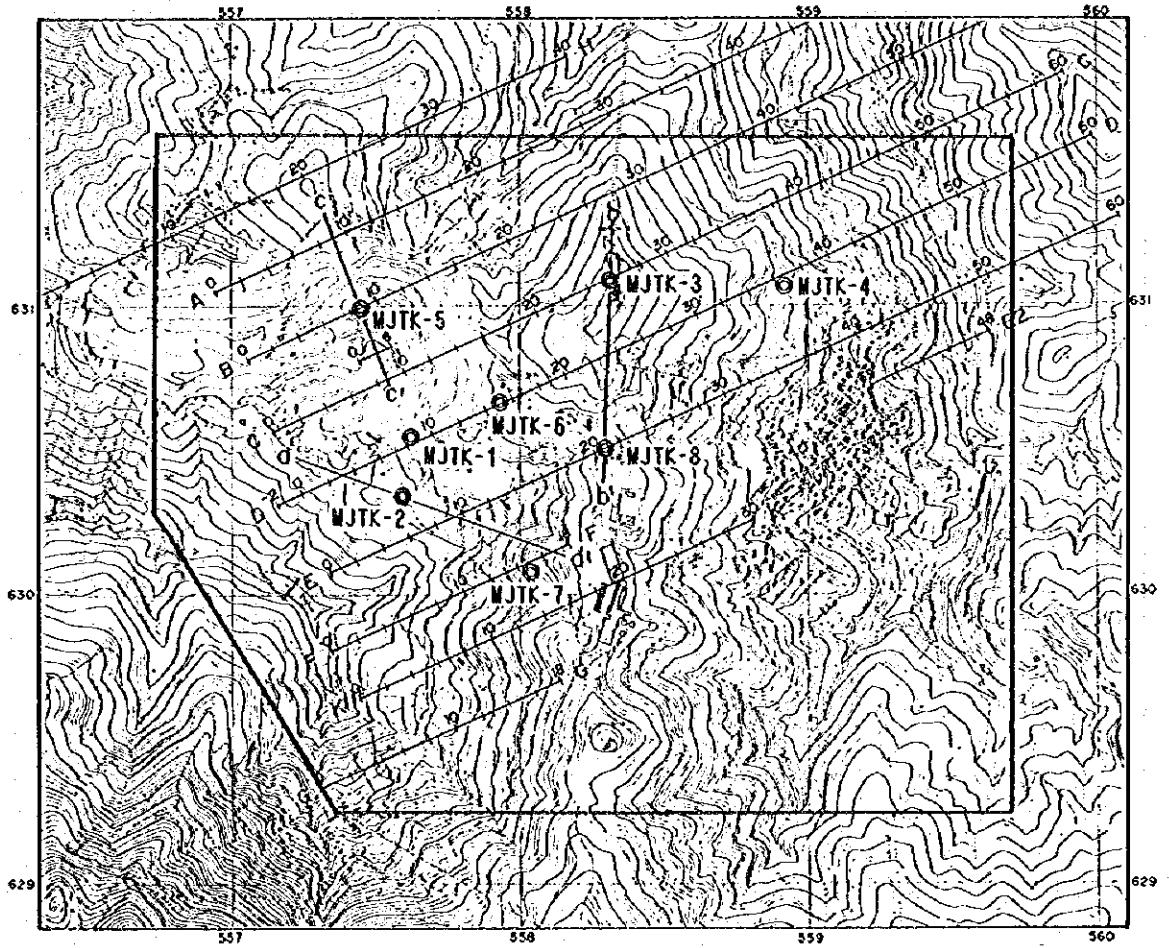
For surface parts, drilling was done by conventional drilling method using HW casing shoe (114 mm in diameter) or NW casing shoe (89 mm in diameter) with inserting HW or NW casing pipes.

For the bedrock zone, wireline method was adopted with NQ and BQ standardized diamond bits (76 mm and 56 mm in diameter respectively) and its core tubes.

Bentonite mud was usually mixed in the circulating drill water. The drilling water was lost in the hole many times because of fractures being developed. For preventing water loss, TELSTOP (squeezed refuse of cottonseed) and oil bentonite (mixture of light oil and bentonite) were injected. The density of mud water was kept in high to prevent the big collapse of wall.

(2) Equipment

The drilling machines were L-44 of Longyear and D-750 of Atlas Copco. Specifications of drilling machine and equipment are shown in Table 2-4.



LEGEND

- A—— CSAMT Surver Line
- b——b' Geological Section
- ⊙ Drill Hole

Fig. 2-11 Location Map of Drill Holes

Table 2-4 Specifications of Drilling Machine and Equipment (Second Phase)

Drilling Machine Model "L-44" Specifications: Capacity Dimension L x W x H Hoisting capacity Spindle speed Engine model "Deutz F5L-912"	1 set 975m(BW), 1,035m(BQ) 2,743mm x 1,448mm x 2,057mm 7,659kg Forward 210, 436, 800, 1,350rpm 81hp / 2,200rpm
Drilling Machine Model "D-750" Specifications: Capacity Dimension L x W x H Hoisting capacity Spindle speed Engine model "Deutz F3L-912"	1 set 425m(BQ) 2,355mm x 900mm x 1,750mm 3,000kg Forward 245, 430, 740, 1,335rpm 36.5hp / 1,800rpm
Drilling Pump Model "DG-130" Specifications: Piston diameter Stroke Capacity Dimension L x W x H Engine	4 set 68.5mm 75mm discharge capacity 130 liter/min 1,600mm x 650mm x 640mm 16hp / 2,000rpm
Generator Specifications: Capacity	1 set 2.7kw 50hz 220v
Derrick for L-44 Specifications: Height Max load capacity	17m 20,000kg
Derrick for D-750 Specifications: Height Max load capacity	7.5m 6,000kg
Drilling tools Drilling rod NQ-WL 3.0m BQ-WL 3.0m Casing pipe HW 1.0m HW 3.0m NW 3.0m BW 3.0m	150 pcs 250 pcs 5 pcs 10 pcs 30 pcs 90 pcs

(3) Working System

Drilling operation was carried out by three shifts per day (8 hours per shift), while the appurtenant works, such as road construction, rig construction, mobilization and demobilization, were done by one shift per day. A shift crew consists of one drilling engineer and three workers normally. Additional six workers were involved in case of the appurtenant work. A base camp for drilling operation was set in Küre mine. The commute between the base camp and drilling site was by car.

(4) Road Construction

A road of 250 m in length for transportation to MJTK-4 was constructed using a bulldozer. A road of 100 m to MJTK-7 was also built.

(5) Transportation

Most of machines and equipments which were used in the second phase, were provided by ETIBANK at Küre mine. All diamond bits were transported from Japan by airplane. A part of mud materials was shipped from Yokohama to Istanbul. After landed, they were transported to Küre mine by trucks.

(6) Drilling Water

Water for drilling was taken directly from water supply pipes in Küre mine or transported by a tank lorry.

(7) Withdrawal

After the completion of drilling programme, the machine, equipment and drilling cores were stored in a drilling warehouse in the Küre Mine.

4-3 Geology and Mineralization of Drill Holes

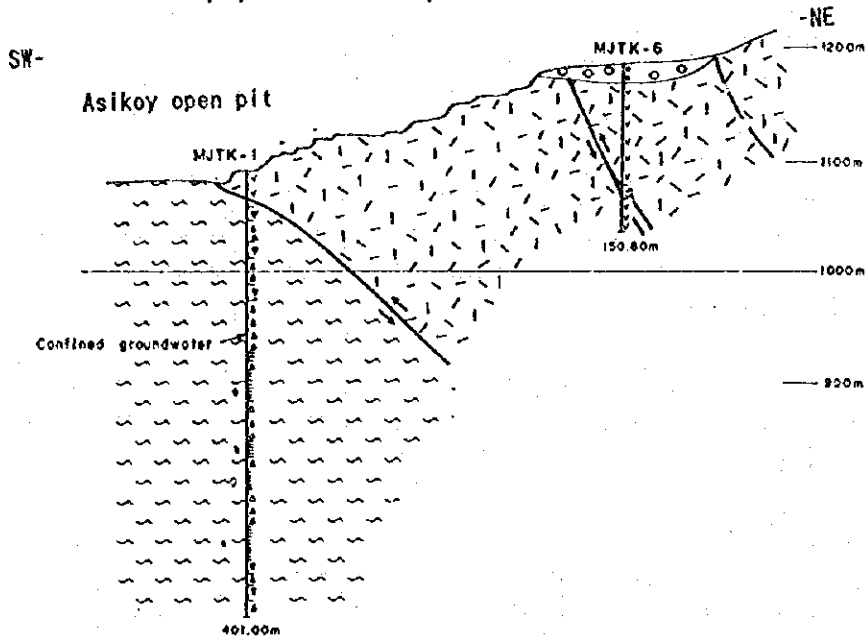
The results of thin section microscopy, polished section microscopy, X-ray diffraction, and ore assay of the cores are shown in Appendix Tables 5-1 - 5-4.

4-3-1 Geology

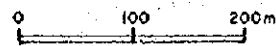
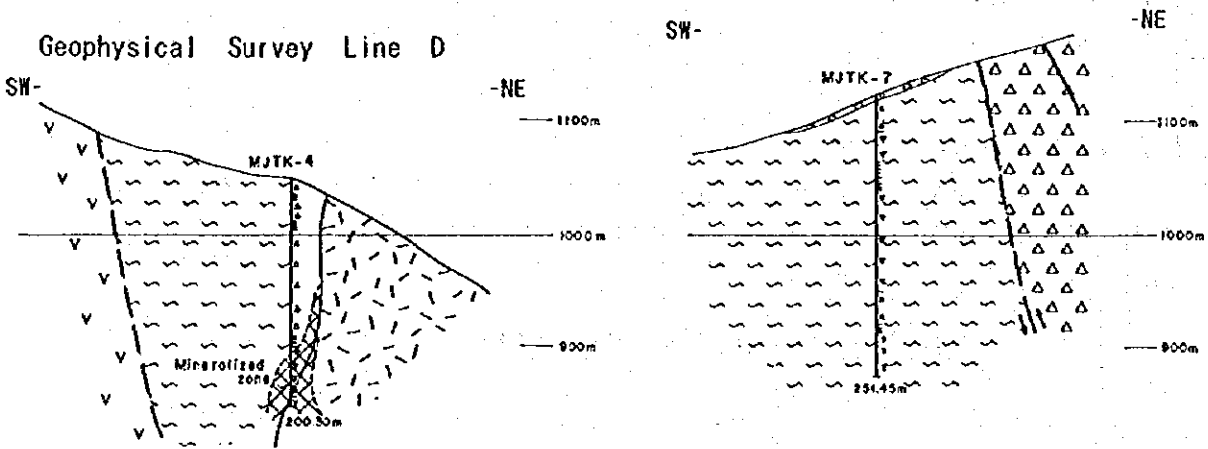
The geology of the area where drilling exploration was carried out this phase is composed of basalt and sedimentary rocks of the Küre Formation.

Basalt consists of pillow lava. Massive basalt and hyaloclastite are observed in drill holes. They are judged as constitutes of massive basalt because the former is interpreted as pillow lobe with tensional cracks, the latter is hyaloclastite between pillow lobes and they are correlated with surface outcrops of massive basalt. Basalt mostly has ophitic texture. Some

Geophysical Survey Line D



Geophysical Survey Line F



- | | | | |
|--|------------------|--|-----------------------------|
| | Talus Deposits | | Black Shale |
| | Breccia | | Graywacke Breccia |
| | Hyaloclastite | | Black Shale - Chert Breccia |
| | Pillow Lava | | Basalt |
| | Massive Basalt | | Fault |
| | Mineralized Zone | | |

Fig. 2-12 Geologic Cross Section along the Drill Holes (Second Phase)

parts of basalt show porphyritic or microspherulitic texture. Altered minerals are quartz, sericite, chlorite, calcite and pyrite.

Sedimentary rocks consist of breccia. Fragments of graywacke, siltstone, black shale, cherty shale and chert are observed. Pyrite fragments are rarely observed.

Breccia of graywacke is composed of massive and graded ones. The former is dominant between them. Fragments of graywacke are composed of quartz, feldspar, mafic minerals, opaque minerals, shale, chert and basic igneous rocks. Maximum size of fragments is 0.3 to 0.7 mm in diameter. Most of quartz grains show wavy extinction. Cracks of graywacke and chert are filled by muddy materials.

Siltstone is graded.

Fragments of cherty shale and chert are lens-shaped and have folded pinch and well structures.

The shape of breccia excluding cherty shale and chert is angular to subangular. The size of breccia ranges from several centimeters up to several meters.

Matrix of breccia is composed of pelitic rocks. Black shale surrounding breccia is sheared and argillized. It has a scaly cleavage. It is easily dissolved in water because it is clayey.

Under the microscope, schistose structure, micro-fault and micro-folding were observed in black shale which looked massive by naked eye. Black shale is composed of quartz, illite, chlorite and bituminous material.

4-3-2 Mineralization

Ore minerals observed in drill cores are pyrite, marcasite, chalcopyrite, chalcocite, sphalerite, bornite and hematite. Gangue minerals are quartz, calcite and chlorite.

The occurrence of ore minerals is breccia, lens and film of sulphides in sedimentary rocks, and veinlets and dissemination of sulphides in basalt.

Ore minerals in sedimentary rocks are pyrite and marcasite. Quartz is rarely observed as gangue mineral.

Veinlets in basalt are composed of a large amount of calcite and a minor amount of copper minerals. Disseminated sulphide mostly consists of pyrite.

CHAPTER 5 DRILLING SURVEY (THIRD PHASE)

5-1 Outline of Drilling

Geological and geophysical surveys of the first phase and the drilling of the second phase enabled the extraction of northern and southern extensions of both Aşıköy and Bakibaba Deposits as the promising targets for further exploration in the Küre area.

The objective of the third phase was set at clarifying the mineral occurrence and the grade of the extensions of the above two deposits by drilling and thereby increasing the copper reserves of the Küre mine. Four holes totaling 953.70 m in length were drilled. The location and the lengths of each hole are shown in Table 2-5. The location of the sites and geologic cross section of each hole are shown in Figures 2-11 and 2-13. Two machines were used for drilling MJTK-2, 3, 5 and 8.

Table 2-5 Coordinates of Drill Holes and Hole Length

Hole No.	Locality	Coordinates		Elevation	Azimuth	Inclination	Drilled Length
MJTK-2	South of Aşıköy	30,342N	57,598E	1,065m	110°	-36°	250.70m
MJTK-3	North of Bakibaba	31,070N	58,330E	1,287m	-	-90°	301.00m
MJTK-5	North of Aşıköy	30,996N	57,435E	1,067m	-	-90°	201.00m
MJTK-8	South of Bakibaba	30,512N	58,315E	1,191m	-	-90°	201.00m

5-2 Drilling Method, Equipment and Progress

(1) Method

For surface and shallow parts, drilling was done by HQ wireline (98 mm in diameter), then reamed by HW casing shoe (114 mm in diameter) and inserting HW casing pipes were inserted.

For the bedrock zone, wireline method was adopted with HQ, NQ and BQ oversized diamond bits (79 mm and 62 mm in diameter respectively) and its core tubes.

Bentonite mud was usually mixed in the circulating drill water. The drilling water was often lost because of the fractures developed. For preventing circulation loss, TELSTOP (squeezed refuse of cottonseed) were injected. Cementing was done when TELSTOP was not sufficient. The density of mud water was kept high to prevent the collapse of wall.

Table 2-6 Specifications of Drilling Machine and Equipment (Third Phase)

Drilling Machine Model "L-44" Specifications: Capacity Dimension L x W x H Hoisting capacity Spindle speed Engine model "Deutz F5L-912"	1 set 975m(BW), 1,035m(BQ) 2,743mm x 1,448mm x 2,057mm 7,659kg Forward 210, 436, 800, 1,350rpm 81hp / 2,200rpm
Drilling Machine Model "L-38" Specifications: Capacity Dimension L x W x H Hoisting capacity Spindle speed Engine model "Deutz 4FL"	1 set 700m(BW), 775m(BQ) 2,440mm x 1,070mm x 1,450mm kg Forward 236, 490, 900, 1,510rpm 60hp / 2,200rpm
Drilling Pump Model "WL-MG-15h" Specifications: Piston diameter Stroke Capacity Dimension L x W x H Engine "Yanmar NFD150"	1 set 68mm 75mm discharge capacity 130 liter/min 2,240mm x 840mm x 1,140mm 15hp / 2,400rpm
Drilling Pump Model "NP-200" Specifications: Piston diameter Stroke Capacity Dimension L x W x H Engine "Isuzu SKR1"	1 set 73mm 75mm discharge capacity 110 liter/min 2,400mm x 560mm x 1,245mm 36hp / 3,600rpm
Generator Specifications: Capacity	2 set 2.7kw 50hz 220v
Derrick for L-44 Specifications: Height Max load capacity	17m 20,000kg
Derrick for L-38 Specifications: Height Max load capacity	6.1m 17,000kg
Drilling tools Drilling rod HQ-WL 3.05m NQ-WL 3.05m BQ-WL 3.05m Casing pipe HW 1.0m NK-NU 1.5m NK-NU 3.0m BX-NU 1.5m BX-NU 3.0m	40 pcs 120 pcs 200 pcs 18 pcs 10 pcs 40 pcs 60 pcs 92 pcs

(2) Equipment

The drilling machines were L-44 and L-38 of Longyear. Specifications of drilling machine and equipment are shown in Table 2-6.

(3) Working System

Drilling operation was carried out by three shifts per day (8 hours per shift), while the appurtenant works, such as road construction, rig construction, mobilization and demobilization, were done by one shift per day. A shift crew consists of one drilling engineer and three workers normally. Additional one worker was involved in case of pumping water. A base camp for drilling operation was set in Küre mine. The commuting between the base camp and the drilling site was by car.

(4) Transportation

L-44 and a part of the equipment were provided by ETIBANK at Küre mine. L-38 and a part of the equipment were rented from MTA. Other equipment, all diamond bits and a part of the drilling mud were shipped by surface freight. After landing at Istanbul they were transported to Küre mine by trucks.

(5) Drilling Water

Water for drilling was taken directly from a spring in the open pit of the Küre mine and transported by a tank lorry to the drilling site or to a tank nearby and then pumped to the site. Also when possible it was hosed to the site from the mine water supply.

(6) Withdrawal

After the completion of drilling programme, the machine and equipment of ETIBANK, and drilling cores were stored in a drilling warehouse in the Küre mine. The drilling machine and equipment of MTA were returned to MTA Ankara. The equipment sent from Japan were shipped by surface freight.

5-3 Geology and Mineralization of Drill Holes

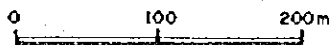
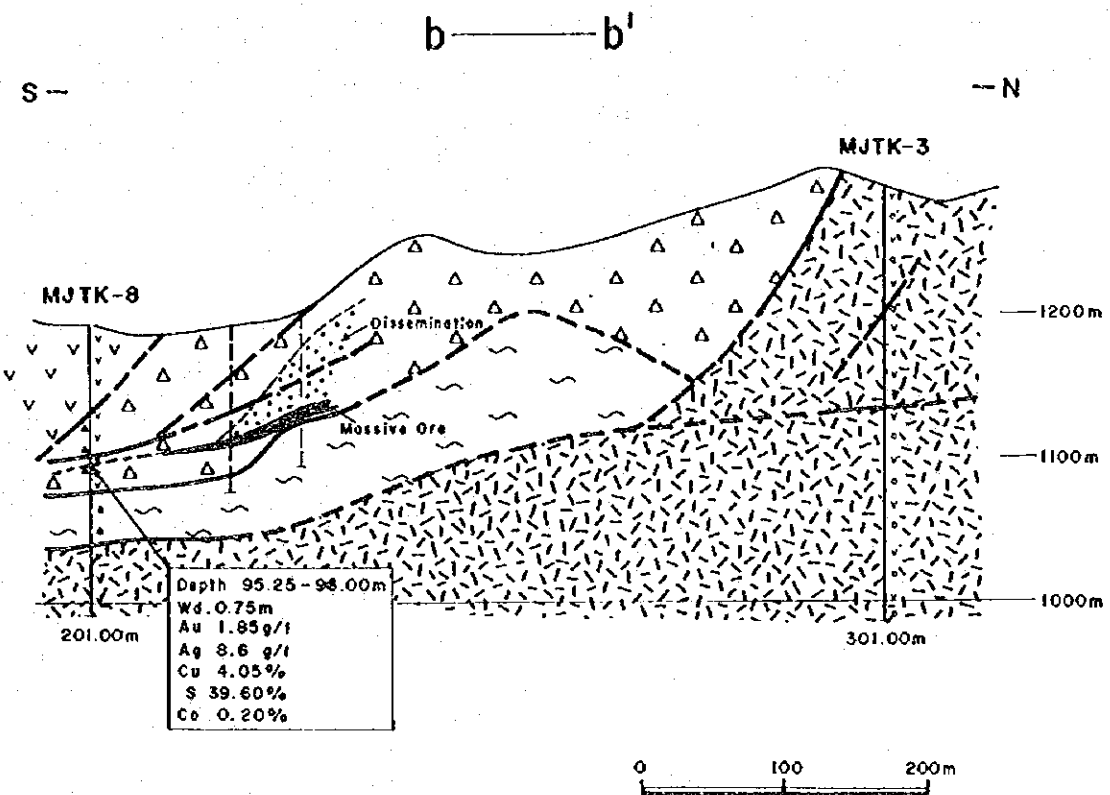
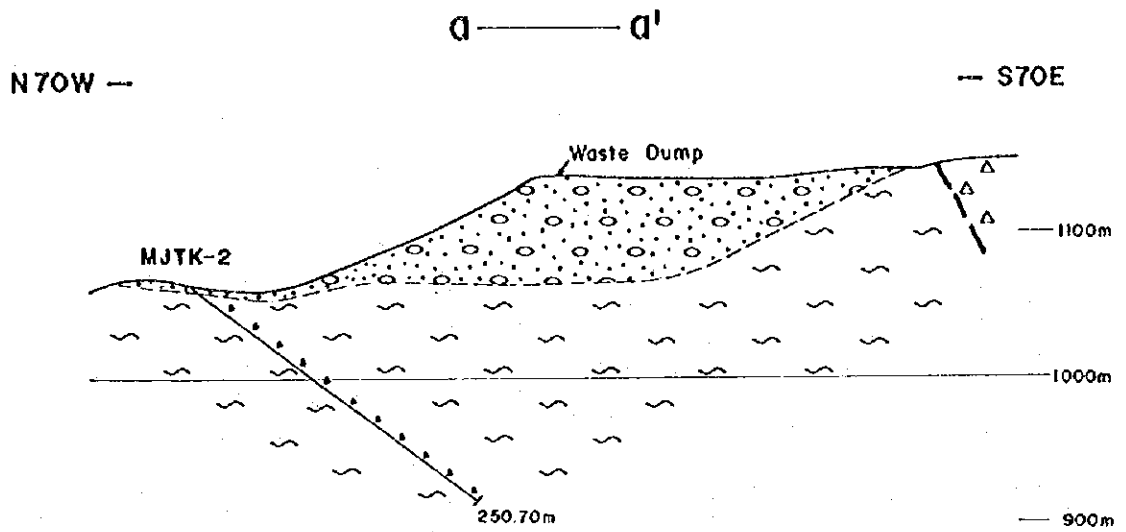
The results of thin section microscopy, polished section microscopy, X-ray diffraction, and ore assay of the cores are shown in Appendix Tables 5-1 - 5-4.

5-3-1 Geology

The rocks drilled during the present third phase are basalt and sedimentary rocks of the Küre Formation.

Basalt consists of pillow lava, massive basalt and hyaloclastite.

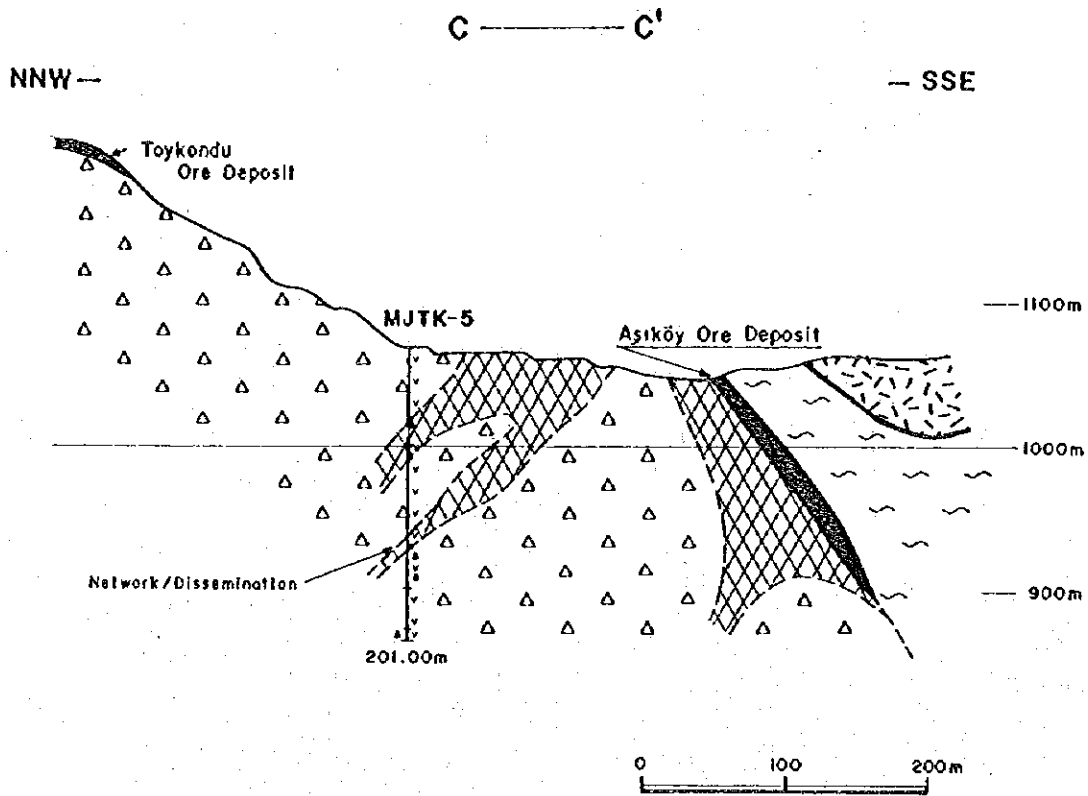
The pillow basalt consists of both close-packed and pillow breccia.



LEGEND

- | | |
|---|---|
| <ul style="list-style-type: none"> Breccia Hyaloclastite Pillow Lava Massive Basalt | <ul style="list-style-type: none"> Fault Drill Hole |
|---|---|

Fig. 2-13 Geologic Cross Section along the Drill Holes (Third Phase, 1/2)



LEGEND

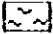

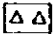

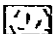
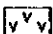
- | | |
|--|--|
|  Breccia |  Fault |
|  Hyaloclastite |  Drill Hole |
|  Pillow Lava | |
|  Massive Basalt | |

Fig. 2-13 Geologic Cross Section along the Drill Holes (Third Phase, 2/2)

5-3-2 Mineralization

Ore minerals observed in drill cores are pyrite, marcasite, chalcopyrite, chalcocite, sphalerite, bornite and hematite. Gangue minerals are quartz, calcite and chlorite.

The mineralization observed in the cores are massive, veinlets to network and dissemination.

In MJTK-8, massive ores are confirmed at 59.25-60.0 m, it appears to the unaided eyes that pyrite and chalcopyrite grains fill the interstices of pyrite fragments (about 1 cm in diameter). It is in fault contact with the upper massive basalt. The alteration of the overlying basalt is weak. The orebody is in contact with the lower hyaloclastite at a high angle. The footwall hyaloclastite is argillized and consists of quartz, chlorite and siderite. The massive ore at this hole is; 75 cm in core width, Au 1.85 g/t, Ag 8.6 g/t, Cu 4.05 %, S 39.6 %.

These microscopic characteristics are similar to those of the Aşıköy and Bakibaba ores.

In MJTK-3 basalt, pyrite-quartz veins, veinlets and pyrite dissemination are observed.

In MJTK-5, pyrite veins, veinlets, network and pyrite dissemination are observed. The ore minerals are pyrite, hematite, chalcopyrite and sphalerite. The gangue minerals are chlorite, quartz and epidote.

CHAPTER 6 ELECTRIC LOGGING AND MEASUREMENT OF PHYSICAL PROPERTIES ON CORES

6-1 Outline

The low CSAMT resistivity anomalies were drilled and electric logging was carried out for the drill holes in order to clarify the physical characteristics of the country rocks and the mineralized zones in the second phase. The measurement of physical properties on cores was done in the third phase.

The quantity of the electric logging is follows

MJTK-4 : 200m

MJTK-6 : 120m

Total length of logging : 320m

The quantity of the measurement of physical properties is thirty core samples.

6-2 Equipment

The GEOLOGGER 3400 manufactured by OYO in Japan was used for this electric logging. The specification is as follows.

Number of channel : two channels

Range of measuring : 50/100/200/500/1K/2k/5k
/10k/20k/50k CPS/ohm-m/F.S.

Clearance of electrode : a=50cm, 100cm

Winding speed : 0 - 20 m/min.

Length of cable : 1000 m

Analog recorder : two pens , 250m/m width,
scale 1/50, 1/100, 1/200, 1/500

Power requirement : AC 100 volts, 50/60 Hz, 30 VA

6-3 Results of Logging

MJTK-4

The following was clarified by this logging.

0 - 174.5m: Mainly black shale, resistivity 70-100ohm-m with small variation. Several resistivity peaks inferred to be caused by graywacke pebbles.

174.5 - bottom: High resistivity due to basalt.

176.9 - 178.9m: Cu 2.6% ore, but resistivity decrease from 120 - 200ohm-m to 80ohm-m. This particularly evident with electrode interval of 50cm.

182.5 - 186.8m: Pyrite dissemination, resistivity decrease to 70ohm-m from 200ohm-m.

Bottom: Sudden increase of resistivity due to silicification of basalt.

It is seen from the above that since the ores at 176.9 - 178.9m. and the pyrite dissemination between 182.5- 186.8m are not sufficiently large to cause the CSAMT anomalies, it is reasonable to consider the source of these low resistivity to the existence of black shale to 175m depth.

MJTK-6

After completion of the hole at 150.3m depth, The strainers by polyvinyl chloride were immediately inserted and logging was carried out. There was a collapse at 120m depth, unfortunately insertion was not completed below 120m .

The following was clarified by this logging.

18.6 - 120.0m: Mainly basalt, resistivity 80-300ohm-m with comparatively wide variation. Several resistivity dips inferred to be caused by tensional cracks
105 - 120: High resistivity due to basalt.
117.2-123.7m: the resistivity are decreased by black shale .

It is seen from the above that it is reasonable to consider the source of these low resistivity to the existence of weathered basalt to 54m depth at this point.

6-4 Physical Properties of the Cores

Thirty core samples were collected for the measurement of physical properties such as resistivity and FE value by the same equipment used in the first phase. Samples were taken each 10 samples from three drill holes, namely MJTK-3, MJTK-5 and MJTK-8. The results are shown for each rock in Table 2-18 and Figure 2-11.

The average values of resistivity are 3,770 ohm-m of massive basalt, 3,705 ohm-m of pillow breccia and 1,730 ohm-m of hyaloclastite in descending order. The lowest average is 137 ohm-m of black shale. A gray shale sample and a silicified rock show 137 and 837 ohm-m respectively.

The rock with the highest FE value, excluding samples with pyrite veinlets and pyrite dissemination, is massive basalt at 6.9% followed by black shale at 5.6%, hyaloclastite, pillow lava and pillow breccia at 1.9%.

Mineralization or argillization normally leads to the decreasing of resistivity and the increasing of FE value. The decreasing of resistivity by pyrite dissemination were observed in this measurement. Low resistivities and high FE values were detected in samples of MJTK-5. It is believed that pyrite veinlets along the direction of electrodes in these samples caused above phenomena.

Limited samples allow that there is a significant difference in resistivity between basalt and sediments, namely black shale and gray shale. Regarding FE values, there is a tendency that dense pyrite veinlets and dissemination cause the increasing of FE value and the drop of resistivity.

The results of physical properties measurement is harmonious with that of the first phase collected from outcrops. It could be confirmed that massive sulfide indicated low resistivity at 7.5 ohm-m, and black shale and some sandstone indicated low resistivity below 250 ohm-m. It is clarified from the work in this phase that pyrite dissemination or argillization in basalt which has high resistivity above 1,000 ohm-m possibly makes low resistivity zone.

CHAPTER 7 DISCUSSIONS

7-1 Geology, Geologic Structure and Mineralization

The geology of the Küre zone consists of pre-Jurassic ultramafic rocks, Jurassic Küre Formation, Lower Cretaceous Karadana Formation, Upper Cretaceous Çaglayan Formation, diorite and dacite which are intruded into the Küre Formation. The known ore deposits occur in the the Küre Formation. The stratigraphic relationship of three formations, namely Küre Formation, Karadana Formation and Çaglayan Formation is unconformity. Ultramafic rocks are in fault contact with Küre Formation.

Küre Formation is composed of basalt, and brecciated formation comprising fragments of pelitic and flysh rocks, and being cemented by pelitic materials.

Basalt is divided into pillow lava, hyaloclastite and massive basalt. The chemical composition of the basalt is characterized by mid-ocean ridge basalt. Secondary minerals such as chlorite, epidote, prenite and actinolite are generally observed in basalt under the microscope.

Breccia is composed of fragments of greywacke and black shale. The fragments are angular to subrounded and their size ranges from several centimeters to several meters. The matrix is pelitic and is either fractured and argillized or has scaly cleavage. This pelitic rock dissolves easily and is argillized. The black shale fragments are generally schistose with minor faults and minor folds in some places. There are in some localities, small basalt bodies within the breccia.

The geologic structure of this area is characterized by many faults and there are many fractured zones and faults in the basalt bodies.

It is thus considered that the Küre Formation is a melange.

The known ore deposits in this zone tend to occur at the boundary between hyaloclastite and black shale of the Küre Formation also within hyaloclastite. Ore is divided into massive, brecciated, disseminated and network ones. Massive

and brecciated ores occur at the boundary between hyaloclastite and black shale. Disseminated and network ores occur within hyaloclastite.

The major part of massive ore is composed of sulphide minerals. The brecciated ore is composed of quartz, clay minerals and sulphide minerals.

The major ore minerals are pyrite and chalcopyrite with a minor amount of bornite, pyrrhotite, magnetite, sphalerite, galena, marcasite, electrum, bravoite and carrollite.

Massive and brecciated ores sometimes contain minute pyrite of colloform and gel-form together with coarse pyrite. In many cases, such pyrite shows cataclastic feature. Chalcopyrite fills the interstices between the pyrite grains.

Alteration zone below massive ores is composed of chlorite, epidote, carbonate minerals, and locally quartz and sericite. Wall rocks of network zone generally show green color. They are silicified, and contain numerous veinlet and dissemination.

Basalt is submarine effusive rock. It is considered that the basalt erupted on the deep ocean floor, because tuffs formed by steam explosion do not occur in this zone. There are massive ores comprising a large amount of pyrite, a small amount of chalcopyrite and sphalerite, and a minor amount of marcasite and pyrrhotite.

Considering to these evidences, the known ore deposits in this zone are interpreted to be a Cyprus-type.

On the basis of these considerations, the process of ore deposit formation and emplacement is inferred as follows.

Hydrothermal systems accompanied by basalt eruption were formed on the mid-ocean ridge. Massive ores were formed from minute pyrite of colloform and gel-form together with coarse pyrite, and chalcopyrite filled among the pyrite grains.

After the formation of ore deposits, ores were covered by deep ocean pelitic sediments. The ores with basalt and pelitic sediments were sheared and mixed with flysh sediments which deposited around the subduction zone by obduction. Thus a melange was formed.

The period of melange formation is interpreted to be Middle Jurassic, prior to the intrusion of dacite.

The Küre Formation which is interpreted as a melange, is characterized by the arrangement of basalt and sedimentary rocks which extend in the direction of N-S to NNW-SSE. This direction is harmonious with the major faults. It agrees with the distribution of pillow lava and hyaloclastite around the Asiköy and Bakibaba ore deposits. It also agrees with the surface elongation of intrusive rocks.

Tectonically dislocated ore deposits are distributed in the same direction

as the distributions of Aşıköy - Toykondü and Bakibaba - Kızılsu ore deposits.

Basalt shows an imbricate structure. The boundary between basalt and sedimentary rocks are proposed as interesting zones for future exploration. The N-S to NNW-SSE extension of the known ore deposits are considered to be promising zones for exploration.

7-2 Geophysical Prospecting and Mineralization

During the first phase, low resistivity anomalies were confirmed by CSAMT and IP survey. These anomalies are considered to be related to ore deposits of Aşıköy, Bakibaba and Kızılsu. Of particular interest is the many small anomalies detected southeast of Aşıköy orebody as these occur as several linearly oriented groups of anomalies and they apparently are continuous to the Kızılsu deposit to the southeast. Also small but continuous anomalies were detected to the north and south of Bakibaba Deposit. Weak anomalies were detected near the mineral showings to the northeast of Bakibaba and these are considered to continue to the Zemberekler mineralized zone.

Also the following three localities were selected to be being promising for future prospecting from study of the results of the above survey as well as those obtained by ETİBANK previously and the conditions of the mineral showings and the known deposits. These areas are; (1) south and north of Aşıköy Deposit, (2) north and south of Bakibaba Deposit, and (3) north-northwestern extension of the Zemberekler mineralized zone.

Eight holes were drilled with the above anomalies as targets. They are; (1) southeast of Aşıköy Deposit MJTK-1,2 and 7, (2) north of Bakibaba Deposit MJTK-3, (3) north of Aşıköy Deposit MJTK-5, (4) southwest of Bakibaba Deposit MJTK-8, (5) NNW extension of Zemberekler mineralized zone, and a locality between Aşıköy and Bakibaba Deposits MJTK-6.

It is now clear from the holes drilled in this study that the low resistivity anomalies identified by CSAMT survey are caused mainly by the existence of massive sulfides, vein network of sulfides, black shale, breccia and shear zone.

7-3 Potential of Resources

The Küre Formation which contains the known ore deposits, is considered as a melange. Basalt and breccia formation are distributed with imbricate structure. All directions of lateral extension of basalt, the distribution of known ore deposits and strike of major faults, are N-S to NNW-SSE.

Basalt shows submarine effusive facies. Tuffs which imply steam explosion do not occur in this zone. It is interpreted that the basalt erupted in deep ocean. Ore deposits are composed of massive, brecciated, network ores with a large amount of pyrite, a small amount of chalcopyrite and sphalerite, and a minor amount of marcasite and pyrrhotite. No hydrothermal alteration zone occurs in the footwall basalt below massive ores. From the above facts, the known ore deposits in this zone are interpreted to be a Cyprus-type.

The Küre Formation is melange and fractured by tectonic movement. However, in the three of the four known deposits namely Aşıköy, Toykondu and Bakibaba Deposits, larger massive orebodies are often accompanied by sulfide network and dissemination. As pelitic rocks of hanging wall have bedding planes parallel to the boundary between basalt and pelitic rocks, some parts of pelitic rocks were also dislocated together with footwall basalt.

If we assume that the scale of the ore deposits anticipated to occur in this area is more or less similar to those of the known deposits, the maximum would be in the order of 400x200x30 m. In the known deposits, however, in places dip steeply, the deposits are cut by faults into small bodies in many localities, and the hanging and foot walls are sometimes in fault contact with the orebodies. Therefore, sufficient numbers and depths of drilling is necessary for evaluating mineral prospects and the extensions of known deposits.

As mentioned above, ore deposits occur very close to a mineralized zone in footwall basalt. The existence of mineralized zone in basalt suggests some possibility of massive ore occurrence in the vicinity of such zones.

Massive sulfide deposit was confirmed at one borehole during the course of the present survey. Although the core width of the orebody was rather thin at 75 cm, assay showed a high grade of Cu 4 %, and this confirmed the existence of a massive sulfide orebody to the southwest of Bakibaba Deposit. This borehole is located to the southwest of Bakibaba and it is also to the south of the mineralized alteration zone on the surface. Drilling conducted this year supports the hypothesis that tracing the mineralized alteration zone is a very effective guide for mineral exploration. The dimensions of this newly found orebody must be determined and thus drilling survey should be continued.

Aşıköy and Toykondu Deposits are accompanied by mineralized hyaloclastite on the footwall side and by black shale on the hanging wall side, and thus it is believed that they retain the stratigraphic relations at the time of ore formation. On the other hand, the network and dissemination zones occur at a stratigraphic position higher than the ore horizon at the Bakibaba Deposit and overturned structure is inferred. It is believed that this overturned structure continues

from Bakibaba Deposit to the southeast of Kizilsu Deposit.

The mineralized alteration zone exposed between the above two deposits is very likely the footwall altered zone of the deposit anticipated to occur in this zone.

Drilling at the northern extension of the Zemberekler mineralized zone results in finding veinlets and dissemination of sulphide minerals in pillow lava. The known massive ore deposits occur in hyaloclastite. The mineralized zone in the drill hole MJTK-4 occurs in pillow lava. As hyaloclastite is considered to occur at the flank of and above pillow lava, new massive ore deposits are possibly expected to occur around this hyaloclastite.

It was clarified from the drilling and studies of the cores of the present survey that; pelitic rocks have low resistivity, and the normally high resistivity values of basalt also decreases when the rock is fractured and the interstices are filled with water. Thus low resistivity does not necessarily indicate the existence of mineralized zones.

It is apparent from the above that the localities for future exploration are; north of Bakibaba Deposit, and the mineralized zone between east of Bakibaba and Zemberekler .

PART 3 TAŞKÖPRÜ ZONE

PART 3 TAŞKÖPRÜ ZONE

CHAPTER 1 Regional Survey

1-1 Outline of the Zone

Taşköprü zone was extracted as a promising zone for a further study after careful geological and geochemical study of the existing information and data of the Küre area.

This zone is located about 25 km east of the Küre Mine and covers an area of 559 square kilometers.

Gökırmak River flows along the south of this zone and the upper reaches of this river lie within this zone. The Kızılkaya is the highest peak of the zone, rising 1,514 m above sea level. This zone is covered by relatively dense vegetation.

The distribution of old slags in the zone is known from existing information, and no mining activity has been recorded.

The location of this zone is indicated in Figures 1-1 and 1-3.

1-2 Geological Survey

1-2-1 Method of the Survey

Field geological survey was carried out using topographic maps on 1:25,000 and the survey results were compiled into a geological map on 1:50,000 scale.

A geological column and a geological map of this zone which were prepared in the course of this project are shown in Figures 3-1 and 3-2 respectively.

1-2-2 Stratigraphy

The geology of this zone is composed of, in ascending order; Devrekani Metamorphic Rocks, Çangal Meta-ophiolite, Kayadibi Formation, Muzrup Formation, Kızacık Formation, Alaçam Formation, and Çayköy Formation.

<Devrekani Metamorphic Rocks>

Type locality of these rocks is in the southeastern part of Yazıcı Village. These rocks occur in the western part of the zone, from southeastern Yazıcı Village to the southwestern part of Mt. Alayürek.

The lithology of this unit is mostly biotite gneiss with some muscovite.

The rocks have gneissose texture and consist mainly of quartz, biotite, chlorite and sericite.

Geologic Age		Formation	Thickness	Rock Facies	Rock Name	Mineralization & Intrusives
Quaternary		Alluvium	150m		Sand, gravel	
Cenozoic	Tertiary	Çayköy F.	11.000m		Çtl:limestone	Dâ:dacite Qt:quartz porphyry
					Çta:andesite lava	
Mesozoic	Cretaceous	Alaçam F.	1500m		Acs:sandstone, marl mudstone	Çangal Granitoids (Çg)
		Kızacık F.	1500m		Kcl:limestone	
	Malm	Huzrup F.	1300m		Mmc:conglomerate	
	Dogger					
	Lias	Kayadibi F.	11.000m		Kls:sandstone Klb:basic rocks	
Pre-Jurassic		Çangal Meta-ophiolites	15.000m		Çlp:pelitic schist	Mineralization (Cu,Py)
					Çlb:meta-basic rocks	
					Çls:serpentine	
Paleozoic		Devrekani Metamorphics	11.000m		Dpg:gneiss	

Fig. 3-1 Schematic Geologic Column of the Taşköprü Zone

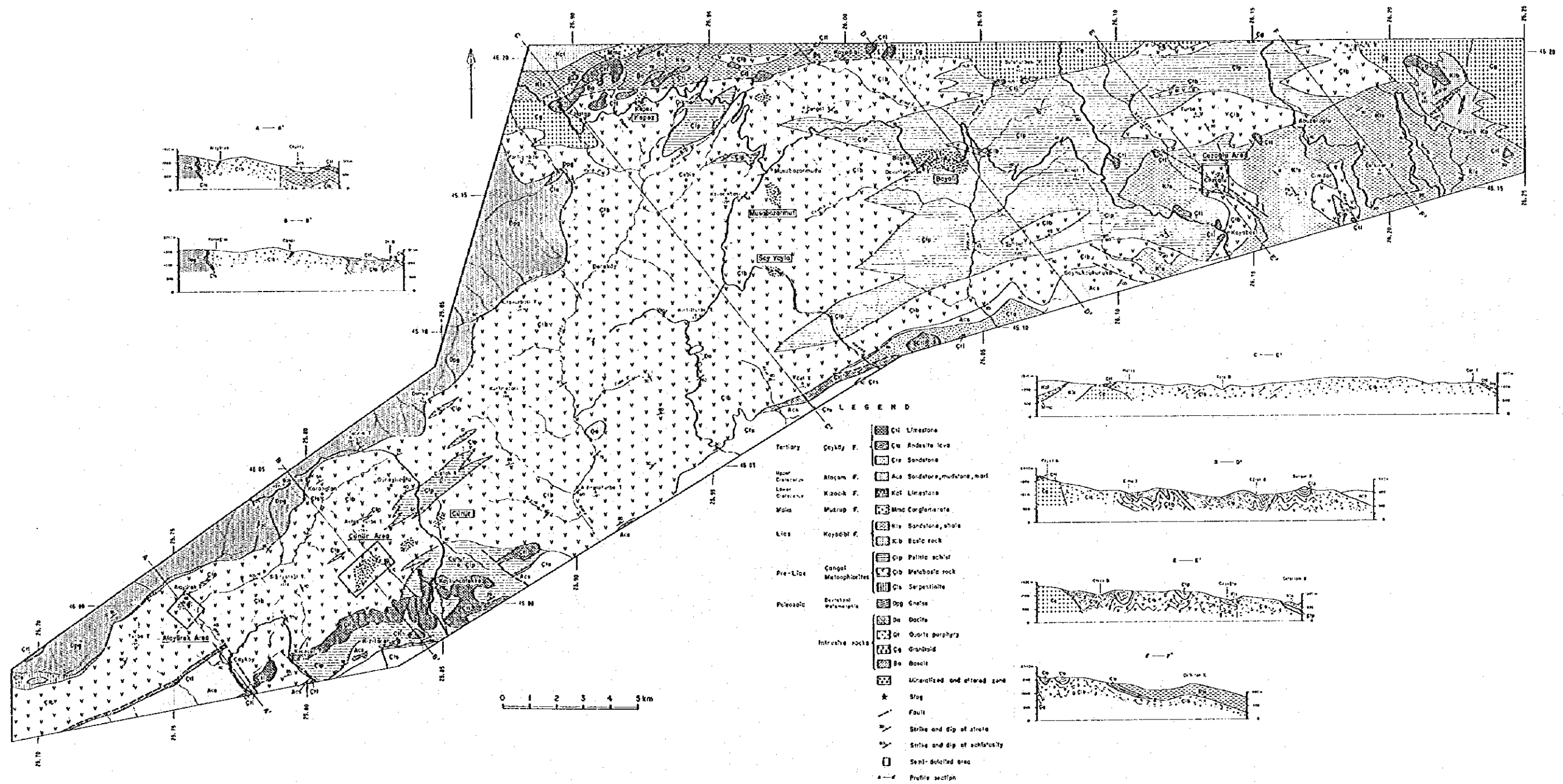


Fig. 3-2 Geologic Map and Cross Section of the Taşköprü Zone

These rocks are in fault contact with the overlying Çangal Meta-ophiolite. This metamorphic unit is considered to have derived from Paleozoic sedimentary rocks and was metamorphosed by orogenesis of the Dogger Epoch.

<Çangal Meta-ophiolite>

Type locality of these rocks is in the southern part of Mt. Çangal. The meta-ophiolite extends 100km in the east-west direction and 30km in the north-south direction. It occupies approximately 70 percent of the survey zone.

This body is composed of serpentinite, green rocks constituting the major part, and pelitic rocks. The orogenesis of the Dogger Epoch strongly affected these rocks and the green rocks were metamorphosed to metabasalt and green schist, and the pelitic rocks to pelitic schist.

Serpentinite occurs at the boundary with the underlying Devrekani Metamorphics and is partly intruded into the lower unit. The occurrence is limited to the western part of the zone and it is narrow with several to several tens of kilometers in length.

The green rock, the major constituent of this unit, consists of metabasalt and green schist. The metabasalt is believed to have derived from basalt and is massive and weakly metamorphosed. The green schist is believed to have derived from pyroclastics. Remnant of brecciated structure is not observed and thus the original rock was most probably tuff. Pelitic schist gradually becomes dominant eastward. Metabasalt is dominant to the west and green schist to the east.

The pelitic schist becomes dominant to the east of Boyalı, but there are also small occurrences around Cünür in the west. It is dominant in the parts delineated as pelitic schist on the geological map. But it also forms alternations with green schist or mixtures that are difficult to distinguish the two schists. The original rocks of the pelitic schist are believed to have been shale, sandstone, mudstone and other sediments.

The metabasalt has intersertal, porphyritic, and ophitic texture characteristic of basalt. Chlorite, epidote, calcite, carbonates increase with the metamorphic degree and granoblastic and nematoblastic texture appears.

The underlying unit is the Devrekani Metamorphic Rocks. The relation with the upper Kayadibi Formation is fault contact at; the northern side of Taşköprü and the west of Kayadibi Village to the north of Mt. Çangal. It is intruded by Çangal Granites to the east of Kayadibi Village. The east-west boundary between the Meta-ophiolite and the Kayadibi Formation is almost linear and a large tectonic line is inferred. In the southern side, the stratigraphically higher Kayadibi, Muzrup, and Kızacık Formations are lacking to the west and the Meta-ophiolite is unconformably overlain by Alaçam and Çayköy Formations. In the east it is overlain unconformably by sandstone of the Kayadibi Formation.

<Kayadibi Formation>

Type locality of this formation is the vicinity of Kayadibi Village. The thickness is over 1,000m. It is distributed in the west of Kayadibi Village and east of Cozoğlu Village.

This formation comprises sedimentary rocks and basalts. The sediments are black shale, siltstone and fine-grained sandstone. Fossils and dendrites are not observed in the sedimentary rocks. The attitudes of these rocks vary considerably in places. The dip is generally steep, 60°-70°. Intercalation of thin limestone has been reported and occurrence of calcareous mudstone was observed in this zone. It has been reported that the basalt is composed of spilite, diabase, gabbro, serpentinite and others, but the body consists of massive basalt near Mt. Cal and basalt dykes in western Kayadibi Village.

This unit overlies the Çangal Meta-ophiolite unconformably and is overlain unconformably by Muzrup and Kızacık Formations at western Kızacık Village, and by limestone of the Çayköy Formation in the depression at eastern Cozoğlu Village. It is correlated regionally to the Akgöl Formation.

<Muzrup Formation>

Type locality of this formation is Muzrup Village (outside the survey zone) to the northwest of Kayadibi Village. The thickness is over 300m. This formation is distributed widely from 4km north of Kepez Village to the Muzrup Village outside the survey zone.

This formation has characteristics similar to alluvial fans in the mountainous areas, and namely it comprises red conglomerate, sandstone, siltstone and psammitic limestone. Fragments of shale, sandstone, diabase, gabbro, granite and granodiorite of the underlying formations are included in the conglomerates and metamorphosed dolomite and marble occurs as pebbles.

This formation unconformably overlies the Kayadibi Formation and is overlain by Kızacık Formation. It is correlated to the Bürnük Formation of latest Dogger to early Malm from the relations to the higher and lower units.

<Kızacık Formation>

Type locality of this formation is Kızacık Village (7km north of Kepez Village, outside the survey zone). The thickness is over 500m. This formation is widely distributed from the northwest corner of the Taşköprü Zone to the Kızacık Village.

This formation is composed of shallow marine gray to bluish gray calcareous rocks extending northward from the south. This was formed by the regional transgression during early Malm Epoch.

This formation overlies the Kayadibi and Muzrup Formations unconformably. The overlying formation is not clear within the survey zone, but is overlain unconformably by Cretaceous sedimentary rocks outside the present area. Index fossils occur in the type locality and this formation is correlated to Inalti Formation.

<Alaçam Formation>

Type locality of this formation is the lower reaches of the Alaçam River. The thickness is over 500m. This formation is distributed from southwestern Cozoğlu to the southern side of Mt. Alayürek.

This formation comprises gray turbiditic sandstone, conglomerate, and dark gray calcareous shale. Bedding with east-west strike and southward dip is developed.

This formation overlies the Çangal Meta-ophiolite unconformably and underlies the Çayköy Formation unconformably. Fossils indicating Upper Cretaceous Epoch occur outside the survey zone and is correlated to the Çağlayan Formation.

<Çayköy Formation>

Type locality of this formation is the vicinity of Çayköy Village. The thickness is over 1,000m. This formation occurs on the southern side of the Taşköprü zone and extends to the outside of the survey zone.

This formation comprises gray well-bedded gray sandstone, grayish purple to reddish brown andesite lava and andesitic pyroclastics, and psammitic limestone in the ascending order. All the constituents have narrow distribution and they occur separately.

The lowermost sandstone occurs on a small scale covering the Çangal Meta-ophiolite and Alaçam Formation in the survey zone. The andesite occurs only in the south-central part of the Taşköprü Zone. Although not studied microscopically, it is believed to be two-pyroxene andesite from hand specimen studies. Psammitic limestone is the uppermost bed and occurs on topographically high localities.

This formation overlies the Çangal Meta-ophiolite and the Alaçam Formation. Fossils are not found, but its relations with strata near indicate Tertiary age.

1-2-3 INTRUSIVE ROCKS

<Çangal Granite>

This granite occurs around Mt. Şuletürbesi in the central-north, the vicinity of Hatap Village in the northwest, and northeastern Mt. Cal in the westernmost part of the zone.

The granite intrudes the Çangal Meta-ophiolite and Kayadibi Formation. The contact of these rocks with the granite is very clear without evidences of thermal metamorphism. There are xenoliths approximately aligned in the east-west direction. The total chemical analysis and microscopic studies indicate coarse-grained diorite.

<Dacite>

The intrusive body considered to be dacite and quartz porphyry occurs with NE-SW trend near Mt. Cal in the eastern part of the survey zone. Here, it is quartz porphyry and has intruded into the basalts of the Kayadibi Formation.

Small bodies of dacite occur along the road between Mt. Kirtiltürbe and Taşköprü and in the middle reaches of Kara Stream. These bodies intrude into the Çangal Meta-ophiolite. These are all silicified and argillized and the alteration mineral is sericite.

1-2-4 Geologic Structure

The Çangal Meta-ophiolite occurs widely in the survey zone and the attitude of the lamina cannot be determined because of the effect of metamorphism. Thus the geologic structure is very difficult to determine. Lithologically, it changes from ophiolitic lava in the west to pelitic rocks in the east. It is in contact with the underlying basement, Devrekani Metamorphics, through NE-SW trending tectonic line. Also it is bordered by the E-W trending lineation with the Çangal Granite and Kayadibi Formation on the northern side.

In the southern side, Cretaceous to Tertiary sediments overlie the Çangal Meta-ophiolite unconformably. These sediments generally are E-W trending. This direction appears to represent the regional trend of this zone. There are faults of N-S and NE-SW systems that intersect the above and they displace and cut into blocs the massif that extends in the E-W direction. These faults are considered, from the geologic units they intersect, to have formed during Tertiary time. The tectonic lines that are inferred to exist at the boundary of the Devrekani Metamorphics and Çangal Meta-ophiolite, and at the Çangal Granite contact are believed to be of older ages.

1-2-5 Mineralization and Alteration

<Boyalı Mineral Occurrence>

It is located 25 km north of Taşköprü. The mineralized and altered zone occurs in the boundary between pelitic schist and green schist.

Limonitization, pyritization and silicification are observed on the surface. The stratiform mineralized part composed of mostly pyrite is distributed widely. Old trenches are found in an area 2 km in the E-W direction and 500 m in the N-S direction.

<Musabozarmut Mineral Occurrence>

It is in the vicinity of Musabozarmut Village, located 15 km north of Taşköprü.

It occurs in an area composed of regionally altered green schists and metabasalts.

Limonitization, pyritization and silicification are observed on the surface. The alteration zone accompanied by mainly pyrite is distributed widely. The superficial extension of this zone is 7 km in the E-W direction and 3 km in the N-S direction.

<Sey Yayla Mineral Occurrence>

It is located 4 km south of Musabozarmut. A hydrothermal alteration zone occurs in metabasalts.

Limonitization, pyritization and silicification are observed on the surface of the zone. The zone consists of mainly pyrite dissemination. The superficial extension of this alteration zone is 500 m in the E-W direction and 200 m in the N-S direction.

Akkus, and the others (1991) carried out geological and geophysical surveys in the area and indicated that the alteration, pyritization and limonitization were observed in a 300 m long zone, and small amount of slag was present within this zone. The recorded anomaly in the IP and SP surveys done and suggested one drill in the area.

<Kepez Mineral Occurrence>

It is located 22 km northeast of Devrekani. It is a hydrothermal mineralization zone in an area composed of pelitic schists and green schists. This zone extends from east to west.

Kepez mineralization is judged to be very weak from geological observation, although limonitization, pyritization and silicification are observed in

Çangal Meta-ophiolites.

<East of Cünür Mineral Occurrence>

It is located 35 km northeast of Kastamonu. A hydrothermal mineralization occurs in an area composed of mostly metabasalts.

Limonitization, pyritization and silicification are observed and chalcopyrite occurs in parts of the surface. The zone consists of mainly pyrite dissemination. The superficial extension of this mineralized zone is wide, ranging more than 7 km in the NEE-SWW direction and it includes Cünür mineralized zone, which will be described later.

1-3 Discussion

The geology of this zone consists of Paleozoic, Mesozoic and Tertiary rocks. The mineralized zones recognized through existing information and regional geological survey, both point only to the copper and zinc mineralization of the Çangal Meta-ophiolite. It was expected that kieslagar-type ore deposits underlie the Taşköprü zone.

These mineralizations are lens-shaped, stratiform and dissemination. A detailed geochemical survey was conducted in the Boyalı and East of Cünür sections by MTA, and a geophysical survey was done in the Sey Yayla prospect by ETİBANK. The results of these surveys are not promising for further exploration.

The other mineralized zones, excluding three zones mentioned later, geologically do not warrant further study.

CHAPTER 2 COZOĞLU PROSPECT

2-1 Outline of the Prospect

This prospect is located in the eastern part of the Taşköprü zone, occupying an area of 1 square kilometer. The name of the prospect is derived from a village that is located in the center of the prospect.

This prospect was extracted as a promising area for further exploration after careful study of existing geological, geochemical information and data and regional geological survey. Semi-detailed geological survey and geophysical exploration were conducted in this exploration programme. The major purpose of the geophysical exploration is to investigate the subsurface electric structure, and to evaluate the potentiality of copper mineralization in this prospect.

2-2 Geological Survey

2-2-1 Method of the Survey

Field geological survey was carried out using an 1:5,000 topographic map enlarged from a 1:25,000 map, and the survey results were compiled into a 1:5,000 geological map.

The geological map of this prospect is shown in Figure 3-3.

2-2-2 Geology and Geologic Structure

The geology in this prospect is composed mainly of Çangal Meta-ophiolite, Kızacik Formation, and Alaçam Formation. The Meta-ophiolite comprises pelitic schist, massive metabasalt and green schist. The Kızacik Formation consists of grayish white limestone and the Alaçam Formation of quartz arenite and black mudstone. Kızacik Formation overlies the Çangal Meta-ophiolite unconformably while the Alaçam Formation is in fault contact.

2-2-3 Mineralization and Alteration

There are two openings of old adits on the surface. A large amount of mine waste is found in the vicinity. These are all in the Çangal Meta-ophiolite.

One of the two old adits has a 7 m long cross cut from the entrance and pyrite dissemination occurs in parts of the green schist with some oxidized copper minerals. Assay of these samples indicate Cu 0.7-0.9% and S 1.8%.

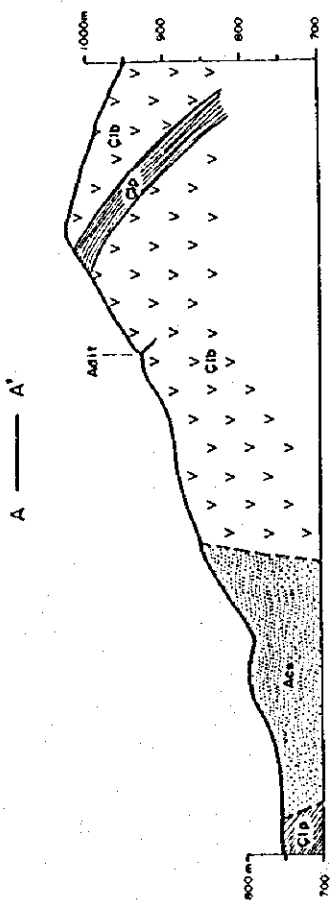
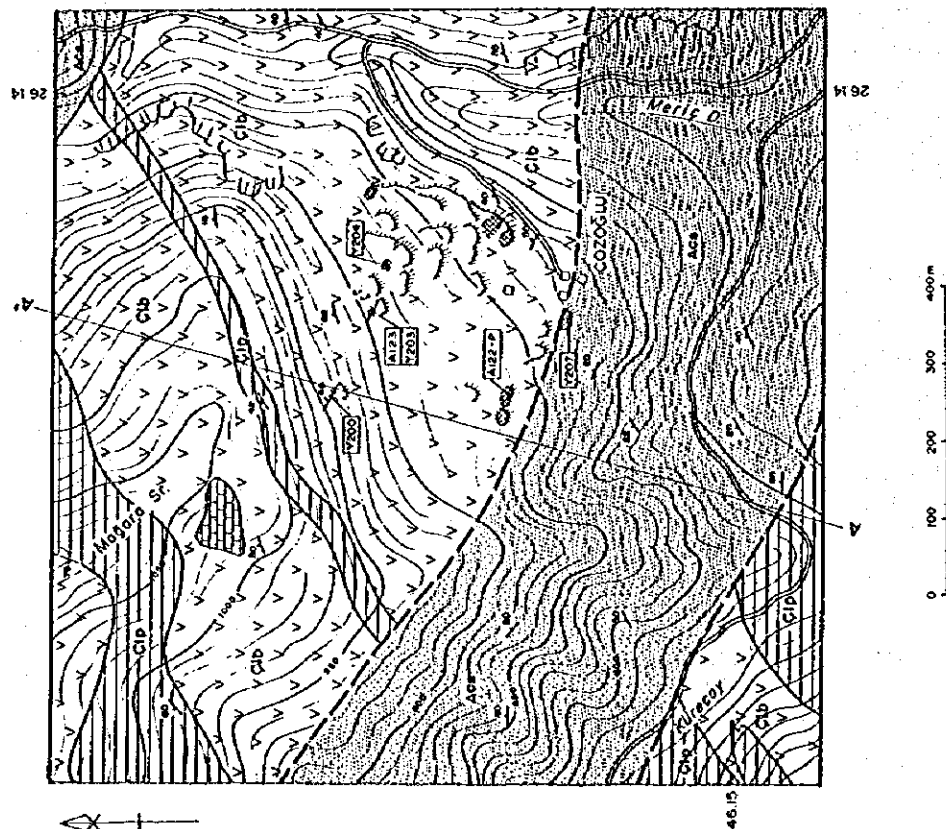
The other opening could be a collapsed incline, a shaft or a ruin of old mining. Near the opening, there is a 30cm thick quartz vein in the green schist with malachite flecks in the cracks. The quartz vein sample shows Cu 2.5%, Zn 0.7% and there could be zinc oxide minerals. There are, however, many segregation quartz veins in the green schist near the mineralized zone and it is believed that the above quartz vein near the adit opening and the copper oxide are not related. Part of the green schist in the vicinity is altered to gray clay.

There are some mine waste dumps within 400x150m range. Samples from two of these dumps show Cu 1.0-4.8% and chalcopyrite and bornite are observed microscopically.

2-3 Geophysical Exploration

2-3-1 Objective and the Outline of the Survey

Electric survey (time-domain IP method) was applied in the Cozoğlu prospect that were considered to be promising by the geological survey carried out during



L E G E N D

- Algeem Formation [Symbol]
- Kizcaik Formation [Symbol]
- Çengel Menephele [Symbol]
- Mineralization and alteration [Symbol]
- Adit [Symbol]
- Dump [Symbol]
- Sediments and shells [Symbol]
- Limestone [Symbol]
- Metabasalt and green schist [Symbol]
- Palitic schist [Symbol]
- Gneiss with quartz veins [Symbol]
- Slope [Symbol]
- Profile section [Symbol]

Sample No.	Ag (g/t)	Cu (%)	Pb (%)	Zn (%)	Ca (%)	S (%)
A122 (Slag)	<0.1	1.19	0.07	0.19	0.17	0.35
A123	<0.1	0.78	0.01	0.04	<0.006	1.61
Y200	<0.1	2.50	<0.01	0.75	0.01	0.18
Y204	<0.1	0.91	<0.01	0.18	0.01	1.22
Y204 (Slag)	<0.1	4.61	<0.01	0.01	<0.006	0.49
Y207 (Slag)	<0.1	1.00	<0.01	0.16	0.11	0.83

Fig. 3-3 Geologic Map and Cross Section of the Cozoglu Prospect

1992. The objective of the survey is to clarify the electric characteristics of the deeper subsurface zones and thus obtain information regarding the mineral potential of these zones.

The outline of the work carried out is as follows. The location map of the survey lines is shown in Figure 3-4.

Total length of survey line : 7,500 m
Number of survey lines : five lines
Interval of lines : 200m
Points of measurement : 230 points

Line	Length(m)	Points of measurement
A	1,500	64
B	1,500	64
C	1,500	64
D	1,500	64
E	1,500	64

<The equipment for IP survey>

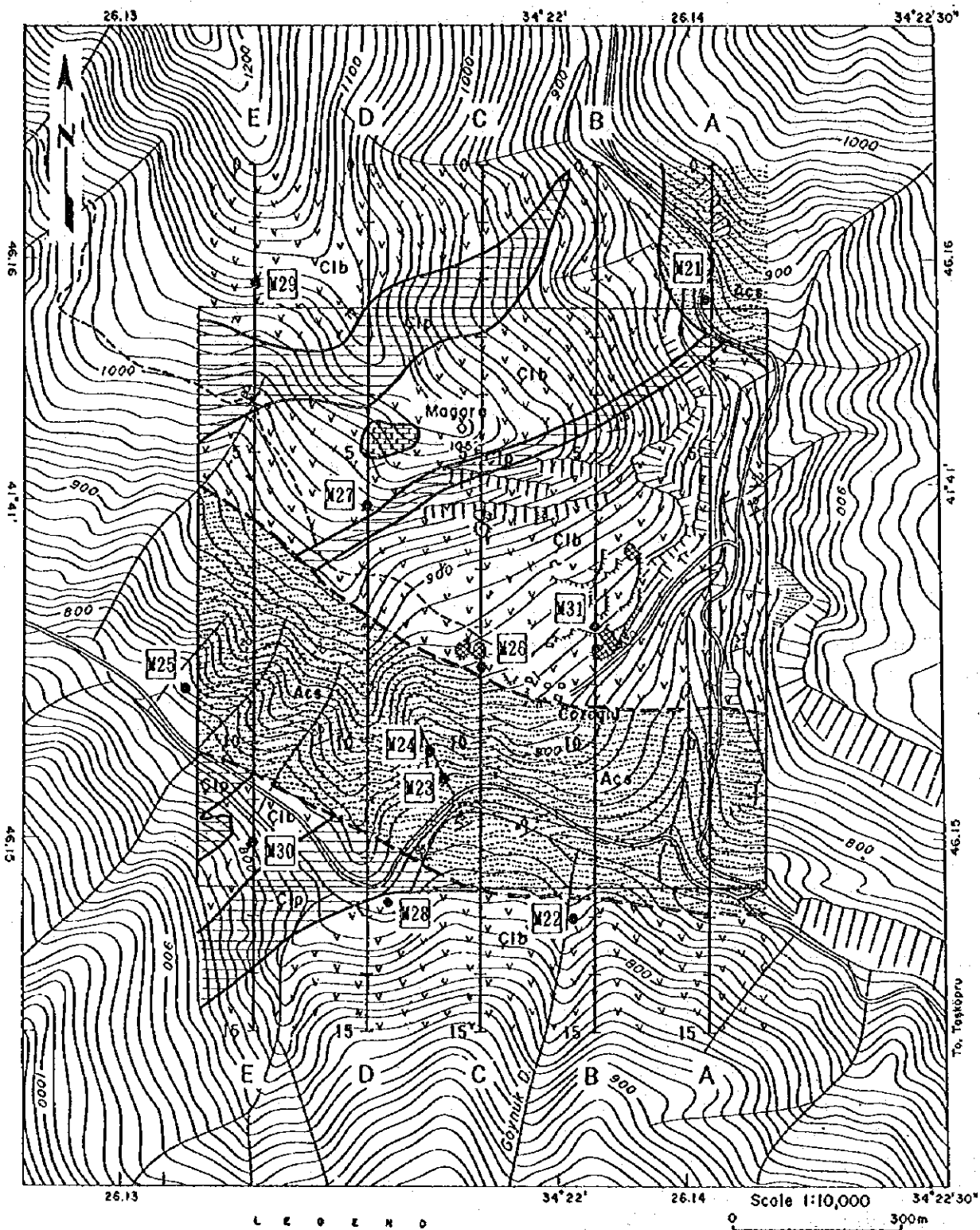
The following equipments were used in this survey.

- a) Receiver Scintrex IPR-12
8 channels, current on/off time 1, 2, 4, 8, 16, 32 sec.
Automatic cancellation of self potential.
Preset 14 windows and automatic measuring and data storage in the semiconductor memory data.
- b) Electrode of receiving dipole : porous pot with Cu-CuSO₄
- c) Transmitter Scintrex TSQ-3
Output power 3000VA, output voltage 300-1350 volts,
output current 10 amp.
Power requirement 230volts, 3 phase, 800 Hz
- d) Generator Briggs and Stratton.
Output power 3500 VA, output voltage 230 volts,
3 phase, 800Hz.
- e) Electrode of transmitting dipole
stainless rods (length 50cm)

<Analysis>

The measured resistivity and chargeability values are shown in tables for each line on the profiles. The subsurface depths are shown on plane maps by the electrode separation index. And the subsurface electric characteristics can be understood from these plane maps and profiles.

The resistivity values were affected by the topography and thus terrain cor-



L E G E N D

Aloğan Formation		Aca	Sandstone and shale		Fault
Kızılcık Formation		Kcl	Limestone		Strike and dip of schist
Çengel Metapelite		Cib	Metabasic and green schist		Strike and dip of schistosity
		Cfp	Pelitic schist		Location and number of sample for ore assay
Mineralization and alteration		Gossan with quartz vein		Slag	
		Adit		Dump	
		Dump			

Fig. 3-4 Location Map of IP Survey Lines in the Cozoğlu Prospect

rection was made by using carbon paper.

Two-dimensional model simulation was carried out for IP anomalies and chargeability and resistivity values were obtained quantitatively for the anomaly sources.

2-3-2 Results of Analysis

<Apparent resistivity>

The measured apparent resistivity values are shown for each line in Figure 3-5. The characteristics of these values are as follows.

- a) Resistivity of 100ohm-m is dominant. The resistivity is generally higher to the north and lower in the central to southern parts.
- b) High resistivity of over 300ohm-m is distributed in the northern side of the survey area and are detected in the shallow subsurface zones with the exception of Line C.
- c) Low resistivity of under 30ohm-m is distributed in the E-W to WNW-ESE direction in the shallow zones of the central part of the survey area. These are detected in the sandstone and shale zone. Two small low zones are found in the deeper parts of Line A and one zone in Line G.

Chargeability

The measured values of chargeability are shown for each line on the profile (Fig.3-6). The following characteristics are noted.

- a) Significant anomaly zones of over 50mV/V are detected in the central part of Lines A and B and also in the southern edge of the survey area.
- b) The former anomalies are noted in the n=1 (-100m) and n=2 (-150m) plane maps, and they are weak anomalies of 30-50mV/V in the deeper parts. These anomalies coincide with the distribution of the slag near the Cozoğlu Village, but they extend eastward. The latter anomalies are detected at the profile ends throughout the Lines A - E and extend further southward.
- c) Negative chargeability anomalies are detected in the central part of the survey area with WNW-ESE trend and also in the northeastern part with NE-SW trend. The former occurs widely corresponding to the sandstone and shale dis-

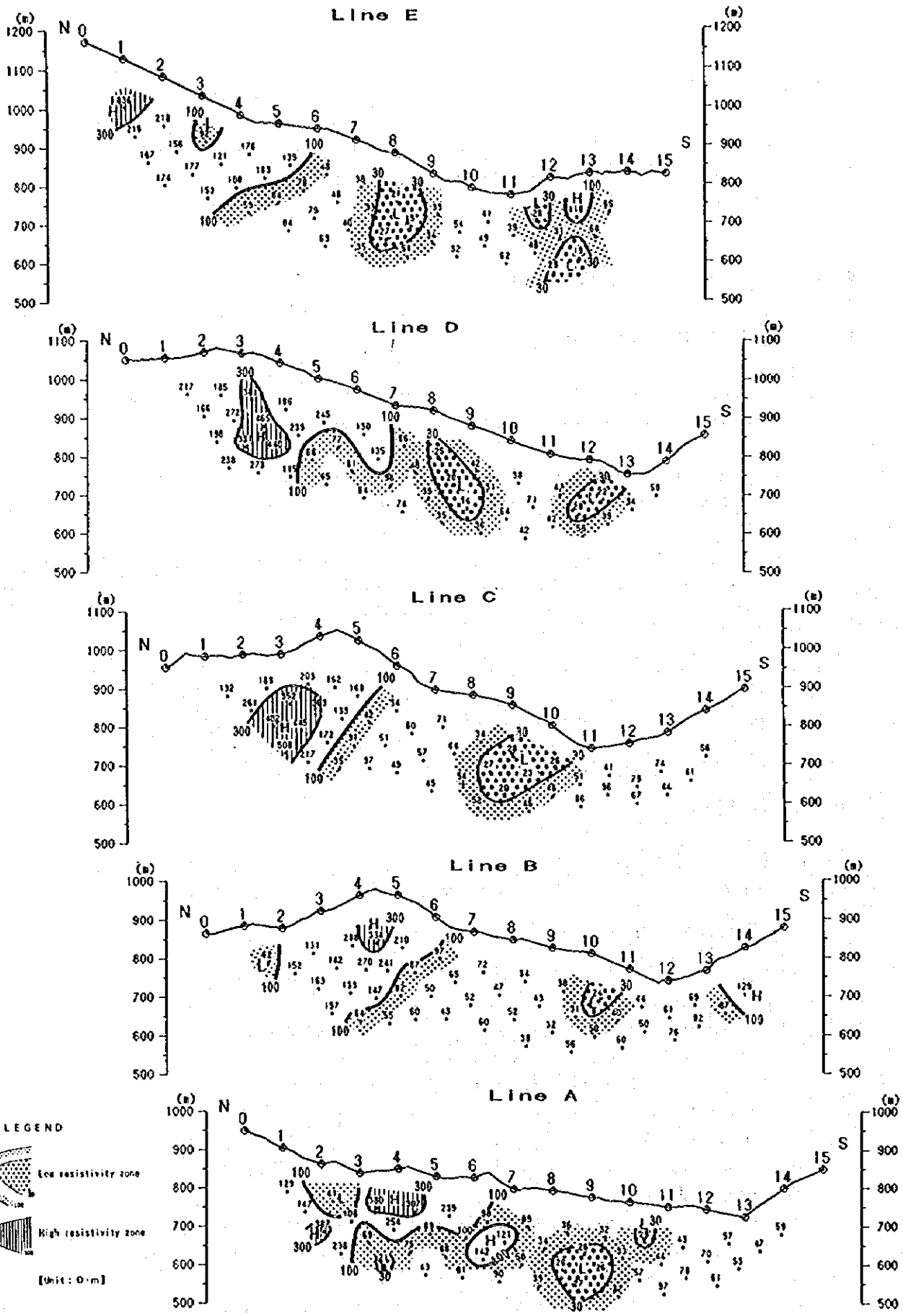


Fig. 3-5 Sections of Apparent Resistivity (Line A - E)

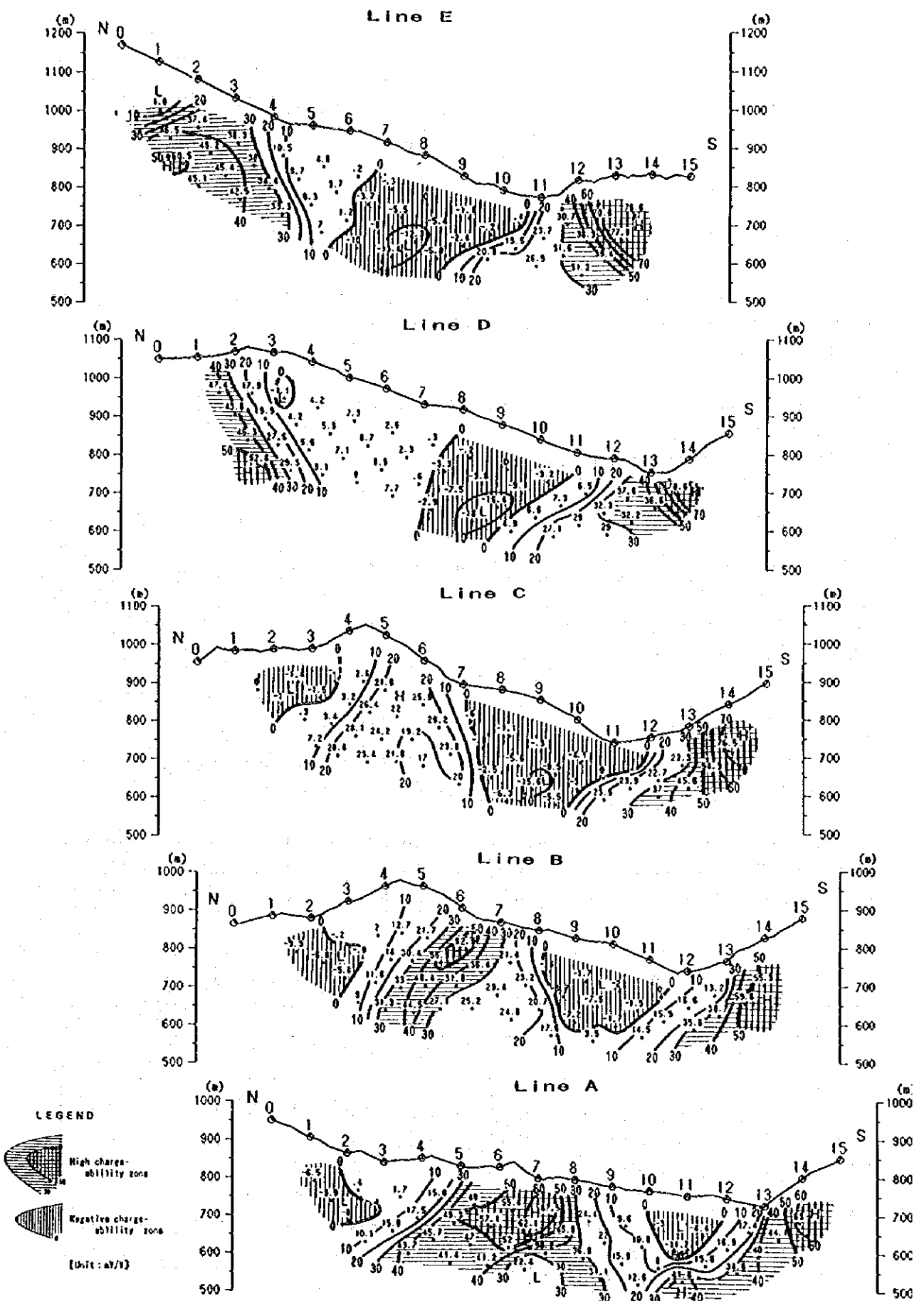


Fig. 3-6 Sections of Chargeability (Line A - E)

tribution, but it becomes narrower in the deeper parts. The latter anomalies are detected in the sandstone, shale and meta-basalt areas, but they become extinct at -200m and -250m depth.

<Physical properties of rock samples>

Resistivity and chargeability were measured by field equipment under field conditions in the laboratory for 11 samples collected from the surface in the field. The results are as follows.

- a) A slag has high chargeability of 485 mV/V and low resistivity of 246ohm-m.
- b) Other samples have chargeability of less than 10mV/V and high resistivity exceeding 750ohm-m with the exception of two samples.

2-3-3 Results of Model Simulation Analysis

Model simulation was carried out for Lines A and B because significant chargeability anomalies were detected.

Line A:

Strong anomaly of 60mV/V was detected at the central part of the line and similar one in the southern edge of the Line.

The prepared model (Fig.3-7) has, at the central and southern end of the line, 50mV/V chargeability and 100ohm-m resistivity source by code 5 and low resistivity zone of 20ohm-m in the sandstone and shale zone.

The results of the simulation agree well with the measured values and thus this is considered to be a reasonable model. The difference from the measured values is the lack of negative zone in the deep central part of the line, and the low value of the chargeability at the southern end.

Line B:

The characteristic of the chargeability and resistivity of this line is similar to those of Line A, and >50mV/V chargeability anomalies are detected in the central and southern parts of the line.

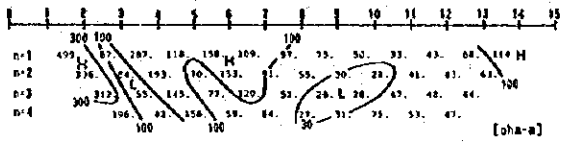
The prepared model (Fig.3-8) has a 100ohm-m, 50mV/V anomaly (code 5) in the central part of the line and this is smaller than that in Line A. The background is set at 100 ohm-m, 10 mV/V (code 1).

Simulation Model Line A

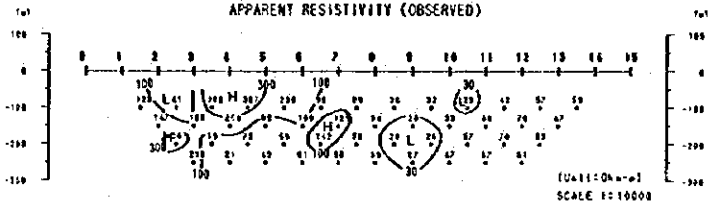
	1	2	3	4	5	6	7	8	9	10	11	12	13	14	15	
1	777	777	777	711	666	666	555	555	501	111	111	111	111	155	555	
2	777	777	777	711	666	666	555	555	501	111	444	444	111	155	555	
100m	777	777	777	711	111	111	155	555	555	501	444	444	111	111	155	555
4	777	777	777	711	111	111	155	555	555	501	444	444	111	111	155	555
8	777	777	777	711	111	111	155	555	555	501	444	444	111	111	155	555
200m	777	777	777	711	111	111	155	555	555	501	444	444	111	111	155	555
1	777	777	777	711	111	111	155	555	555	501	444	111	111	111	155	555
2	777	777	777	711	111	111	155	555	555	501	444	111	111	111	155	555
100m	777	777	777	711	111	111	155	555	555	501	444	111	111	111	155	555
4	777	777	777	711	111	111	155	555	555	501	444	111	111	111	155	555
8	777	777	777	711	111	111	155	555	555	501	444	111	111	111	155	555
200m	777	777	777	711	111	111	155	555	555	501	444	111	111	111	155	555
1	777	777	777	711	111	111	155	555	555	501	444	111	111	111	155	555
2	777	777	777	711	111	111	155	555	555	501	444	111	111	111	155	555
100m	777	777	777	711	111	111	155	555	555	501	444	111	111	111	155	555
4	777	777	777	711	111	111	155	555	555	501	444	111	111	111	155	555
8	777	777	777	711	111	111	155	555	555	501	444	111	111	111	155	555
200m	777	777	777	711	111	111	155	555	555	501	444	111	111	111	155	555
1	777	777	777	711	111	111	155	555	555	501	444	111	111	111	155	555
2	777	777	777	711	111	111	155	555	555	501	444	111	111	111	155	555
100m	777	777	777	711	111	111	155	555	555	501	444	111	111	111	155	555
4	777	777	777	711	111	111	155	555	555	501	444	111	111	111	155	555
8	777	777	777	711	111	111	155	555	555	501	444	111	111	111	155	555
200m	777	777	777	711	111	111	155	555	555	501	444	111	111	111	155	555
1	777	777	777	711	111	111	155	555	555	501	444	111	111	111	155	555
2	777	777	777	711	111	111	155	555	555	501	444	111	111	111	155	555
100m	777	777	777	711	111	111	155	555	555	501	444	111	111	111	155	555
4	777	777	777	711	111	111	155	555	555	501	444	111	111	111	155	555
8	777	777	777	711	111	111	155	555	555	501	444	111	111	111	155	555
200m	777	777	777	711	111	111	155	555	555	501	444	111	111	111	155	555
1	777	777	777	711	111	111	155	555	555	501	444	111	111	111	155	555
2	777	777	777	711	111	111	155	555	555	501	444	111	111	111	155	555
100m	777	777	777	711	111	111	155	555	555	501	444	111	111	111	155	555
4	777	777	777	711	111	111	155	555	555	501	444	111	111	111	155	555
8	777	777	777	711	111	111	155	555	555	501	444	111	111	111	155	555
200m	777	777	777	711	111	111	155	555	555	501	444	111	111	111	155	555
1	777	777	777	711	111	111	155	555	555	501	444	111	111	111	155	555
2	777	777	777	711	111	111	155	555	555	501	444	111	111	111	155	555
100m	777	777	777	711	111	111	155	555	555	501	444	111	111	111	155	555
4	777	777	777	711	111	111	155	555	555	501	444	111	111	111	155	555
8	777	777	777	711	111	111	155	555	555	501	444	111	111	111	155	555
200m	777	777	777	711	111	111	155	555	555	501	444	111	111	111	155	555

CODE	RESISTIVITY	CHARGEABILITY
	Ohm-m	mV/V
1	100.	10.0
2	50.	-5.0
3	20.	-3.0
4	20.	10.0
5	100.	50.0
6	300.	10.0
7	300.	-5.0
8	0.	.0
9	0.	.0

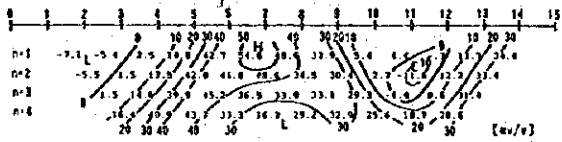
APPARENT RESISTIVITY



APPARENT RESISTIVITY (OBSERVED)



CHARGEABILITY



The result of the simulation is shown in the lower right of the figure and it is seen that they are harmonious with the measured results.

2-4 Discussions

The geology in this prospect is composed mainly of Çangal Meta-ophiolite, Kizacik Formation, and Alaçam Formation. Blind mineralized zones are expected to occur in the Çangal Meta-ophiolite of the prospect similar to the other mineralized zones in the Taşköprü zone.

Mineral showings were not observed on the surface by the geological survey with the exception of slag.

It is difficult to determine the type of mineralization from the surface showings. A similar type of the Aşıköy deposit in the Küre Zone or stratiform copper-zinc deposit is a possible type of deposit. The reasons are; lack of strong alteration of green schist on the surface, the occurrence of copper and zinc oxide minerals, and the existence of a large amount of slags.

IP measurements were carried out during the second year. Chargeability anomalies of 60mV/V were detected corresponding to the distribution of slag and those of 30-50mV/V in the northwestern part and anomalies in the southern part in Lines A-E. The former anomalies extend further eastward and their western limit is inferred to be Line C. The resistivity is low at 50-100ohm-m, similar to that of sandstone and shale, and as this is not due to massive deposits, the possibility of the existence of large massive deposits is low. Of the latter anomalies, that of the southern end is confirmed by all lines, but the total feature is not clear because of the fact that it is at the end of the traverse lines. The anomaly is strong and it is continuous for significant distance. The shape of the anomaly suggests sulfide dissemination, but manifestation of mineralization are not found in the surface rocks (sandstone, shale, pelitic schist) of the anomalous zone.

The interpretation for the former geophysical anomaly is harmonious with the fact that the attitude of the old adit is steep. The existence of the stratiform or vein-type ore deposits is promising from the comprehensive interpretation of the survey results. Drilling survey is further necessary to confirm the geophysical anomalies.

CHAPTER 3 CÜNÜR PROSPECT

3-1 Outline of the Prospect

This prospect is located on the western side of the Cünür Village in the

southwestern part of the Taşköprü Zone and covers an area of 2 square kilometers.

The prospect was extracted as a promising area for further exploration after careful existing geological and geochemical information and data study and regional geological survey. Semi-detailed geological survey and geophysical exploration were conducted in this exploration programme. The major purpose of the geophysical exploration is to investigate the subsurface electric structure, and to evaluate the potentiality of copper mineralization in this prospect.

3-2 Geological Survey

3-2-1 Method of the Survey

Field geological survey was carried out using an 1:5,000 topographic map enlarged from a 1:25,000 map, and the survey results were compiled into a 1:5,000 geological map.

The geological map of this prospect and geological sketch of the mineralized zone are shown in Figures 3-9 and 3-10 respectively.

3-2-2 Geology and Geologic Structure

The geology of the prospect is Çangal Meta-ophiolite consisting of pelitic schist, massive basalt, and green schist. The pelitic schist strikes NE-SW and the dip is mostly within the range of 20°-70° N.

3-2-3 Mineralization and alteration

The mineralized zones comprise eight lenses and bedded gossan bodies in green schist. The gossans extend in the NE-SW direction harmonious to the bedding and the maximum lateral extension is 400x50m. They are silicified and argillized parts of mafic rocks with quartz-limonite-pyrite network veinlets and limonite dissemination. Azurite and chrysocolla occur in parts of the gossan in the central part of the zones and the assay of the sample is Cu 4.3%, Zn 1.4%. Pyrite veinlets occur in the gossan in the northeastern part of the zone with assay result of Au 1.9g/t, Ag 115g/t and S 40%.

Silicified rocks occur widely around the gossans. These silicified bodies are derived from mafic rocks and limonite does not occur.

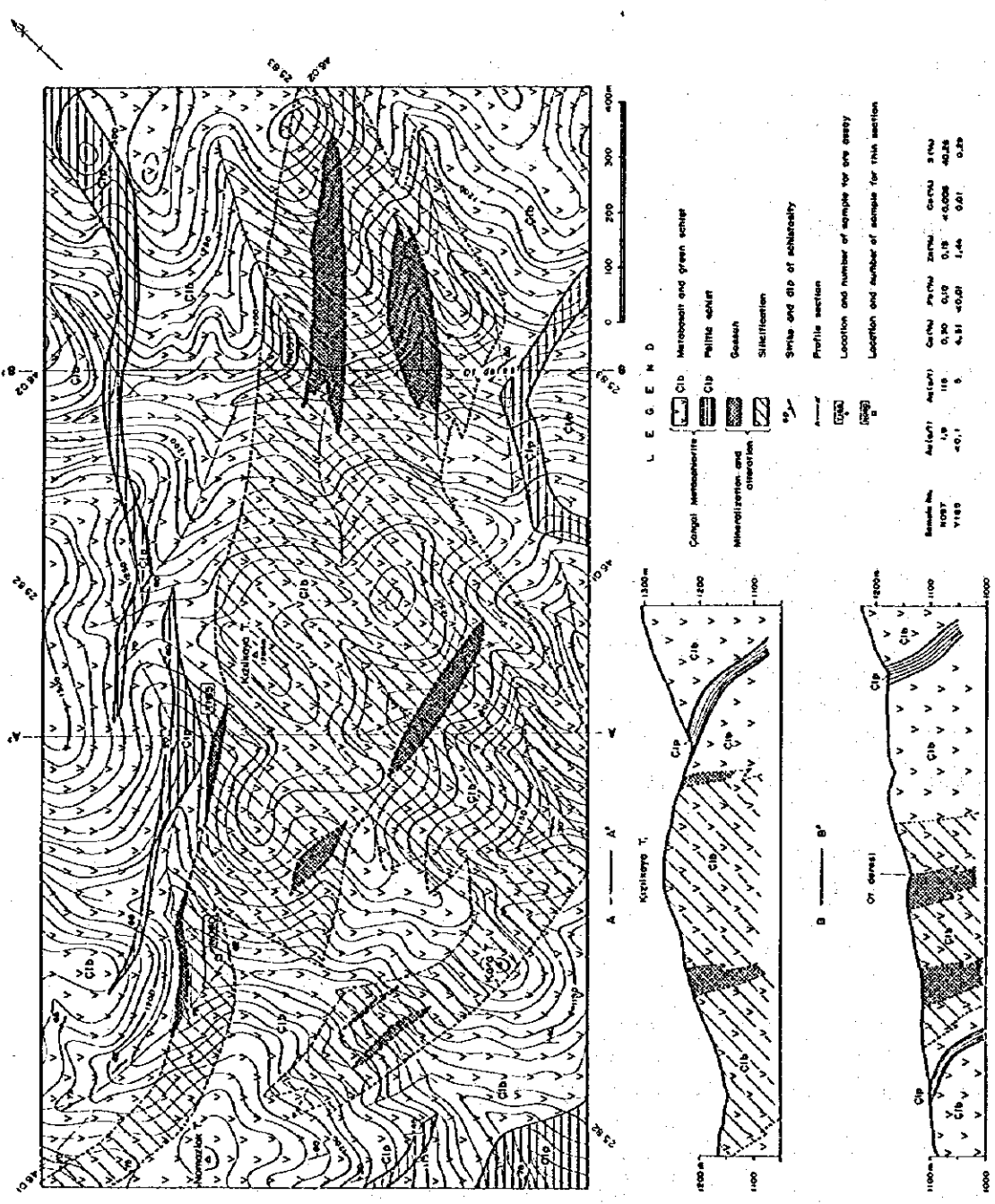


Fig. 3-9 Geologic Map and Cross Section of the Cünür Prospect

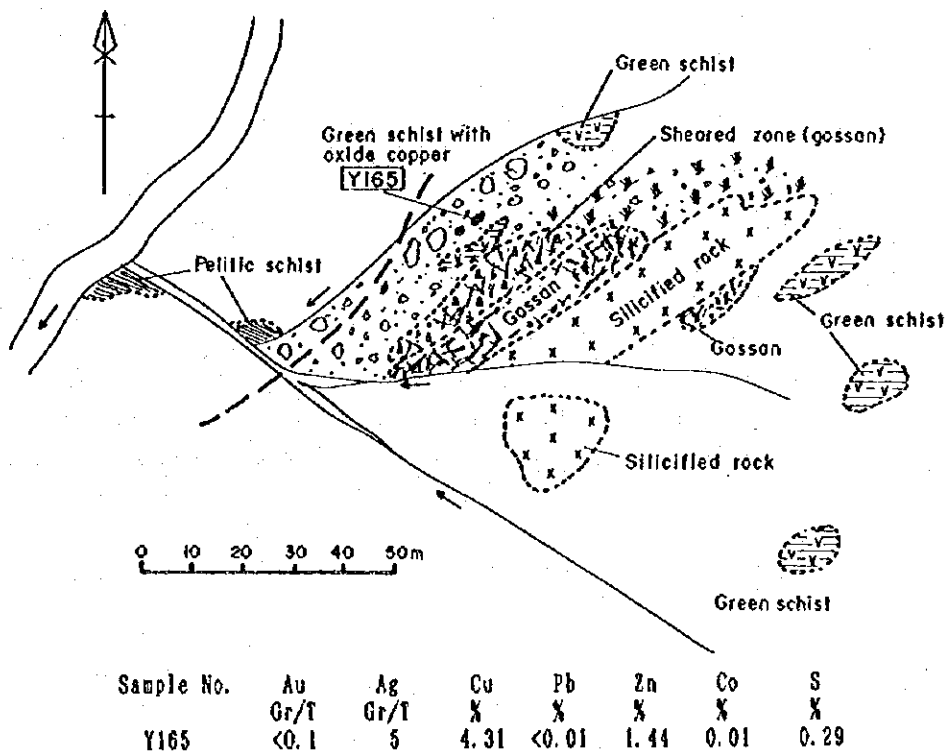


Fig. 3-10 Sketch of Mineralized Zone in the Cünür Prospect

3-3 GEOPHYSICAL PROSPECTING

3-3-1 Objective and the Outline of the Survey

Electric survey (time-domain IP method) was applied in the Cünür area that was considered to be promising by the geological survey. The objective of the survey is to clarify the electric characteristics of the deeper subsurface zones

and thus obtain information regarding the mineral potential of the prospect.

The location of IP survey lines in the Cünür area is shown in Fig.3-11, and geology and location of rock specimen for the laboratory test are shown in same figure.

The outline of the work carried out is as follows.

Total length of survey line: 13,500 m

Number of survey lines: nine lines

Interval of lines: 150m 300m

Points of measurement: 414 points

Line	Length(m)	Points of measurement
A	1,500	64
B	1,500	64
C	1,500	64
D	1,500	64
E	1,500	64
F	1,500	64
G	1,500	64
H	1,500	64
I	1,500	64

<Profile lines and leveling>

The line intervals were set relatively wide in order to cover the total survey area with limited profile length. Interval of 300m was used for most of the CÜNÜR area with denser profile of 150m interval in the promising zones with mineral showings.

The equipment and the methods of measurement and analysis are same as those of the Cozoglu prospect.

3-3-3 Results of Analysis

<Measured values>

The measured apparent resistivity values are laid out for each line in Figure 3-12.

The characteristics of the apparent resistivity values of this prospect are as follows.

- a) The resistivity values are predominantly in the 100-300 ohm-m range.
- b) High apparent resistivity values (>300ohm-m) are detected in the eastern part of the survey area for the shallow subsurface zones and in the northern and north-western parts for the medium to deep zones.

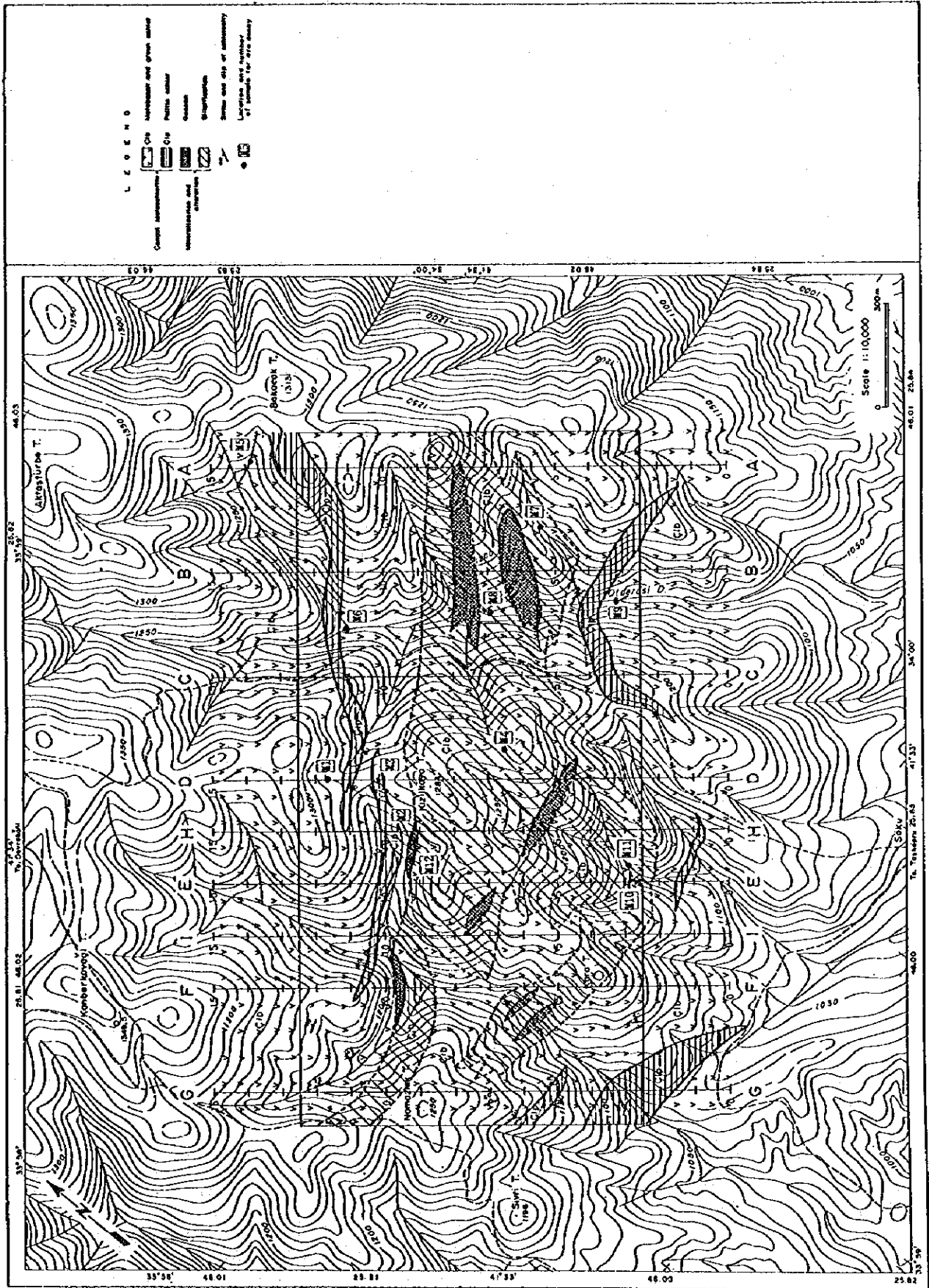


Fig. 3-11 Location Map of IP Survey Lines in the Cünür Prospect

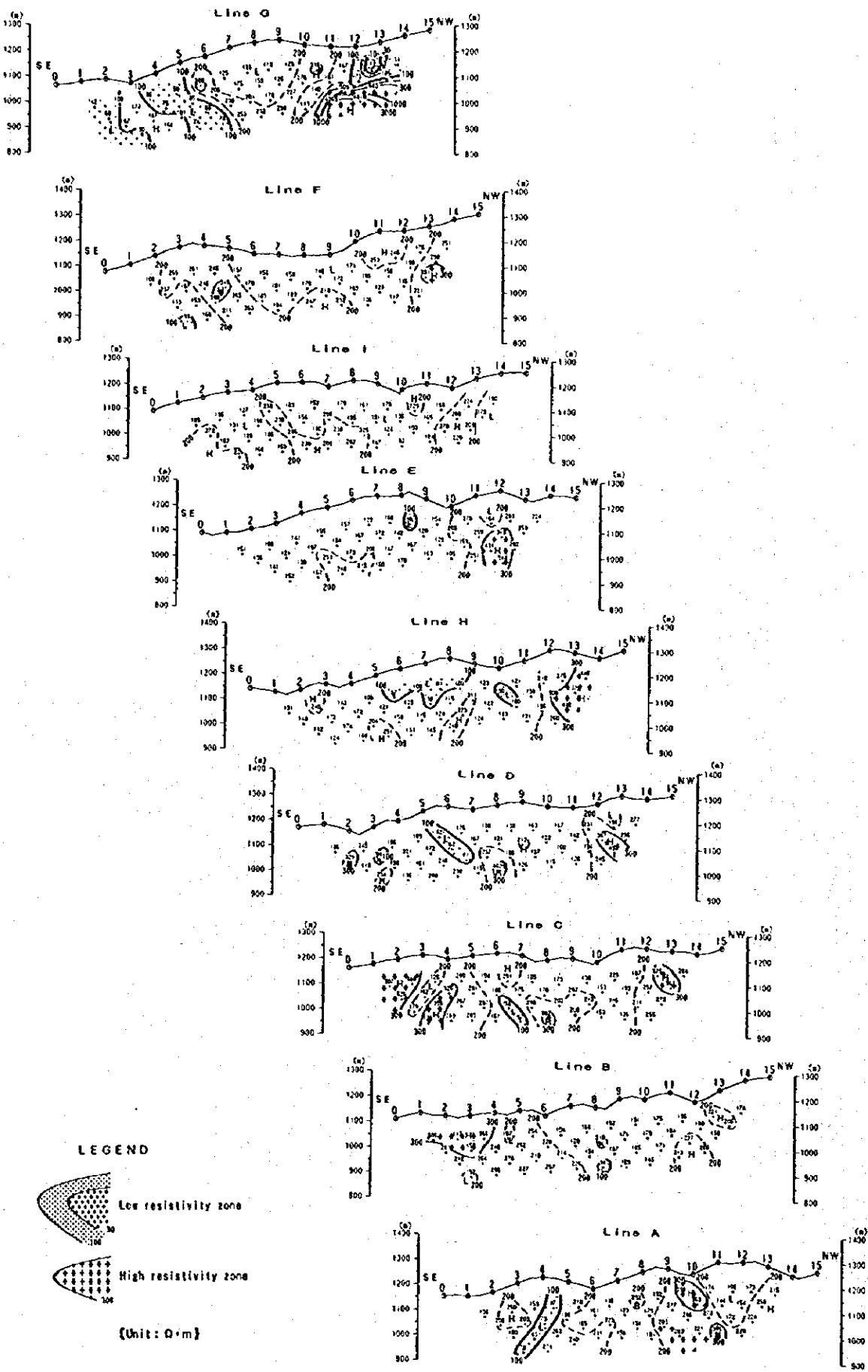


Fig. 3-12 Sections of Apparent Resistivity (Line A - I)

- c) Low apparent resistivity (<100ohm-m) is detected in the west-southwest and the central parts of the survey area for the shallow zones, and for the medium to deep zones low anomalies of small scale occur scattered throughout the survey area.

The measured chargeability values are shown for each line in Figure 3-13.

The characteristics of these values are as follows

- a) The chargeability values are predominantly low (<10mV/V).
- b) Weak chargeability anomalies within the range of 10-50mV/V are detected for the shallow subsurface zones along Lines H - I, particularly H. For the deep zones weak anomalies are detected in the southwestern part on Line G.
- c) Regarding the mineralized alteration zone at Station No. 9 on Line H where Cu 4.3% and Zn 1.4% values were obtained during the previous year, the anomaly value is only slightly higher than the vicinity and thus the mineralization is considered to be of very small scale.

<Physical properties of rock samples>

Resistivity and chargeability were measured for 11 samples collected from the surface in the laboratory with the field equipment under field conditions.

The results are as follows.

- a) Many of the samples showed high resistivity exceeding 1000ohm-m and three samples showed low values near 500 ohm-m.
- b) Chargeability is highest, 7.44mV/V, for massive basalt with pyrite dissemination, other samples have low values (<3.5mV) and the average of nine samples is 2.24mV/V. The value for a sample which was collected from the alteration zone is 6.24mV/V and is somewhat higher than others.

3-3-4 Results of Model Simulation Analysis

High chargeability anomalies exceeding 30mV/V in the southeastern parts of Lines E and H and thus model simulation was carried out for these two lines as follows.

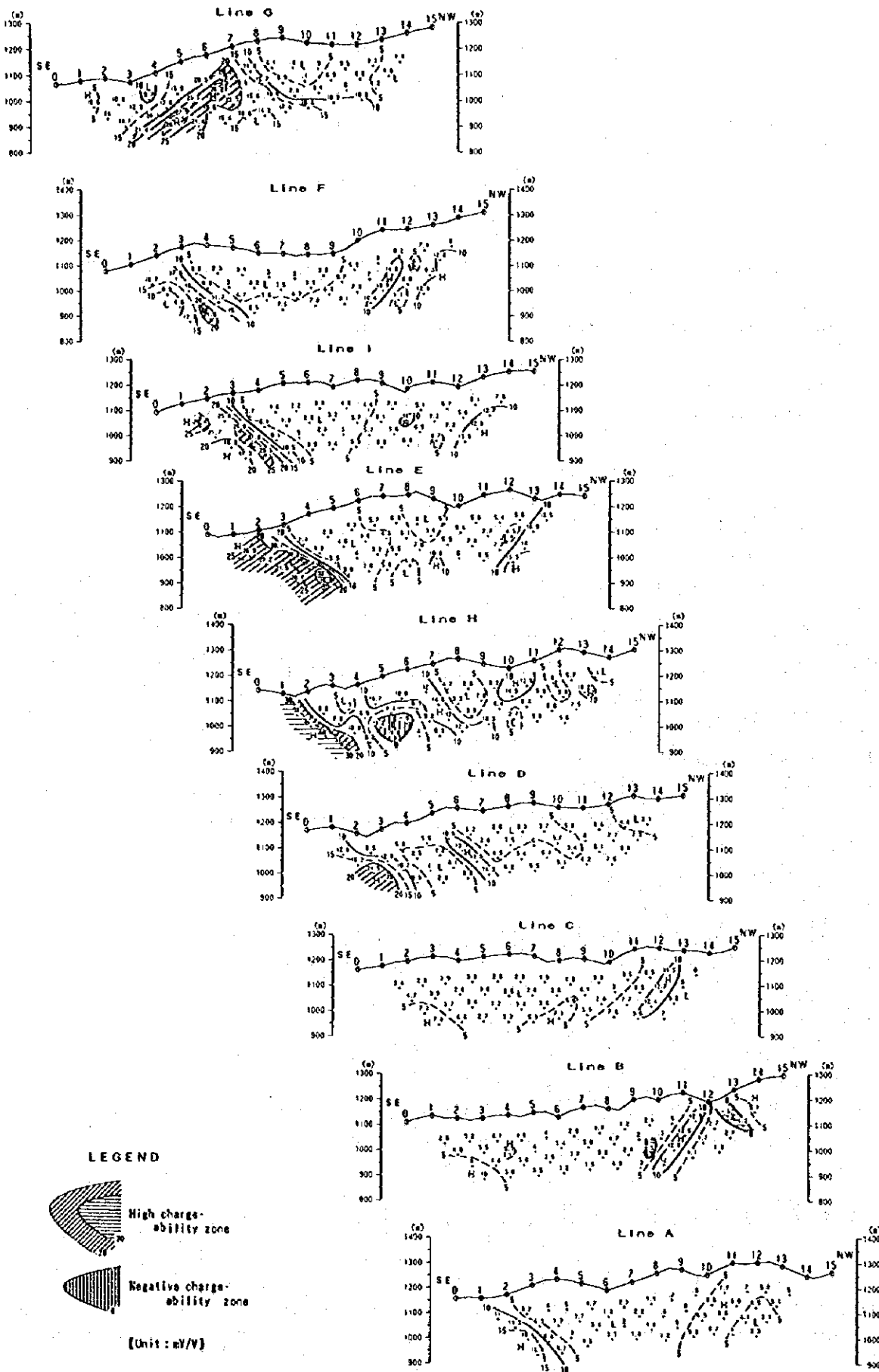


Fig. 3-13 Sections of Chargeability (Line A - I)

Line E (Fig.3-14):

The high chargeability below Stations Nos.1-5 and the high resistivity below Nos. 11-13 are the characteristics of this line. The high chargeability anomaly of Nos. 1-5 is also detected in the adjacent lines and is the most promising anomaly of this area.

In the model constructed, a high chargeability zone (15-30 mV/V) is set below Nos. 0-2, and a high resistivity anomaly on the northwestern side of this zone. Also as resistivity and chargeability increase toward the northwestern edge of this line, 15mV/V, 400ohm-m zone was established in the model at this edge.

The results of the simulation are harmonious with the measured results and thus it is considered to be a reasonable model.

The source of the anomaly in the southeastern part of this line is assumed to lie in the zone between shallow subsurface to 200m in depth. But since the total anomaly cannot be clarified by that detected at the southeastern edge of the line, it is difficult to determine whether the anomaly source is limited to the shallow parts or not.

The high resistivity in the northwestern part corresponds to the distribution of meta-basalt and green schist bodies and mineralization in the deeper zones is anticipated.

Line H (Fig.3-15):

In this line, 30mV/V anomaly was detected at Nos. 1-3 and negative chargeability in the deeper zone under Nos. 4-6. Also gossan containing azurite and chrysocolla occurs near No. 9. The resistivity of the most part is within the range of 150- 250ohm-m and somewhat high zones over 200ohm-m occur in the central part and at the northwestern edge of the line.

In the model, 40mV/V, 150-300ohm-m zone was established at the southeastern edge of the line and a zone with higher chargeability(15mV/V) than the background in the shallow part below Nos.3-7.

Figures and contours harmonious with the measured values were obtained by the simulation. The high chargeability and resistivity at the southeastern end of this line are interpreted to indicate the possible occurrence of sulfide minerals accompanied by silicification.

3-4 Discussions

The geology of the prospect consists of Çangal Meta-ophiolite. The mineralized zones comprised Quartz-Limonite-Pyrite networks and limonite dissemina-

tion are distributed in the leached and silicified/argillized basic rocks. Silicified rocks occur widely around the gossans.

These zones are considered to be promising for copper and zinc from the chemical data with the good possibility of blind Kure-type deposit.

The results of careful analysis and interpretation of the model simulation results and the tests on the collected rock samples indicate the following.

Time-domain IP survey was carried out in an area centered around the silicified zone. Anomalies related to the outcrops of gossan and other evidences of mineralization confirmed on the surface could not be detected. Although the silicified zone is distributed widely in the survey area, high resistivities do not occur in this zone, while such anomalies exceeding 300ohm-m occur in the unaltered northwestern and eastern parts of the area. This indicates that the silicification is not strong and the existence of mineralization comprising magnetite, pyrrhotite and other sulfide minerals lowered the resistivity.

The chargeability values are generally not high in this area, they range in the order of 5-10mV/V (background). This is interpreted to be the result of relatively weak mineralization or oxidation or leaching of the sulfide minerals that accompanied silicification. The electrode interval of this survey was relatively large at 100m and it is difficult to detect small deposits and narrow mineralized zones. Information is available only to the depth of 250m and if oxidation and leaching occur to this depth, the low chargeability of the silicified zone can be explained.

Two profile lines were added for studying the weak anomaly (>20mV/V, Lines D and E) detected in the southeastern part of the survey area and the promising gossan.

The weak anomaly is continuous in the E-W direction that is the same as the trend of the elongation of the known gossan and it has the shape of anomalies of the dissemination deposits. This weak anomaly extends westward and wedges out at Line F in the shallow zones, but is considered to continue to the weak anomaly of Nos. 5-7 of Line F. This is considered to be caused by sulfide dissemination because of the relatively high resistivity at 150ohm-m, chargeability of 20-30mV/V and the relatively wide spread of the anomaly. The chargeability plane of -200m and -250m indicate that this anomaly connects with that of Line G and is elongated in the E-W to NE-SW direction as one mineralized zone.

Regarding the mineralized alteration zone of Lines E and No.9 of H, from which Cu 4.1% and Zn 1.4% were obtained in the previous year, the resistivity is within the background values and the chargeability is somewhat lower than the vicinity. Thus the mineralized zone is considered to be of small scale and prob-

ably has been oxidized and leached considerably because of the occurrence of azurite and chrysocolla. Extensive mineralization cannot be expected from this zone.

CHAPTER 4 ALAYÜREK PROSPECT

4-1 Outline of the Prospect

The prospect is located at the southwestern end of the Taşköprü Zone, 7km west of the Cünür prospect and covers an area of 1 square kilometer.

The prospect was extracted as a promising area for further exploration after careful study of existing geological, geochemical information and data and regional geological survey. Semi-detailed geological survey was conducted in this exploration programme.

4-2 Geological Survey

4-2-1 Method of the Survey

Field geological survey was carried out using an 1:5,000 topographic map enlarged from an 1:25,000, and the survey results were compiled into an 1:5,000 geological map.

The geological sketch of the mineralized zone and geological map of this prospect are shown in Figures 3-18 and 3-19 respectively.

4-2-2 Geology and Geologic Structure

The Çangal Meta-ophiolite is the geologic unit in the prospect. The lithology is pelitic schist, massive basalt, and green schist. The attitude of the pelitic schist is NE-SW strike and 30° N dip. There are many faults of N-S and E-W systems in the southeastern part of the area.

4-3-2 Mineralization and Alteration

The mineralization consists of pyrite dissemination and limonite network at two localities. One is stratiform dissemination-network zone extending in the east-west direction over 600 x 70m in the western part. The mineralizations differ by the nature of the host rock. Strong dissemination occurs in green schist while network veinlets are developed in massive basalt. The higher of the assay values of the network samples is Au 1.5g/t, Ag 100g/t, Cu 0.9%. The green schist is almost totally non-altered, but the massive basalt is partly silicified.

The other mineralized zone occurs to the east of the above zone and is a relatively small pyrite dissemination over 100 x 10m extending N-S along faults. In

the vicinity of this zone bounded by N-S and E-W faults, mafic rocks have been silicified and bleached with large amount of quartz, some sericite and chlorite. The silicified zone does not contain metallic minerals.

4-3 Discussions

These mineralized zones are characterized by weak alteration with the exception of silicified parts and the occurrence of copper minerals. This indicates the possibility of blind deposits similar to the Kure type. Geophysical prospecting followed by drilling exploration is necessary to confirm this possibility.

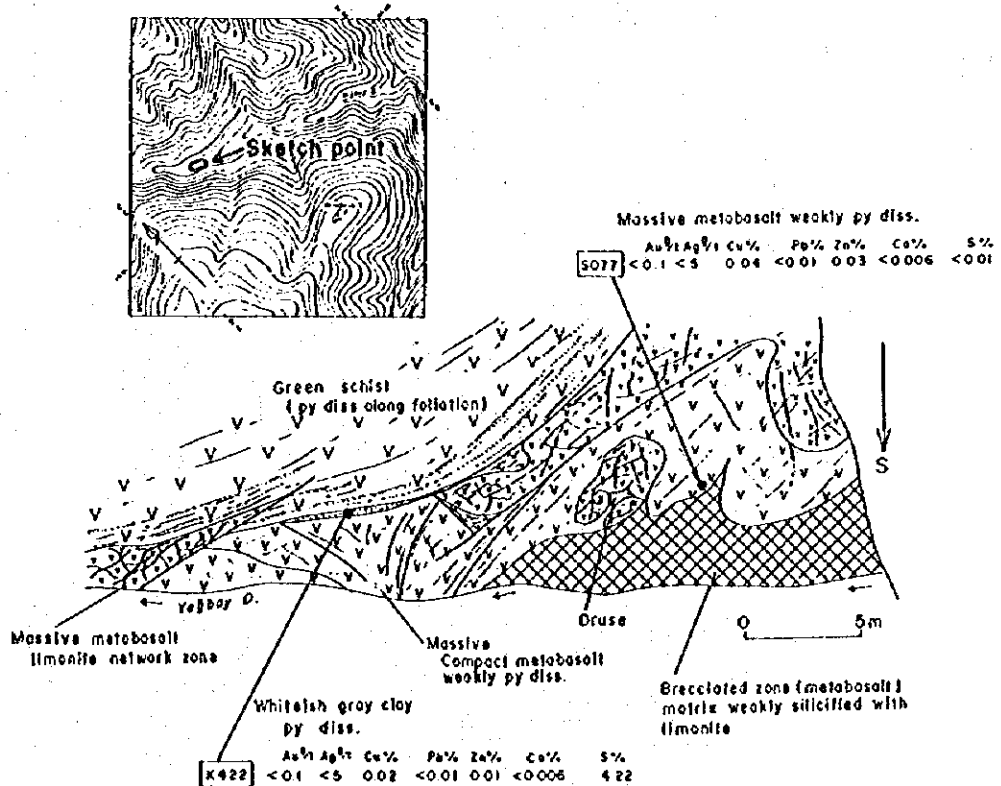
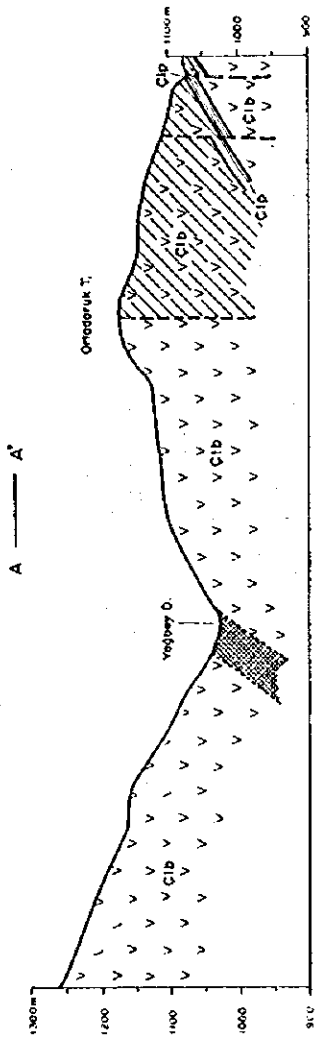
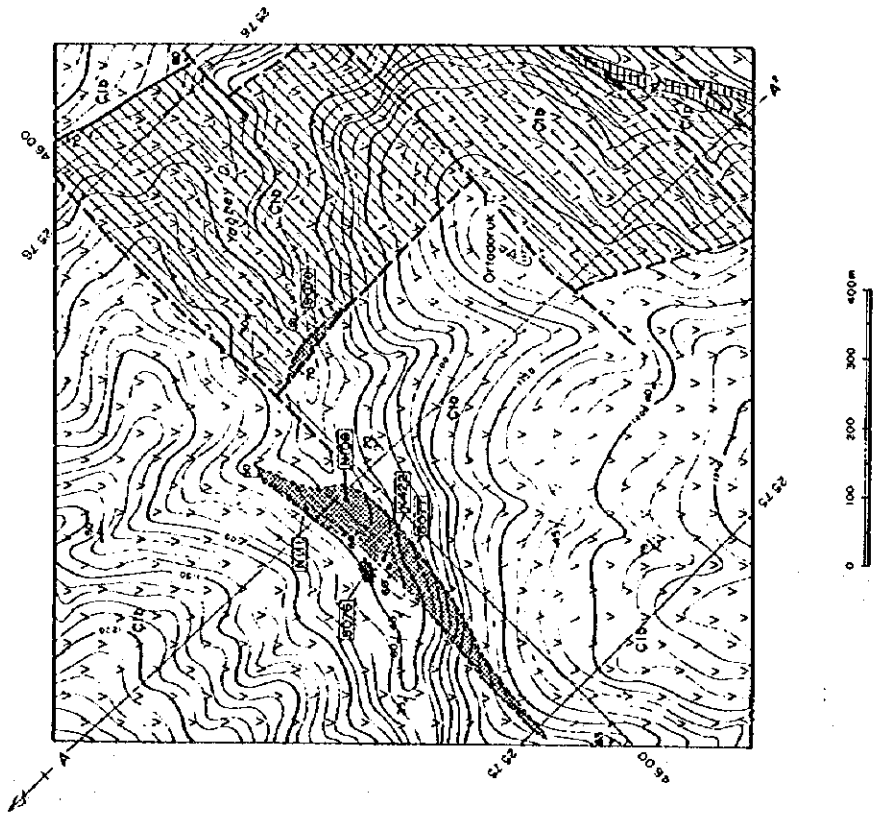


Fig. 3-16 Sketch of Mineralized Zone in the Alayurek Prospect



L E G E N D

- Conger metamorphites
- Cib
- Orogork T
- Vagbey D
- Fault
- Stream and dip of schistosity
- Location and number of sample for XRF assay
- Location and number of sample for X-ray diffraction analysis
- Pyrite section

- Massive and green schist
- Pyrite schist
- Disseminated pyrite and partly amphibolitic foliation
- Sillification
- Sillig

Sample No.	As (ppm)	Ag (ppm)	Cu (%)	Pb (%)	Zn (%)	Co (%)	S (%)
N422	<0.1	<5	0.02	<0.01	<0.01	<0.008	4.72
N108	0.2	<5	0.91	<0.01	0.03	<0.008	128.1
Mill	1.5	100	0.17	0.89	0.05	<0.008	1.75
8076 (R19)	<0.1	15	1.02	0.04	1.56	<0.008	1.39
8077	<0.1	<5	0.04	<0.01	0.03	<0.008	<0.01

Fig. 3-17 Geologic Map and Cross Section of the Alayurek Prospect

PART 4 DIKMENDAG ZONE

PART 4 DIKMENDAG ZONE

CHAPTER 1 Regional Survey

1-1 Outline of the Zone

Dikmendağ zone was extracted as a promising zone after careful geological and geochemical study of the existing information and data of the Küre area.

This zone is located about 15 km west of the Küre mine and covers an area of 66 square kilometers.

The Oluklu mountain is the highest peak in the zone, rising 1,388 m above the sea. This zone is a mountain district and is covered relative dense vegetation.

The location of this zone is indicated in Figures 1-1 and 1-2.

1-2 Geological Survey

1-2-1 Method of the Survey

Field geological survey was carried out using 1:25,000 topographic maps and the survey result were compiled into a 1:50,000 geological map.

The geologic column and geological map of this zone are shown in Figures 4-1 and 4-2.

1-2-2 Stratigraphy

The geology of this zone consists of Küre Formation of Lias Series, Köstekciler Formation and Satıköy Formation of Cretaceous System.

<Küre Formation>

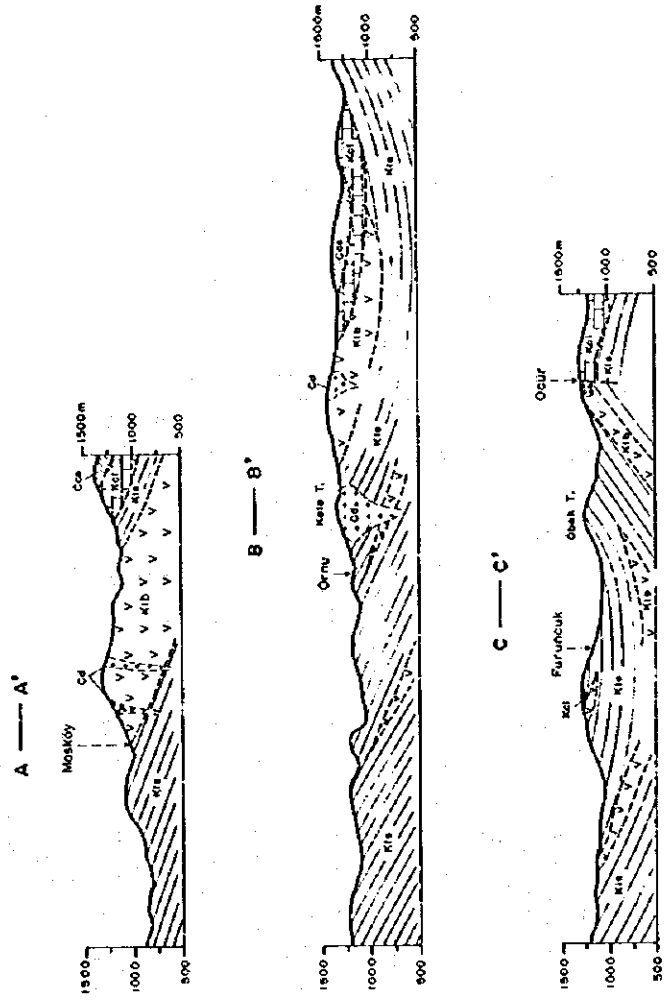
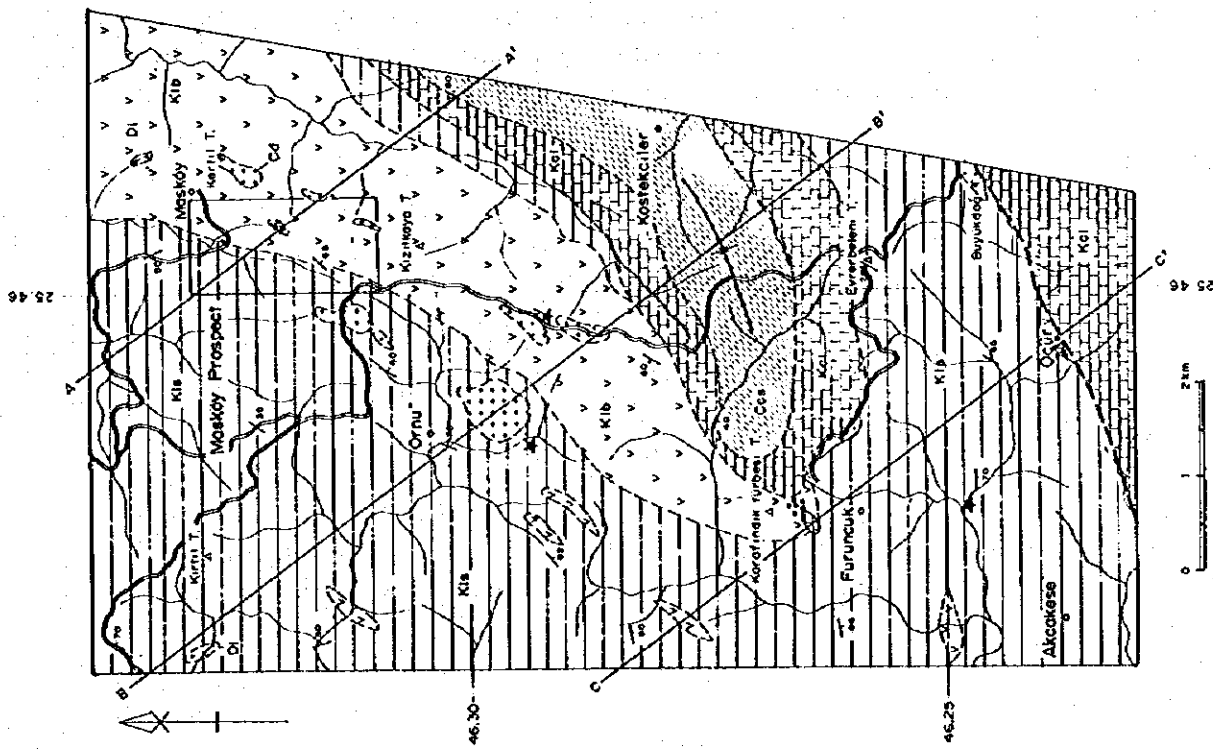
This formation is composed of sedimentary rocks and basalts. Sedimentary rocks are black shale, siltstone and fine sandstone. Basalts occur mostly between Masköy and Furuncuk Villages, while sedimentary rocks occur widely on the western side of the Dikmendağ Zone.

The attitude of the sedimentary units varies considerably and the dip is generally in the range of 60°-70°. The basaltic rocks are very similar to those of the Küre Area with characteristics of spilite and diabase. They have porphyritic texture microscopically and the chemical composition is somewhat felsic; close to that of andesite. Basalt lava occurs in the sedimentary rocks.

This formation occupies the lowermost horizon of the zone and is overlain unconformably by Köstekciler Formation.

Geologic Age		Formation	Thickness	Rock Facies	Rock Name	Mineralization & Intrusives
Quaternary						
Cenozoic	Cretaceous	Upper	1400m	Ccs	Ccs:sandstone/mudstone	
		Lower	1200m	Kcl	Kcl:limestone	
	Jurassic	Malm				
		Dogger				
Lias	Küre F.		Kls Klb	Kls:sandstone/shale Klb:basic rocks	↑ Dacite (Çd) ↑ Py-cp mineralization	

Fig. 4-1 Schematic Geologic Column of the Dikmendağ Zone



- L E G E N D**
- Sarıköy F. Sandstone and mudstone
 - Kövekçiler F. Limestone
 - Küre F. Alternation of sandstone and shale
 - Intrusive rocks
 - Kib Basic rock
 - Gs Dacite
 - Di Diorite
 - Dissemination of pyrite / slag
 - Probable fault
 - Syncline axis
 - Strike and dip
 - Profile section
 - Survey area

Fig. 4-2 Geologic Map and Cross Section of the Dikmendağ Zone

<Köstekciler Formation>

Type locality of this formation is north and south of Köstekciler Village. The thickness of this unit is over 200m.

This formation overlies the Küre Formation unconformably and occurs between Köstekciler and Satıköy Villages. A synclinal axis passes through the above two villages.

The rocks constituting the formation are gray to bluish gray calcareous rocks and calcareous sandstone. These are shallow marine sediments extending from the south northward. They were formed during the regional transgression in the Malm Epoch.

This formation underlies the Satıköy Formation unconformably. This is correlated to the Çağlayan Formation of the Küre Area, and regionally to the İnalti Formation.

<Satıköy Formation>

Type locality of this formation is the vicinity of Satıköy Village. The thickness is over 400m. This unit occurs between the Satıköy and Köstekciler Villages, similar to the distribution of the Köstekciler Formation.

The rocks constituting this formation are yellow to grey turbiditic sandstone, conglomerate, and dark grey calcareous shale. They occur as well bedded formation in the synclinal part of the above zone.

This formation unconformably overlies the Köstekciler Formation.

1-2-3 Intrusive Rocks

<Dioritic Rocks>

Diorite is intruded into sedimentary rocks of the Küre Formation in a relatively small scale. It is holocrystalline and is microscopically gabbroic in nature with idiomorphic plagioclase surrounded by hornblende and augite. Minor amount of opaque titanium minerals occur as an accessory.

<Dacite>

Many dacite with a shape of dome occur arranged in the NNE-SSW direction between Masköy and Ornu Villages. These are all small intrusive bodies with maximum dimensions of 500 x 500m at southern Ornu Village. It has been intruded into the Küre Formation. These bodies are partly sericitized.

1-2-4 Geologic Structure

The altitude of the sedimentary rocks of the Küre Formation varies considerably on strike and dip. Small scaled basalt bodies occur within sedimentary rocks. Muddy rocks with scaly cleavages are distributed in a basalt body like

mud dykes. Black shale of the Küre Formation has scaly cleavage. Therefore, the Küre Formation is considered to be a melange.

A NE-SW trending synclinal axis passes through the vicinity of the center of the zone and Köstekciler and Satıköy Formations are distributed in the synclinal part.

A NEE-SW trending fault occurs in the south and there are pyrite disseminations in the basaltic rocks cut by this fault.

1-2-5 Mineralization and Alteration

Masköy Mineralized Zone is located in the northeastern part of the zone and weak mineralization accompanied by pyrite dissemination is observed in the basalt at north of Furuncuk Village and in Öcür Village in the southern part of the zone. The Masköy Mineralized Zone is described in following chapter.

The mineralization north of Furuncuk is located at the southern end of the basalt and is at the southern extension of the synclinal axis. The mineralization in Öcür is cut by a NEE-SW fault and to the south of the fault is Köstekciler Formation, while to the north is basalt which occur rarely in the sedimentary rocks.

Old slags were found in the following three localities in this zone.

1km south of Ornu Village

1.6km southeast of Ornu Village

1km south of Furuncuk Village

A sample with malachite recognizable with the unaided eyes contained Cu 3.25%.

1-3 Discussion

The Küre Formation is extensively distributed in this zone and is composed of sedimentary rocks and basalts. Basalts is megascopically similar with those of the Küre zone, though whole rock chemical composition of these rocks is of andesitic.

Network and/or dissemination of pyrite are observed in these basalts. Old slags are clustered in the other places. These features are analogous of the Küre zone, excluding the scale of these appearance. The difference between two zone is that massive basalt is large in superficial distribution and pillow lava is small in the Dikmendağ zone. Hyaloclastite which is expected to occur in the footwall of the ore deposits is not found in the zone.

The mineralization of the zone is small in size at the surface. Therefore the priority for mineral exploration is relatively low in comparison with that of other zones, although we could not find any field evidences to deny the existence of Cyprus-type mineralization in the zone.

Chapter 2 MASKÖY PROSPECT

2-1 Outline of the Prospect

The semi-detailed geological survey was conducted in this prospect, because Masköy Mineralized zone is located in this prospect and is promising for Cyprus-type mineralization as a result of the regional geological survey.

This prospect is located in the northeastern part of the Dikmendağ zone and covers an area of 2 square kilometers.

2-2 Geological Survey

2-2-1 Method of the Survey

Field geological survey was carried out using an 1:5,000 topographic map enlarged from an 1:25,000 map, and the survey result were compiled into a geological map on a scale of 1 to 5,000.

The geological map of this prospect and geological sketch of Masköy Mineralized zone are shown in Figure 4-3 and 4-4.

2-2-2 Geology and Geological Structure

The geology around this prospect consists of the Küre Formation, dacite, and diorite.

The rocks constituting the Küre formation are basalt, black shale, siltstone and sandstone. The basalt is mostly massive, but is also partly pillow lava. Black shale and siltstone are the thicker units. These sedimentary units have NE-SW strike and the dip in most areas ranges 20°- 65° SE.

Dacite occurs as small stocks and dykes in the basalt and the sedimentary rocks. Diorite occurs as dykes in the sedimentary units.

2-2-3 Mineralization and Alteration

This mineralized zone consists of limonite network/veinlets and pyrite dissemination over an area of 300 x 50m and gossan. It extends in the NE-SW direction. The host rock is basalt and it is silicified to dark grey in the pyrite disseminated parts of the zone. Both Cu and Zn grades of the rock samples from this zone are low.

Dacite occurs in the vicinity, but it is fresh without evidences of alteration.

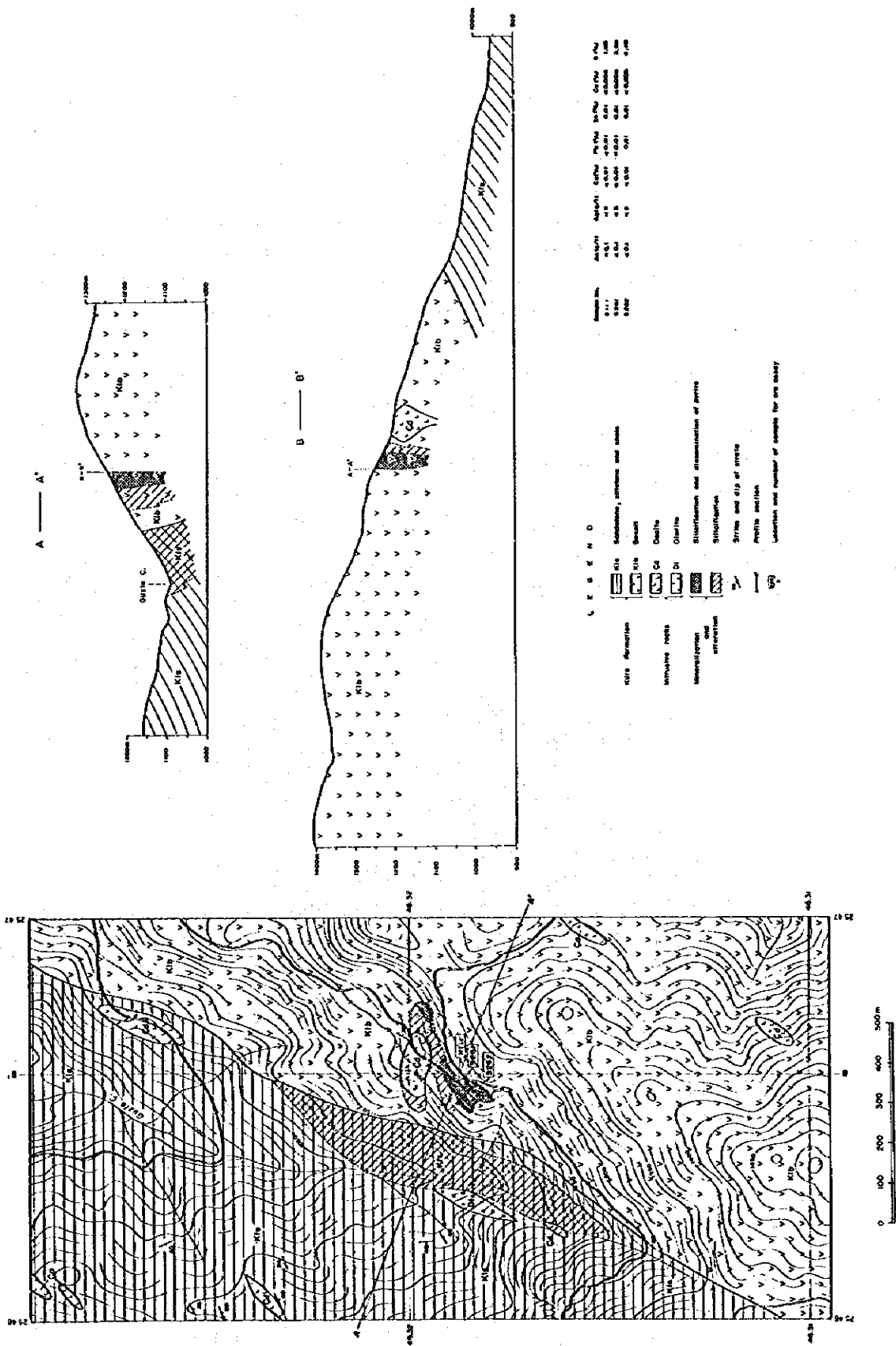


Fig. 4-3 Geologic Map and Cross Section of the Masköy Prospect

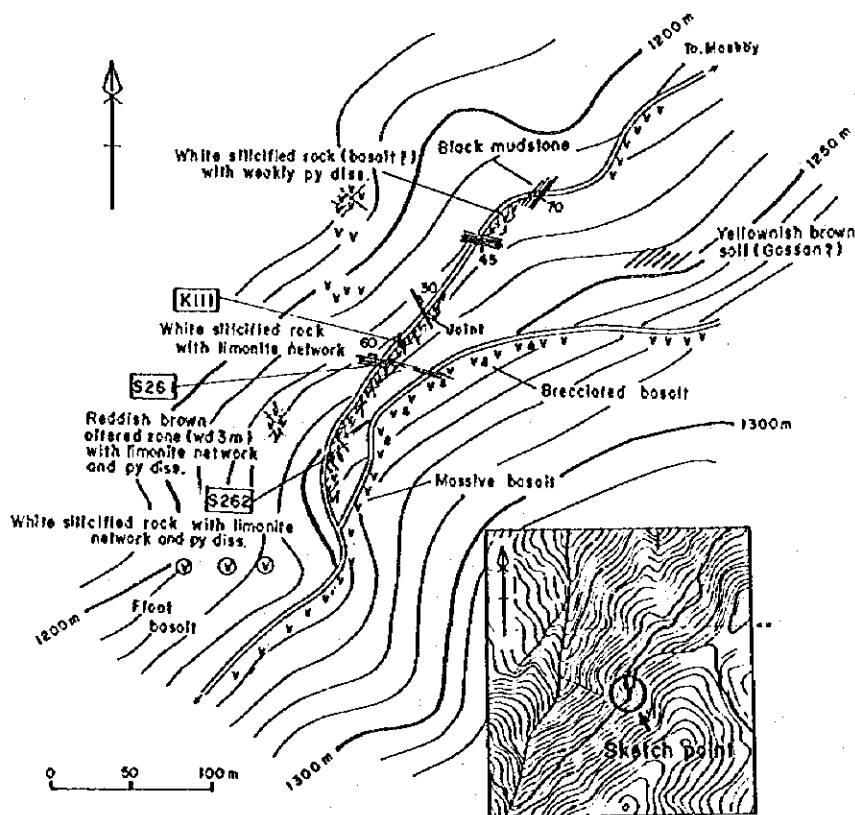
2-3 Discussion

The mineralization is composed of limonite network/veinlet and pyrite dissemination. The host rock of the mineralization is basalt. These features in the Masköy mineralized zone is similar to those of the mineralized zones in the Küre zone

A silicified zone is close by this mineralized zone and dacite further. This silicification, then, may be interpreted to be caused by the dacite intrusion. Any evidences which suggest the intrusion to invite this silicification, however, is not found, as any silicification and/or mineralization is absent around the other dacite bodies in the Dikmendağ zone

We will only give a possibility that this mineralization is similar to the Cyprus-type mineralization, because field data are not enough to discuss it further.

It is recommended for the further exploration that geophysical survey for Küre-type mineralization is essential, following which drilling is necessary to confirm the existence of ore deposits, but the priority order for the supplementary explorations is lower than that in the other mineralized zones, because the superficial extent of the known mineralized zone is considerably small.



Sample No.	Au Gr/T	Ag Gr/T	Cu %	Pb %	Zn %	Co %	S %
K111	<0.1	< 5	< 0.006	<0.01	0.01	<0.006	1.93
S261	<0.1	5	< 0.006	<0.01	0.01	<0.006	43.58
S262	<0.1	< 5	< 0.006	0.01	0.01	<0.006	4.48

Fig. 4-4 Sketch of Mineralized Zone in the Masköy Prospect

**PART 5 PREPARATORY INVESTIGATION
FOR GEOCHEMICAL PROSPECTING**

PART 5 PREPARATORY INVESTIGATION FOR GEOCHEMICAL PROSPECTING

CHAPTER 1 Geochemical Prospecting

1-1 Purpose of investigation

Küre Mine (Cyprus-type massive sulfide mineral deposit) is present in Küre area and basalt is widely distributed around the mineral deposit. The basalt has been studied mainly on major elements of it through chemical analysis as the country rock. However, trace elements of the basalt have hardly been studied.

Therefore, geochemical prospecting was preparatorily executed to extract designated elements related to mineralization from the behavior of trace elements of basalt distributed around mines and use the geochemical prospecting as one of the mineral deposit prospecting techniques. At the same time, botanical geochemical prospecting was executed to study its applicability.

1-2 Investigation area

The following two zones were selected as objective areas of investigation: Küre zone where generally known Küre mineral deposit originates and Dikmendağ zone.

1-3 Samples to be collected

In Küre zone, 121 samples of basalt were collected mainly on Aşıköy and Bak-ibaba ore bodies which are main ore bodies on the ground surface and 33 samples were collected in the gallery every 100 m in principle (every 10 to 50 m in the vicinity of an ore body). Resultingly, the total of 154 samples of rocks were collected. Moreover, to study the applicability of plant

leaves to the geochemical prospecting in this zone, three types of plants which are universally distributed in this zone were selected and 64 samples of plant leaves were collected at the same point as the rock sampling position.

In Dikmendağ zone located approx. 40 km east of Küre zone, 54 samples of rocks were collected mainly in Masköy prospect (33 samples).

Figure 5-1 shows the rock sampling position in Küre zone, Figure 5-2 shows the rock sampling position in Dikmendağ zone (excluding Masköy prospect), and Figure 5-3 shows the rock sampling position in Masköy site, Dikmendağ zones.

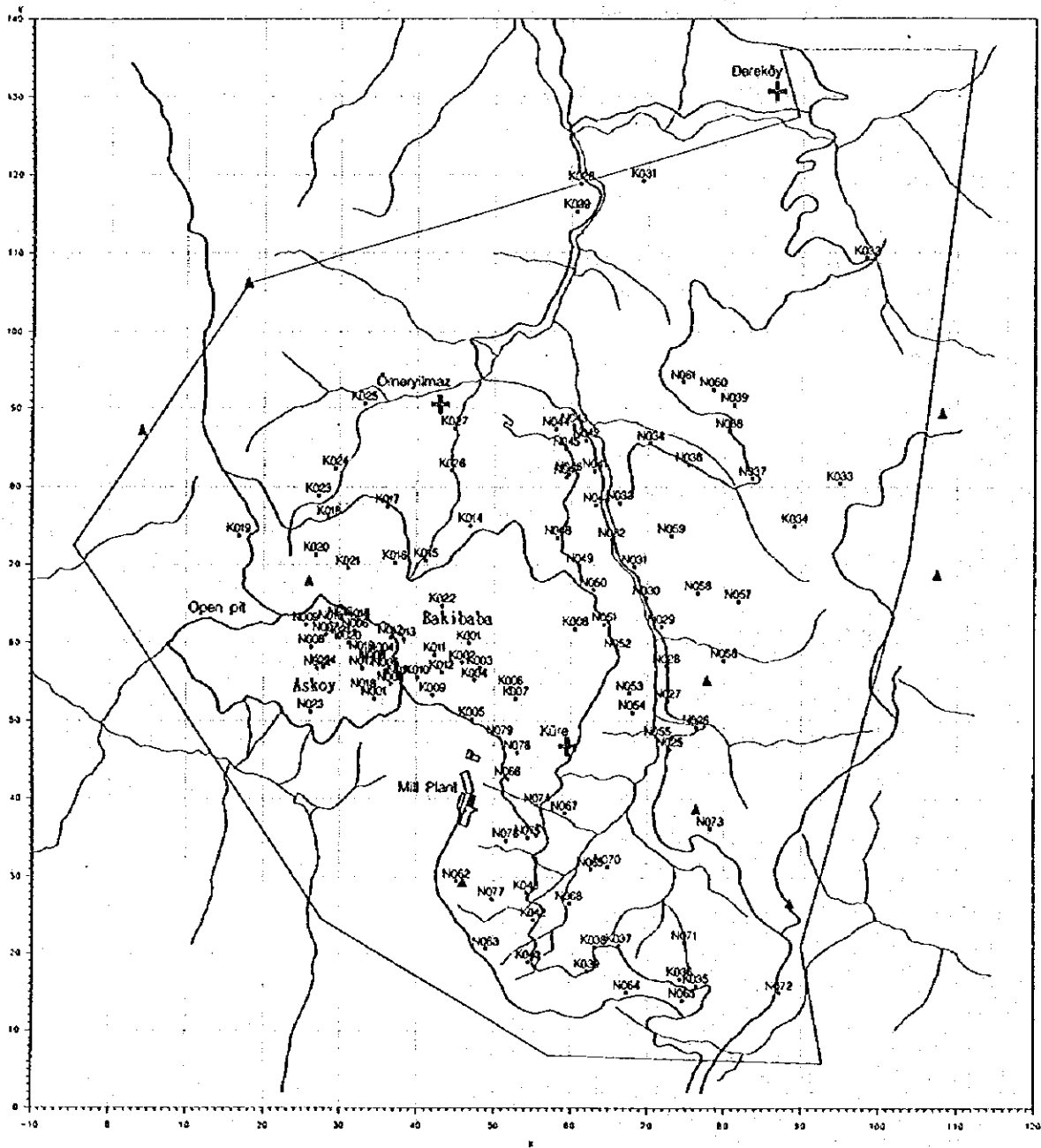


Fig. 5-1 Sampling Points of Rocks in the Küre Zone

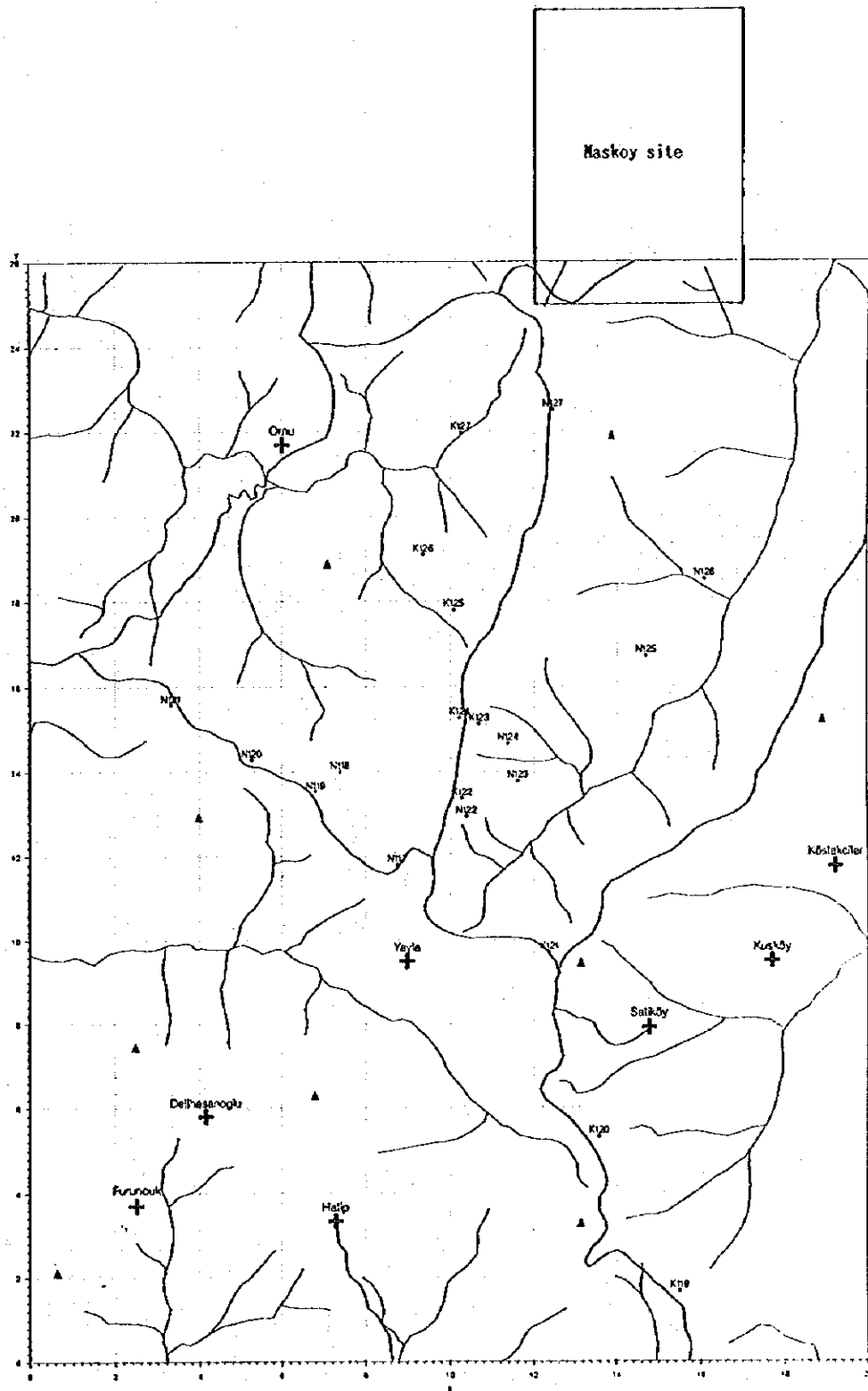


Fig. 5-2 Sampling Points of Rocks in the Dikmendağ Zone

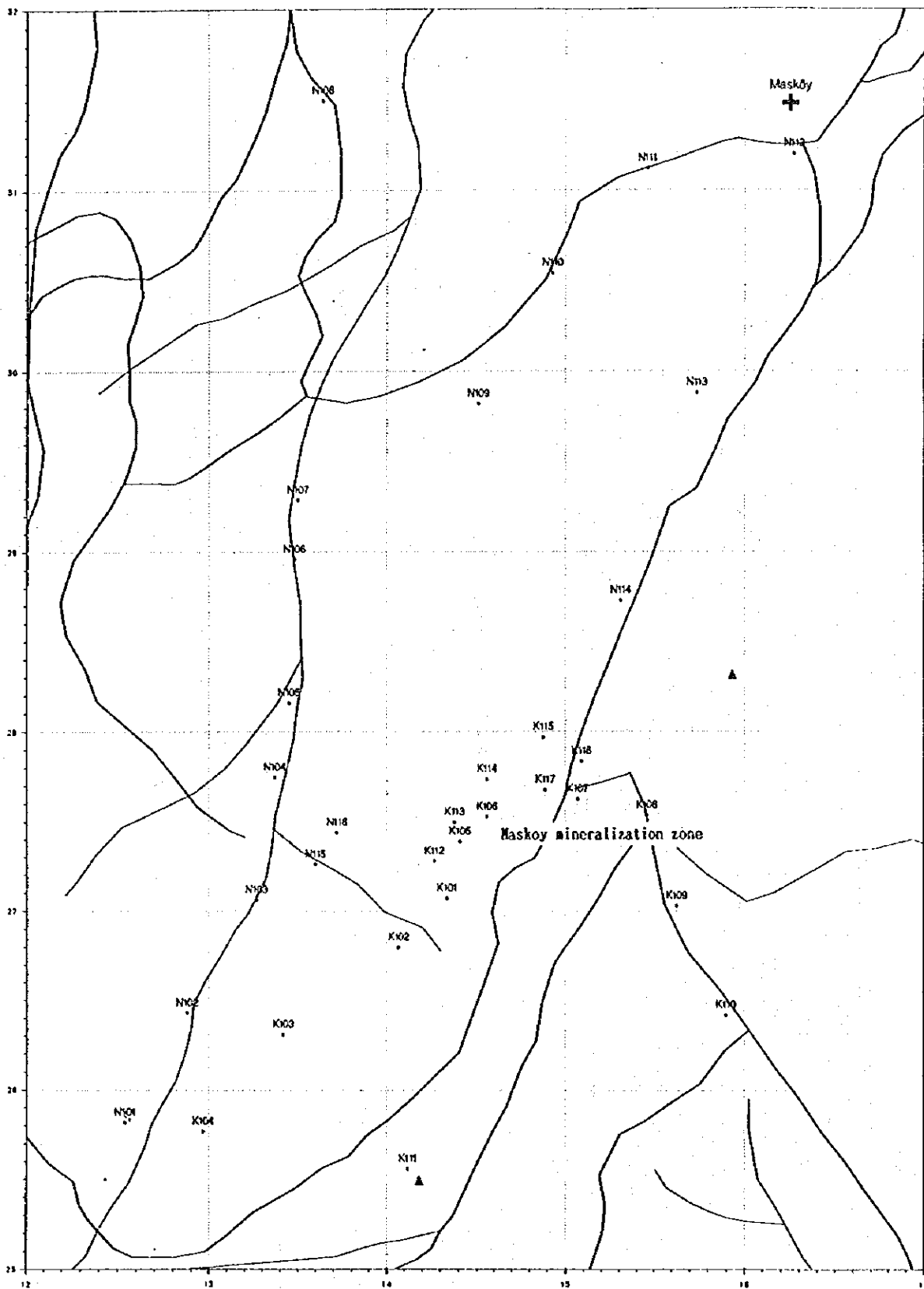


Fig. 5-3 Sampling Points of Rocks in the Masköy Prospect, Dikmendağ Zone

1-4 Chemical analysis

Collected samples were directly sent to Chemex Labs. Ltd. in Canada from the Küre Mine by air and chemical analysis was executed for 33 components. Table 5-1 shows the analysis components, analysis method, and detection limit.

1-5 Study results

Table 5-2 shows the basic statistical calculation results of rocks in Küre zone and Table 5-3 shows the basic statistical calculation results of plants. Moreover, Table 5-4 shows the basic statistical calculation results of rocks in Dikmendağ zone. The above basic statistical results were subdivided for each zone to study them in accordance with a geochemical anomaly map drawn for each element.

(1) Küre Zone

<1> Rocks

As a known ore body comes nearer on the ground surface, the quality of the four elements of Mo, Tl, Co, and Cu showed a high anomaly. This is a natural result because Cu and Co are originally major elements of a mineral deposit.

In particular, however, Mo showed a very high anomaly of +2.5 SIGMA (standard deviation) or more (see Fig. 5-4). Three elements of Na, Ca, and Sr showed a low anomaly near the ore body.

Among samples collected in the gallery most, elements showed a high anomaly of +2.5 SIGMA or more or -2.5 SIGMA or less as Bakibaba ore body comes nearer which is distributed at a place approx. 860 m separate from the mine mouth (see Fig. 5-5).

Regardless of degree, 16 elements showed a high anomaly trend and 7 elements showed a low anomaly.

The same trend as in the gallery was observed on seven elements which showed an anomaly on the ground surface. A remarkable trend was observed particularly on Mo and Sr elements other than major elements of the mineral deposit. It is estimated that Na and Ca showed a low anomaly because they were leached due to mineralization.

<2> Plants

Among three types of plants, only "MESE (sample No.P1) called by the native is distributed in entire Küre zone. Because other two types of plants have a small distribution range, it is difficult to grasp the trend of quality distribution.

Therefore, as the result of studying only MESE, it is found that high anomaly

Table 5-1 Chemical Method and Detection Limit

Rock samples

element	method	detection limit	element	method	detection limit
Ag	AAS	0.2 ppm	Mg	ICP-AES	0.01%
Al	ICP-AES	0.01ppm	Mn	ICP-AES	5 ppm
As	AAS	2 ppm	Mo	ICP-AES	1 ppm
Au	FA-NAA	1 ppb	Na	ICP-AES	0.01%
Ba	ICP-AES	10 ppm	Ni	ICP-AES	1 ppm
Be	ICP-AES	0.5 ppm	P	ICP-AES	10 ppm
Bi	AAS	0.1 ppm	Pb	AAS	2 ppm
Ca	ICP-AES	0.01%	S	LECO	0.001%
Cd	AAS	0.1 ppm	Sb	AAS	0.2 ppm
Co	ICP-AES	1 ppm	Se	AAS	0.2 ppm
Cr	ICP-AES	1 ppm	Sr	ICP-AES	1 ppm
Cu	ICP-AES	1 ppm	Ti	ICP-AES	0.01%
Fe	ICP-AES	0.01%	Tl	AAS	0.1 ppm
Ga	AAS	1 ppm	V	ICP-AES	1 ppm
Hg	AAS	10 ppb	W	ICP-AES	10 ppm
K	ICP-AES	0.01%	Zn	ICP-AES	2 ppm

Plant samples

element	method	detection limit	element	method	detection limit
Ag	ICP-AES	0.10ppm	Mg	ICP-AES	50 ppm
Al	ICP-AES	50 ppm	Mn	ICP-AES	15 ppm
As	ICP-AES	2 ppm	Mo	ICP-AES	0.50ppm
Ba	ICP-AES	5 ppm	Na	ICP-AES	50 ppm
Be	ICP-AES	0.20ppm	Ni	ICP-AES	0.50ppm
Bi	ICP-AES	1.00ppm	P	ICP-AES	5 ppm
Ca	ICP-AES	50 ppm	Pb	ICP-AES	0.50ppm
Cd	ICP-AES	0.20ppm	Sb	ICP-AES	2 ppm
Co	ICP-AES	0.50ppm	Sc	ICP-AES	2 ppm
Cr	ICP-AES	0.5 ppm	Sr	ICP-AES	0.50ppm
Cu	ICP-AES	0.50ppm	Ti	ICP-AES	50 ppm
Fe	ICP-AES	50 ppm	Tl	ICP-AES	5 ppm
Ga	ICP-AES	5 ppm	U	ICP-AES	5 ppm
Hg	ICP-AES	1 ppm	V	ICP-AES	1 ppm
K	ICP-AES	50 ppm	W	ICP-AES	10 ppm
La	ICP-AES	5 ppm	Zn	ICP-AES	2 ppm

Table 5-2 Basic Statics of Rock Data in the Küre Zone

Variable	Label	N	Mean	Std Dev	Minimum	Maximum
LAG	Ag (ppm)	154	-0.9781	0.1771	-1.0000	0.6812
LAL	Al (%)	154	0.8403	0.1622	-0.2366	0.9921
LAS	As (ppm)	154	0.5699	0.4541	0.3010	2.6435
LAU	Au (ppb)	154	0.8763	0.4743	-0.3010	3.6532
LBA	Ba (ppm)	154	1.1501	0.4043	0.6990	2.6335
LBE	Be (ppm)	154	-0.5956	0.0806	-0.6021	0.3979
LBI	Bi (ppm)	154	-1.2595	0.1984	-1.3010	0.2304
LCA	Ca (%)	154	0.3453	0.6414	-1.5229	1.1446
LCD	Cd (ppm)	154	-1.2718	0.2118	-1.3010	0.4150
LCO	Co (ppm)	154	1.5444	0.3659	0.0000	3.5276
LCR	Cr (ppm)	154	2.2054	0.3610	1.1139	3.1430
LCU	Cu (ppm)	154	1.6292	0.6704	-0.3010	4.0000
LFE	Fe (%)	154	0.7951	0.1816	0.2175	1.3979
LGA	Ga (ppm)	154	0.9659	0.1691	-0.3010	1.4314
LHG	Hg (ppb)	154	1.9943	0.5576	1.3010	4.2553
LK	K (%)	154	-0.7562	0.3698	-1.6990	0.3617
LMG	Mg (%)	154	0.5144	0.2839	-0.7959	1.3502
LMN	Mn (ppm)	154	2.8315	0.3519	1.3010	3.4440
LMO	Mo (ppm)	154	-0.1723	0.3001	-0.3010	1.7160
LNA	Na (%)	154	0.2085	0.4879	-1.6990	0.6730
LNI	Ni (ppm)	154	1.7460	0.4149	0.0000	3.2810
LP	P (ppm)	154	2.5529	0.3052	0.6990	3.0899
LPB	Pb (ppm)	154	0.0637	0.2501	0.0000	1.8573
LS	S (%)	154	-1.7704	0.9873	-3.0000	1.6646
LSB	Sb (ppm)	154	-0.6443	0.5584	-1.0000	1.4472
LSE	Se (ppm)	154	-0.8562	0.3423	-1.0000	1.2455
LSR	Sr (ppm)	154	1.7505	0.5114	0.0000	2.4330
LTI	Ti (%)	154	-0.2917	0.2625	-2.0000	0.0531
LTL	Tl (ppm)	154	-0.9484	0.3071	-1.3010	0.0792
LV	V (ppm)	154	2.3336	0.1591	1.3222	2.7427
LW	W (ppm)	154	1.0508	0.2261	0.6990	2.1461
LZN	Zn (ppm)	154	1.7932	0.2919	0.9031	3.1004

Table 5-3 Basic Statics of rock Data in the Dikmendağ Zone

Variable	Label	N	Mean	Std Dev	Minimum	Maximum
LAG	Ag (ppm)	54	-0.9833	0.1229	-1.0000	-0.0969
LAL	Al (%)	54	0.8169	0.2864	-0.4815	1.0107
LAS	As (ppm)	54	0.5888	0.3446	0.3010	1.4150
LAU	Au (ppb)	54	0.5426	0.5223	-0.3010	1.6435
LBA	Ba (ppm)	54	2.4403	0.3744	1.0000	2.9638
LBE	Be (ppm)	54	-0.4506	0.2253	-0.6021	0.1761
LBI	Bi (ppm)	54	-0.9299	0.3896	-1.3010	0.0792
LCA	Ca (%)	54	0.1475	0.5602	-1.0458	1.3979
LCD	Cd (ppm)	54	-1.2843	0.1229	-1.3010	-0.3979
LCO	Co (ppm)	54	0.9869	0.2407	0.0000	1.5315
LCR	Cr (ppm)	54	1.8405	0.4420	0.0000	2.7380
LCU	Cu (ppm)	54	0.9823	0.4393	0.0000	1.8513
LFE	Fe (%)	54	0.3842	0.2305	-0.7447	0.6776
LGA	Ga (ppm)	54	1.0374	0.2915	-0.3010	1.2788
LHG	Hg (ppb)	54	1.8638	0.6111	1.0000	3.6990
LK	K (%)	54	0.1740	0.3578	-1.0458	0.6201
LMG	Mg (%)	54	-0.0126	0.3087	-0.8861	0.5977
LMN	Mn (ppm)	54	2.5944	0.2815	1.6990	3.0453
LMO	Mo (ppm)	54	-0.2230	0.1454	-0.3010	0.3010
LNA	Na (%)	54	0.1948	0.3916	-1.1549	0.6484
LNI	Ni (ppm)	54	1.1726	0.3964	0.3010	2.0253
LP	P (ppm)	54	2.6569	0.1970	1.8451	2.8808
LPB	Pb (ppm)	54	1.2880	0.3053	0.6021	1.9731
LS	S (%)	54	-2.0377	1.1020	-3.0000	0.4814
LSB	Sb (ppm)	54	-0.6059	0.5226	-1.0000	0.7782
LSE	Se (ppm)	54	-0.9331	0.1392	-1.0000	-0.3979
LSR	Sr (ppm)	54	2.0489	0.3324	1.3617	2.9335
LTl	Tl (%)	54	-0.6706	0.3187	-2.0000	-0.3468
LTL	Ti (ppm)	54	-0.3905	0.2578	-1.0000	0.6990
LV	V (ppm)	54	1.6913	0.2519	1.1761	2.2480
LW	W (ppm)	54	0.7213	0.0796	0.6990	1.0000
LZN	Zn (ppm)	54	1.7075	0.2668	0.7782	2.1461

Table 5-4 Basic Statics of Plant Data in the Küre Zone

Variable	Label	N	Mean	Std Dev	Minimum	Maximum
LAG	Ag (ppm)	64	-1.2587	0.1183	-1.3010	-0.6990
LAL	Al (ppm)	64	2.1404	0.2895	1.6990	3.0212
LAS	As (ppm)	64	0.0000	0.0000	0.0000	0.0000
LBA	Ba (ppm)	64	1.0416	0.5222	0.3979	2.1761
LBE	Be (ppm)	64	-1.0000	0.0000	-1.0000	-1.0000
LBI	Bi (ppm)	64	-0.2963	0.0376	-0.3010	0.0000
LCA	Ca (ppm)	64	3.9416	0.0892	3.7324	4.1523
LCD	Cd (ppm)	64	-1.0000	0.0000	-1.0000	-1.0000
LCO	Co (ppm)	64	-0.1518	0.3116	-0.6021	0.9294
LCR	Cr (ppm)	64	0.4959	0.3401	-0.6021	1.2553
LCU	Cu (ppm)	64	1.2929	0.5009	0.5441	2.5911
LFE	Fe (ppm)	64	2.2892	0.2533	2.0000	3.2041
LGA	Ga (ppm)	64	0.3979	0.0000	0.3979	0.3979
LHG	Hg (ppm)	64	-0.2963	0.0376	-0.3010	0.0000
LK	K (ppm)	64	3.8033	0.0772	3.6435	3.9868
LLA	La (ppm)	64	0.3979	0.0000	0.3979	0.3979
LMG	Mg (ppm)	64	3.4145	0.1926	3.0414	3.8976
LMN	Mn (ppm)	64	2.7623	0.2685	2.1614	3.3222
LMO	Mo (ppm)	64	-0.5879	0.0641	-0.6021	-0.3010
LNA	Na (ppm)	64	1.6158	0.2530	1.3979	2.9031
LNI	Ni (ppm)	64	0.4022	0.4304	-0.6021	1.0414
LP	P (ppm)	64	3.1127	0.1443	2.8513	3.5340
LPB	Pb (ppm)	64	-0.2465	0.1590	-0.3010	0.4771
LSB	Sb (ppm)	64	0.0047	0.0376	0.0000	0.3010
LSC	Sc (ppm)	64	-0.3010	0.0000	-0.3010	-0.3010
LSR	Sr (ppm)	64	1.0802	0.1730	0.6990	1.4472
LTI	Ti (ppm)	64	1.4026	0.0376	1.3979	1.6990
LTL	Tl (ppm)	64	0.3979	0.0000	0.3979	0.3979
LU	U (ppm)	64	0.4356	0.1003	0.3979	0.6990
LV	V (ppm)	64	-0.2289	0.2191	-0.6021	0.6021
LW	W (ppm)	64	0.3979	0.0000	0.3979	0.3979
LZN	Zn (ppm)	64	1.2884	0.1076	1.0607	1.5315

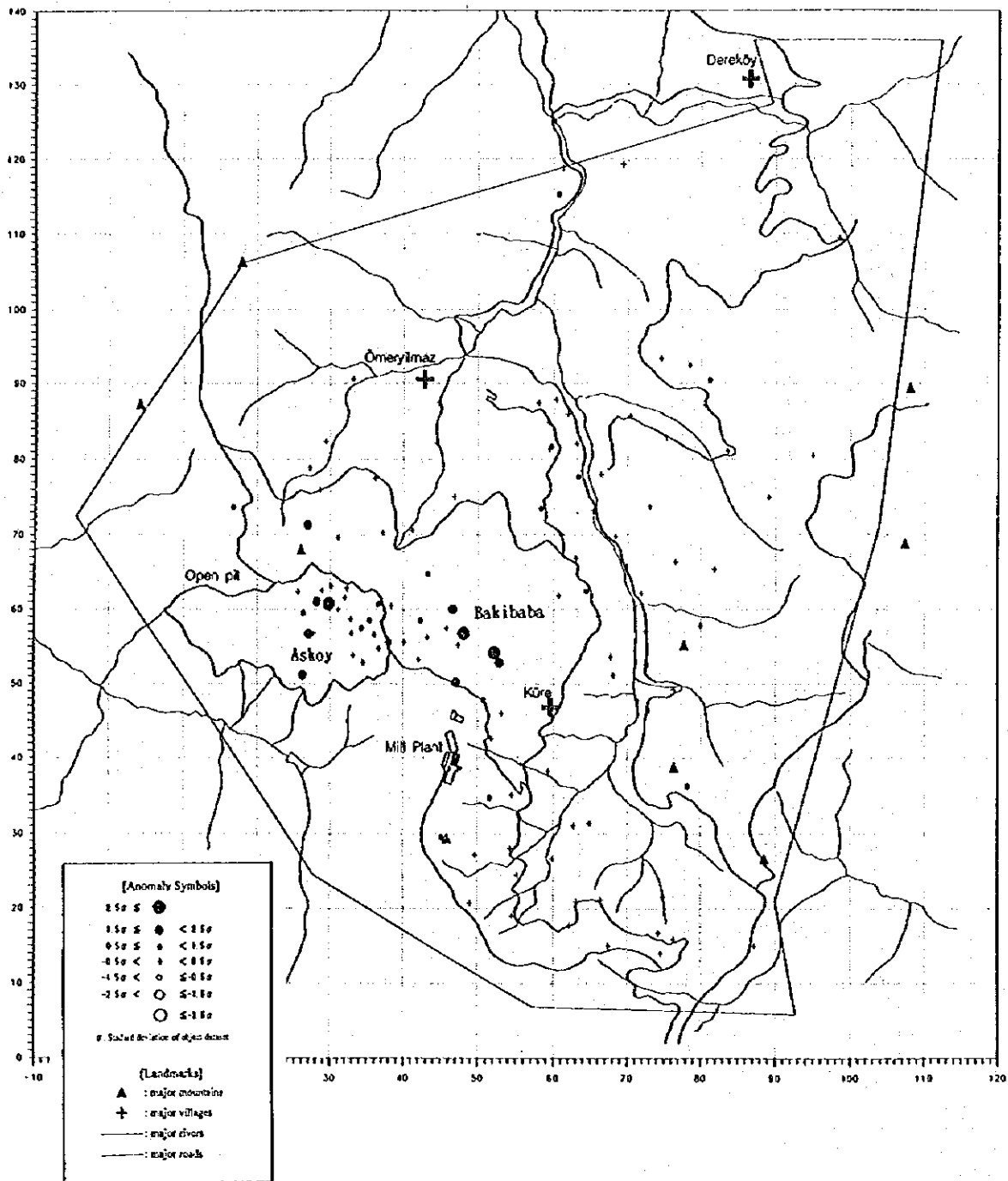


Fig. 5-4 Geochemical Anomaly Map of Rock Data in the Küre Zone (Mo)

area of Cu and Co directly related to a mineral deposit particularly harmonizes with the origination area of the known mineral deposit (see Fig. 5-6).

Eight other elements of P, Ni, Na, Mo, Ag, Cr, Mn, and Zn also showed a high anomaly in the vicinity of the mineral deposit and V showed a low anomaly.

(2) Dikmendağ Zone

In this zone, rocks were sampled throughout the zone mainly in Masköy site.

As a result, a high anomaly was recognized on the three elements of Se, S, and Hg mainly at a place where an ore sign was observed particularly in Masköy site (see Fig. 5-7). On the contrary, however, a low anomaly was recognized on Be and Sr (see Figs. 5-8 and 5-9).

In the case of Be, it is characteristic that the anomaly is clearly different in the northwest and southeast of the site.

1-6 Consideration

In the case of Küre zone, it is considered that geochemical contamination widely expands on the ground surface due to waste water and dust discharged from a sedimentation pond and a processing plant because Küre Mine which is a operating mine is present particularly in Küre zone. This can be explained with the fact that only seven elements showed a geochemical anomaly on the ground surface though most elements showed an anomaly in the gallery as an ore body comes nearer.

Moreover, the geochemical prospecting using Cu as a designated element can also be applied to plants because MESE is universally distributed in this zone and a geochemical anomaly is recognized on Cu directly related to a mineral deposit.

As the result of principal component analysis performed simultaneously with the above study, it is estimated that a factor positively controlling the first principal component relates to mineralization and a factor negatively controlling the first principal component is due to rock-forming minerals of basalt particularly on the rocks sampled in Küre zone (Table 5-5).

Cu and Co which are major ore elements of Küre mineral deposit are positively controlled by the sixth principal component and negatively controlled by the second principal component. However, the contribution rate is low as a whole. This can also be explained as the fact that ore bodies of Küre mineral deposit were supplied by melange and only slightly related to the basalt around the mineral deposit.

As described above, judging from the geochemical prospecting of this area, it is possible to apply the botanical geochemical prospecting by using Cu as an object element. Also for basalt, because seven elements showing a geochemical anomaly on the ground surface also showed an anomaly in the gallery (Küre zone),

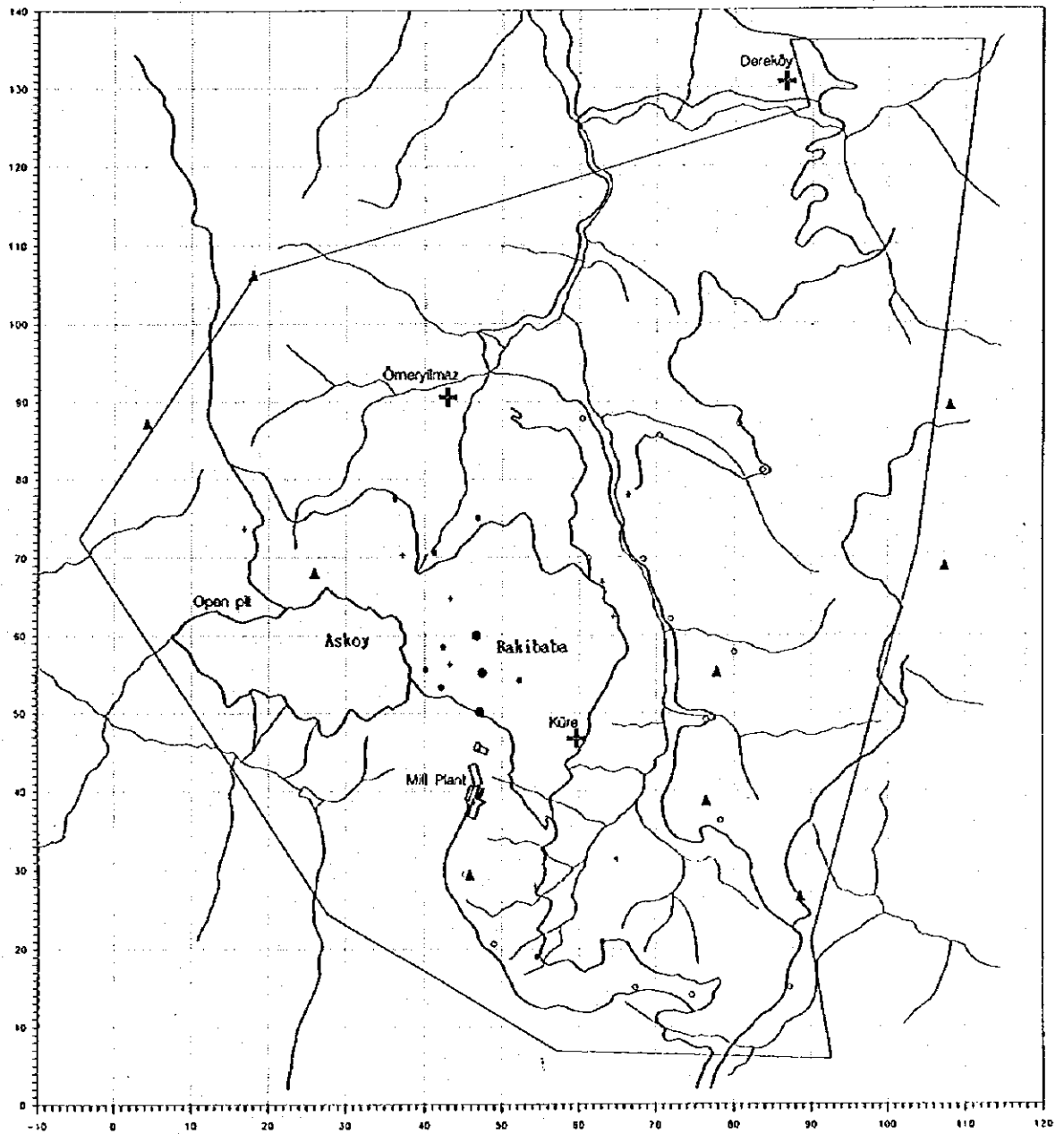


Fig. 5-6 Geochemical Anomaly Map of Plant Data in the Küre Zone (Cu)

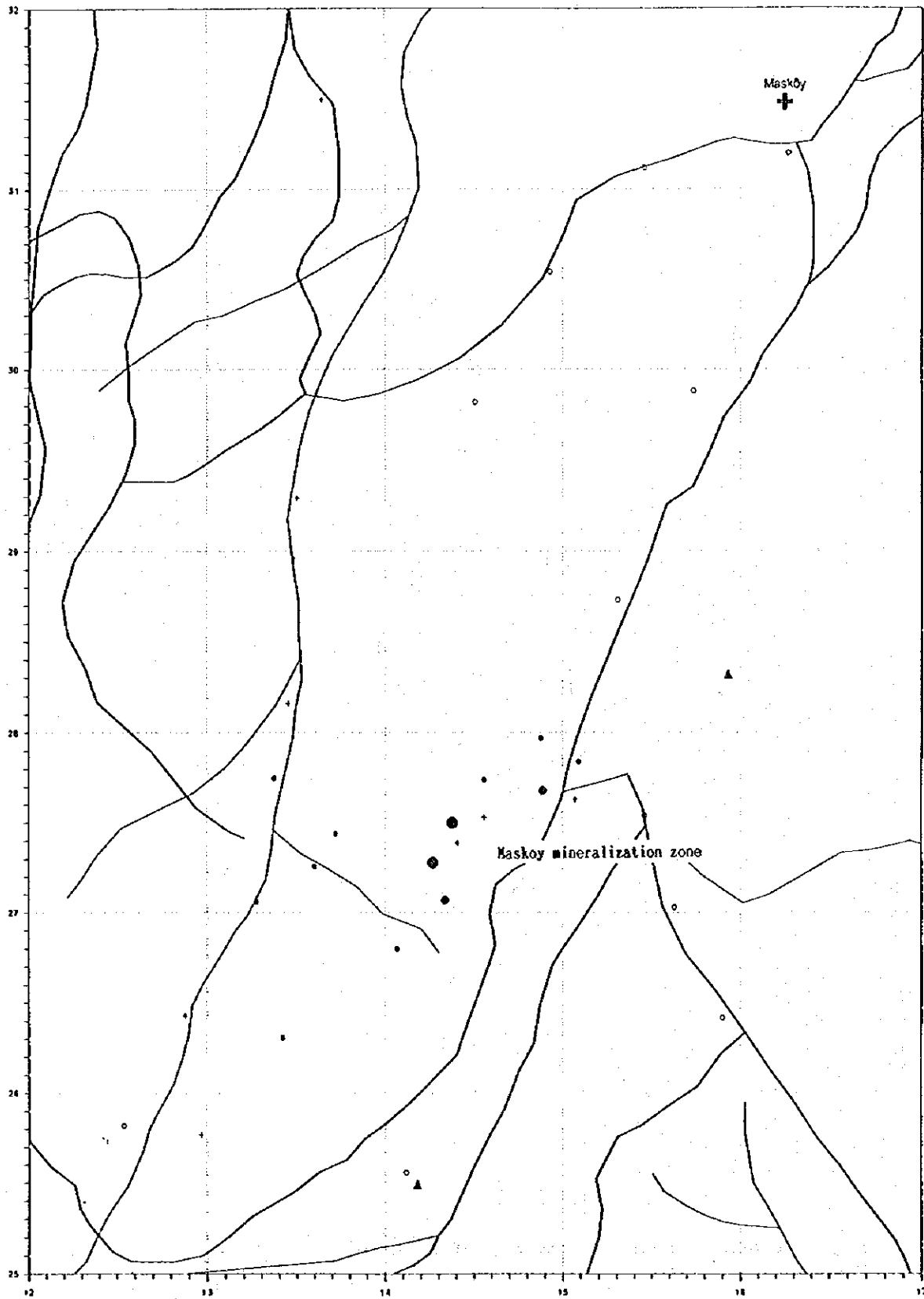


Fig. 5-7 Geochemical Anomaly Map of Rock data in the Masköy Prospect, Dikmendağ Zone (Hg)

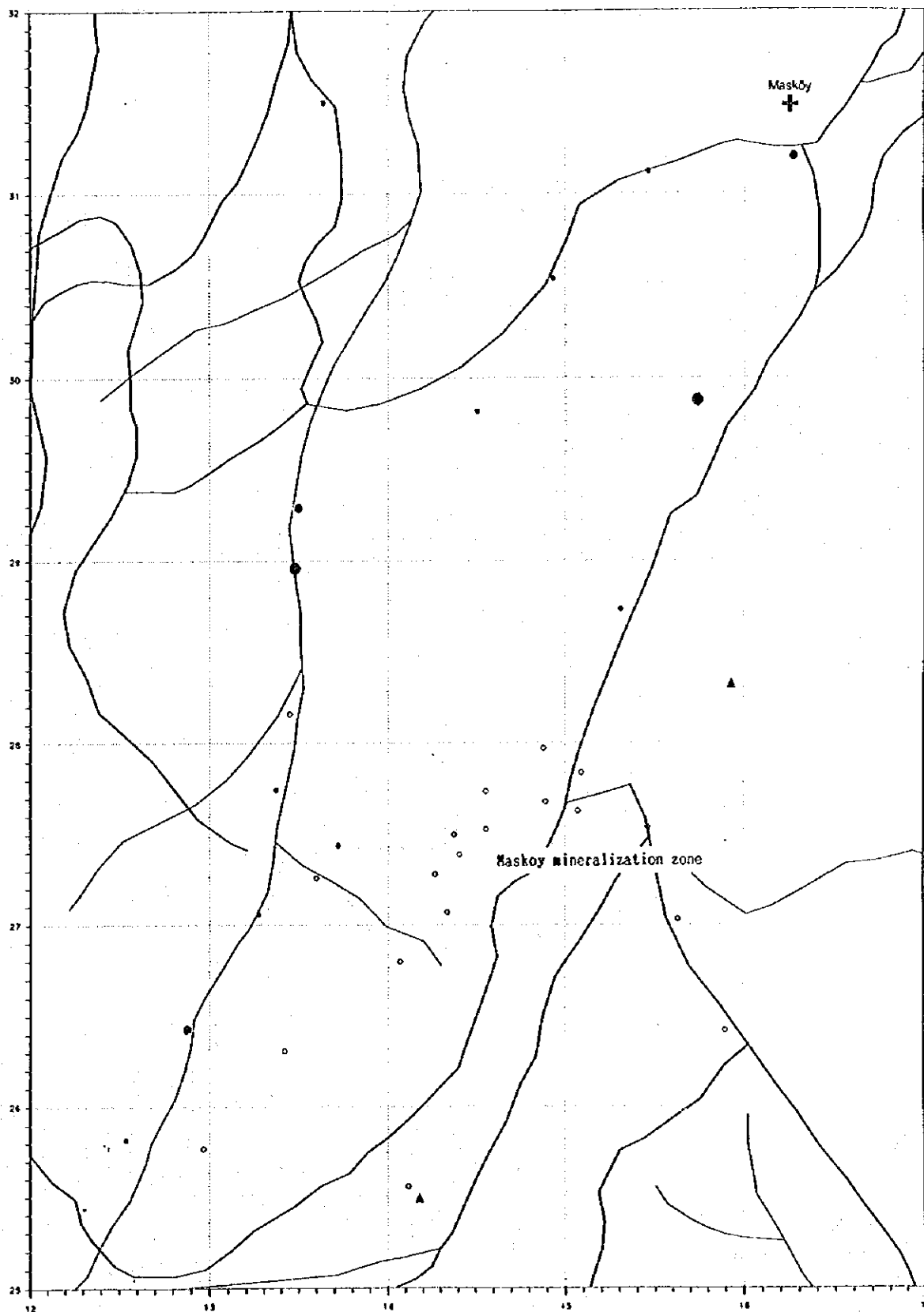


Fig. 5-8 Geochemical Anomaly Map of Rock data in the Masköy Prospect, Dikmendağ Zone (Be)

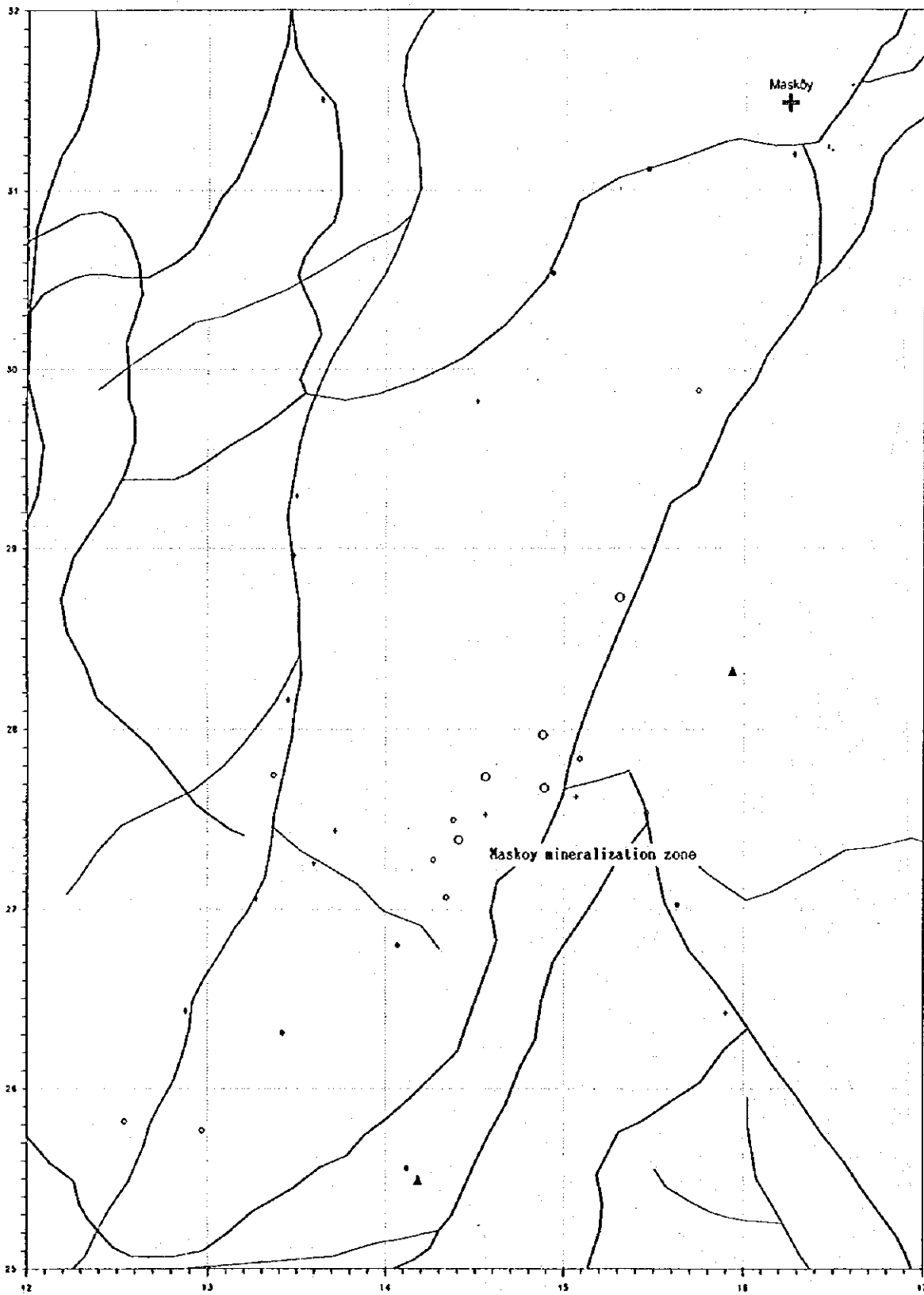


Fig. 5-9 Geochemical Anomaly Map of Rock data in the Masköy Prospect,
Dikmendağ Zone (Sr)

Table 5-5 Principal Components Loading Pattern of Rock Data
in the Kure Zone

Top-PC	Element	PC-1	PC-2	PC-3	PC-4	PC-5	PC-6	PC-7	PC-8	PC-9
1	Bi	0.85506	0.22409	0.13381	0.06310	-0.06532	0.23763	-0.10220	-0.08607	0.18730
1	Mg	0.84696	-0.04203	-0.13362	0.07396	0.03151	0.13591	-0.11265	-0.03805	0.13594
1	Ag	0.79016	0.13395	0.16155	-0.08859	0.13024	0.24329	-0.12399	0.19071	0.15950
1	Se	0.67923	0.15109	0.04392	-0.07465	0.09883	0.39858	0.19303	0.19767	-0.04290
1	Pb	0.58063	0.25212	0.32895	0.20163	-0.23949	0.00157	-0.27007	-0.20136	0.03244
1	Au	0.55527	0.11265	-0.04136	-0.10262	0.00203	0.32818	0.04867	0.44349	0.21655
1	Cd	0.55084	-0.23940	0.14715	0.31849	0.15716	-0.29198	-0.29404	0.20335	-0.18182
1	P	-0.53157	0.36537	-0.26844	0.39057	0.16959	0.19043	-0.18672	-0.25234	0.17796
1	V	-0.58339	-0.07488	-0.52139	0.27281	0.06821	0.15323	-0.01066	0.08038	0.03208
1	Ti	-0.59890	0.16085	-0.54343	0.42473	0.09055	0.15119	-0.01799	-0.09799	0.08841
1	Sr	-0.66124	0.42287	0.38578	0.06897	0.18067	0.16002	-0.00846	0.12687	0.19911
1	Ca	-0.66472	0.03832	0.48782	0.02870	0.38567	0.15532	-0.04750	-0.01486	0.13305
1	Mn	-0.73125	-0.24932	0.31405	0.22175	0.22822	0.14691	-0.12198	-0.00673	-0.01160
1	Na	-0.73164	0.35636	0.28023	0.10056	0.28487	-0.08102	-0.08286	0.13753	0.01123
1	Al	-0.79221	0.00099	-0.21952	0.28134	-0.16736	-0.08987	0.05621	0.15158	-0.06126
2	Hg	0.42490	0.53297	-0.10520	0.20107	0.16027	-0.25450	0.41947	0.14479	-0.15842
2	Sb	0.32470	0.52079	0.00553	0.19559	0.08336	-0.35621	0.28180	0.12597	0.18359
2	Co	0.27973	-0.71237	-0.10017	0.25167	-0.05343	-0.18681	-0.17855	0.28676	0.04879
2	Mg	-0.46392	-0.75395	0.00651	-0.02916	-0.09998	-0.07580	0.06435	0.17755	-0.05916
2	Ni	-0.20166	-0.76445	0.32385	0.07907	-0.11085	-0.03831	0.32083	-0.06418	0.19364
3	Tl	0.10191	-0.02391	0.54770	0.23704	-0.10512	0.02776	-0.13991	-0.19746	-0.24678
3	Ba	-0.20540	0.37920	0.39216	0.37776	-0.39175	0.08829	0.21057	0.23244	0.04100
3	Fe	0.54718	-0.40101	-0.60005	0.24713	-0.09034	0.02593	-0.07807	0.02636	0.08452
3	Ga	-0.36473	0.26589	-0.63498	0.06635	-0.34782	0.17712	0.21561	0.00339	0.00680
4	Zn	0.24536	-0.43118	0.18857	0.65838	0.07063	-0.17119	-0.01212	0.04349	-0.17026
4	S	0.36623	0.07136	-0.02639	0.47586	0.34884	-0.02145	0.09158	-0.04713	-0.26951
5	Be	0.06960	0.22493	0.20255	0.30905	-0.63970	0.03770	-0.18164	-0.28937	0.10121
6	Cu	0.44053	-0.23283	0.05470	0.41596	0.12019	0.45633	0.39082	-0.13666	-0.16075
6	As	0.45369	0.43144	-0.02038	0.21458	0.11860	-0.48042	0.20784	-0.21685	0.04008
7	Cr	-0.03041	-0.52056	0.34472	-0.01348	-0.06518	-0.02700	0.68506	-0.23144	0.27737
8	K	-0.35579	0.25379	0.28820	0.30230	-0.43341	-0.09047	-0.03028	0.44460	0.00515
9	W	0.28773	-0.26391	-0.10740	0.37186	0.18577	-0.29616	-0.14180	0.00522	0.57441

the geochemical prospecting can be applied to these elements. Also in Dikmendağ zone, it is necessary to notice Sr which showed a geochemical anomaly same as in Küre zone.

PART 6 CONCLUSIONS AND RECOMMENDATIONS

PART 6 CONCLUSIONS AND RECOMMENDATIONS

CHAPTER 1 CONCLUSIONS

1-1 Küre Zone

In the first phase survey, the conducted works were; compilation of available geological and geophysical information, geological survey, and geophysical survey comprising CSAMT and IP.

In the second phase, four holes totaling 1,003.55m in length were drilled in the promising areas of the Küre zone, which were delineated by the geological and geophysical surveys during the previous year. Also two holes were electrically logged.

In the third phase, drilling exploration comprising four holes totaling 953.70m in length continued.

Following conclusions are obtained as the results of the above works.

(1) The geology of the zone consists of pre-Jurassic ultramafic rocks, Jurassic basalt, sedimentary rocks of the Küre Formation, grayish white fossiliferous limestone of the Lower Cretaceous Karadana Formation, pale brown and white marl of the Upper Cretaceous Çağlayan Formation, talus deposits and intrusive diorite and dacite.

(2) The major part of the zone is occupied by the Jurassic Küre Formation. The basalt is composed of pillow lava, hyaloclastite, and massive basalt. Sedimentary facies of the Küre Formation is composed of angularly fragmented greywacke and tectonically sheared/argillized black shale. The matrix consists of pelitic materials.

Basalt and brecciated sediments of the Küre Formation are interpreted as a constituent of melange. The period of melange formation is inferred to be Middle Jurassic, since intrusion into the melange is inferred to be Later Dogger epoch.

(3) The geologic structure of this zone is characterized by many faults. They are divided into two systems; N-S and E-W. The former system is crosscut by the latter. With the exception of the diorite and dacite intrusive bodies and the Karadana Formation, the boundaries of all geologic units, including ultramafic bodies, have been dislocated. The surface elongation of the intrusive bodies is harmonious with the strike of the faults in the vicinity and with the boundary between sediments and basalt of the Küre Formation.

Basalt is distributed extending to N-S and NNW-SSE direction with imbricate structure.

(4) The known ore deposits are the Cyprus-type deposits. The new ore deposits of the same type are expected to occur in the zone. They occur at the boundary between hyaloclastite and black shale of the Küre Formation and also within hyaloclastite. They consist of massive ore, brecciated ore, network ore and disseminated ore.

(5) Ore deposits together with footwall mineralized zone and hanging-wall pelitic rock are considered to be dislocated by the tectonic movements.

(6) Drilling in this study resulted in locating a massive ore with the drilled length 75 cm long and 4% Cu grade at the area to the southwest of the Bakibaba Deposit. The location and depth of ore correspond a weakly low resistivity zone defined by CSAMT. The characteristic of ore is similar to that of the known ore deposits. The potential of the Cyprus-type was confirmed by the drilling.

(7) A low resistivity zone obtained at the north of Bakibaba Deposit by CSAMT consists of basalt. Veinlets composed mainly of pyrite were observed in this zone. The lithology and mineralization of this hole are considered not to cause this low resistivity. Argillization similar to that observed in the above mentioned drill hole occurs in this hole. Thus, the area in the vicinity of this hole is promising for the future exploration.

(8) Drilling at the northern extension of Zemberekler mineralized zone results in finding a mineralized zone. The zone which is located in the N-S and NNW-SSE extensions from the Zemberekler mineralized zone with low resistivity anomalies, are promising for future exploration.

(9) In the low resistivity zone to the south of Aşıköy Deposit, it was anticipated that massive orebodies would occur in the shallow parts due to displacement by a fault. The results of the survey in the second and this phase indicate that this low resistivity zone represents pelitic rocks and fault fractured zone. Therefore, it is considered that the possibility of the existence of massive orebodies of the scale of Aşıköy is low. The existence of massive orebodies expected to occur in the deep parts could not examine due to the shortness of the drilling length.

(10) Limonite network and dissemination are widely developed near the Bakibaba Deposit. The past exploration of this area covered only a limited location and depth. An aggressive exploration covering a wide area is necessary.

(11) The massive deposit confirmed at the south of Bakibaba Deposit is accompanied by a silicified zone. Noting this characteristic, the silicified zones of Mt. Bakibaba to the north of Bakibaba Deposit and Mt. Karacakaya between the Bakibaba and Kizilsu Deposits will be targets for exploration.

(12) Vein network and dissemination occur over the orebody at Bakibaba Deposit. Overturned structure is inferred in the surrounding area. The main orebody of Kizilsu Deposit is believed to be the vein network in the footwall side of the orebody.

On the basis of the above evidence, it is concluded that the gossan which is exposed between Bakibaba and Kizilsu Deposits is most probably the altered products in the footwall side of the mineralized zone.

(13) On the basis of the results of drilling survey done in the past two years, the low resistivity anomalies by CSAMT are considered to indicate zones dominated by pelitic rocks and/or fractured zones aside from some ore deposits. From the results of physical properties measurement in the first and third phase, it has been proved that massive ore, sulfide network, black shale and some sandstone cause low resistivity anomalies. Therefore, the suitable method for the exploration in this zone is the IP survey. As the size of known massive orebodies is small except Aşiköy Deposit, it is necessary to conduct such IP survey that has the line and station allocation of short distances.

1-2 Taşköprü Zone

In the first phase survey, the conducted works were; compilation of available geological and geophysical information, and geological survey.

In fiscal 1993, geophysical survey (IP, 21 line-km) was carried out at Cünür and Cozoğlu of the Taşköprü zone since these were concluded to be promising by geological survey during the first year.

Following conclusions are obtained as the results of the above works.

(1) The geology of the zone consists of Devrekani metamorphics, Çangal meta-ophiolite, Kayadibi Formation, Muzrup Formation, Kızacik Formation, Alaçam Formation and Çayköy Formation in ascending order.

(2) Mineralization occurs in Cozoğlu, Cünür, Alayürek, Boyalı, Musabozarmut, Sey Yayla, Kepez and East of Cünür.

(3) The geology around the Cünür prospect is the Çangal meta-ophiolite consisting of pelitic schist, massive basalt, and green schist. The mineralized

zone in this prospect is composed of eight lenses and bedded gossans in green schist. The gossans consist of quartz-limonite-pyrite network and limonite dissemination in the silicified and argillized parts of mafic rocks.

The results of time-domain IP survey show that resistivities of the zone extended below gossans are similar to those of the surrounding non-mineralized zone, and chargeabilities are lower than those of the surrounding silicified zones. The size of mineralized zones expected to occur below gossans is estimated to be small.

Blind mineralized zones may not be expected below the extensively silicified zone which occurs around gossans, because chargeabilities of the zones below silicified zone are similar to those of surface outcrops.

High chargeability anomalies are identified at the southern margin of the zone. These anomalies are located adjoining to the silicified zone. The shape on cross sections, chargeabilities, resistivities of these anomalies and geology suggest that these anomalies may indicate the existence of disseminated sulphide minerals.

(4) The geology around Cozoğlu prospect is composed mainly of the Çangal meta-ophiolite, the Kızacik Formation, and the Alaçam Formation. The meta-ophiolite consists of pelitic schist, massive metabasalt and green schist. The Kızacik Formation consists of grayish white limestone and the Alaçam Formation of quartz arenite and black mudstone.

There are two openings of old adits, a large amount of slag and waste dumps on the surface. They are distributed in the Çangal meta-ophiolite.

The mineralized zone observed in outcrops in this prospect is only a weak dissemination of pyrite.

The results of geophysical survey in the second phase show that high chargeability anomalies are distributed from the above zones which are covered by slags and waste dumps to the eastern part of this prospect. The shape of these anomalies on cross sections and the geology may indicate that bedded cupriferous pyrite deposits probably occur within these zones.

The other high chargeability anomalies having similar values to the above mentioned anomalies are identified in the southern margin of the prospect, where is covered by the Çangal meta-ophiolite. It is considered that bedded cupriferous deposits may occur in these anomalous zones.

1-3 Dikmendağ Zone

In the first phase survey, the conducted works were; compilation of available geological and geophysical information, and geological survey.

Following conclusions are obtained as the results of the above works.

(1) The geology of the zone consists of Küre Formation of Lias, Köstekciler Formation of Lower Cretaceous, Satıköy Formation of Upper Cretaceous and, intrusive dacite and diorite.

(2) Masköy mineralized zone is located in the northeastern part of the zone. Aside from this zone, pyrite dissemination in basalt occurs in the north of Furuncuk village and around Ornu village. Slag is also distributed 1 km south and 1.6 km southeast of Ornu, and 1 km south of Furuncuk.

(3) The size of pyrite dissemination is small except of Masköy mineralized zone. The order of priority for the future exploration in these mineralized locations is lower than that of Masköy prospect.

(4) Masköy mineralized zone consists of limonite network and pyrite dissemination over an area of 300x50m. The host rock is basalt and it is silicified to dark gray in the pyrite disseminated part of the zone. Dacite occurs in the vicinity, but it is fresh without evidences of alteration. There is not enough geological data to discuss whether this mineralization is Cyprus-type because surface manifestation of the mineralization is weak.

CHAPTER 2 RECOMMENDATIONS FOR THE FUTURE EXPLORATION

2-1 Küre Zone

It is recommended that drilling exploration should be carried out in the following localities for the purpose of clarifying the conditions of subsurface copper mineralization.

(1) Detailed drilling survey in the vicinity of MJTK-8, the south and the north of Bakibaba Deposit

(2) An area between Bakibaba and Kızılsu Deposits

(3) An area from the east of Bakibaba Deposit to Zemberekler mineralized zone

IP survey is recommended to carry out over the low resistivity zones by CSAMT, where have not been explored by drilling in this study.

2-2 Taşköprü Zone

In Cozoğlu prospect, it is recommended that drilling works should be carried out in the geophysical anomalies which are identified in the east of the locali-

ties where are occupied by slags for the purpose of clarifying the conditions of subsurface copper mineralization.

2-3 Dikmendağ Zone

It is considered that geophysical prospecting is necessary for Masköy prospect for the future exploration, but the order of priority for the work is lower than that for above mentioned two zones because the surface manifestation of the mineralization is small.

REFERENCES

REFERENCE

Geology

- Balley, E.H., Barnes, J.W. and Kupfer, D.H. (1986): Geology and Ore Deposits of the Küre District, Kastamonu Province, Turkey.
- Cas, R.A.F. (1992): Submarine Volcanism: Eruption Style, Products, and Relevance to Understanding the Host-Rock Successions to Volcanic-Hosted Massive Sulfide. *Mining Geology*, v. 87, p. 511-541
- Etibank (1990): Küre ve Civarındaki Bakır Zuhurlarında Yapılan Çalışmalar Hakkında Rapor (unpublished in Turkish).
- Ichige, Y., Furuno, M., Sakimoto, T. and Sowanaka, M. (1991): Exploration of the El Roble Mine and its Vicinity, Republic of Colombia, *Mining Geology*, 41, 77-93 (in Japanese).
- Ichige, Y., Furuno, M., Hori, M. and Sowanaka, M. (1992): Application of stable Isotope and Minor Elements Analyses to the Exploration of Massive Sulfide Deposits.-An Example in and around the El Roble Mine, Republic of Colombia.-, *Mining Geology*, 42, 101-117 (in Japanese).
- Iwasaki, M. (1972): Some Problems on the Ophiolite Suite in Relation to its Lithologic Sequence, Special Issue of *Mining Geology* (in Japanese).
- Kosaka, H. and Kubota, Y. (1973): Lithogeochemical Study on the Diabase of the Shimokawa Mine, Hokkaido, *Mining Geology*, 23, 153-161 (in Japanese).
- Kosaka, H. (1975): Geochemical Characteristics of the Shimokawa Diabase Sheets, Hokkaido, *Mining Geology*, 25, 161-174 (in Japanese).
- Küre Bakırlı Pirit İşletmesi Müessesesi (1988), Etibank Bülteni, Sayı 112- 113, Sa 47-57
- Miyake, T. (1965): Texture of the Ore Minerals from the Shimokawa Mine, *Mining Geology*, 15, 120-129 (in Japanese).
- Miyake, T. (1965): On Spilitic Rocks of the Shimokawa Mine and their Genetical Relations to the Ore Deposits, *Mining Geology*, 15, 1-11 (in Japanese).
- MTA (1962): Geology of the Sinop District, quadrangle series, scale 1:500,000.
- Nielsen, H. (1979): Sulfur Isotopes, Lectures in Isotope Geology, Edited by E. Jäger and J.C. HUNZIKER, Springer-Verlag, p. 283-312.
- Sawkins, F.J. (1984): Metal Deposits in Relation to Plate Tectonics, Springer-Verlag, p. 143-151.
- Searle, D.L. (1972): Mode of Occurrence of the Cupriferous Pyrite Deposits of Cyprus. *Inst. Mining Metallurgy Trans.* 81, B189-B197

Takashima, K. (1977): Copper-Zinc-Lead Deposits of Turkey, Chishitu News, No.275, p.45-57 (in Japanese).

Ünsal, A. and Kafadar, S. (1990): Copper Exploration Project in the Vicinity of Küre-Taşköprü in Kastamonu (unpublished), Etibank.

Ünsal, A ve Dirim, M.S. (1990): Küre Civarındaki Bakır Zuhurlarında Yapılan Çalışmalar Hakkında Rapor, Etibank MAD Rap No.1445

Ünsal, A. (1991): Küre Bakırlı Pirit İşletmesi Sahalarında Yapılan Arama Çalışmaları ve Rezervlerine, ilişkin özet rapor

Yamagishi, H. (1987): Studies on the Neogene Subaqueous Lavas and Hyaloclastites in Southwest Hokkaido. Rep. Geol. Surv. Hokkaido, No.59, p.55-117

Geophysics: CSAMT Method

Cagniar, L. (1953) : Basic Theory of the Magnetotellurics Method of Geophysical Prospecting, Geophysics, 37, 605-635

Goldstein, M.A. and Strangway, D.W. (1975) : Audio Frequency Magnetotellurics with a Grounded Electric Dipole Source, Geophysics, 40, 669-683.

Kaufman, A.A., and Keller, G.V. (1981): The Magnetotelluric Sounding method, Elsevier, p.595.

Murakami, H., (1983): Basic Theory of Magnetotelluric Method, Butsuri-Tankou 36(6), 382-391

Ogawa, Y. (1988): Fortran Program Codes for Two-Dimensional Magnetotelluric Forward and Inverse Analyses, Open File Report Geol. Surv. Japan No.59

Ogawa, Y. and Takakura, S. (1990): CSAMT Measurements across the 1986 C Craters of Izu-Oshima Island, Japan J. Geomag. Geoelectr., 42, 211-224

Strangway, D.W., Swift, C.M. and Holmer, R.C. (1973): The Application of Audio Frequency Magnetotellurics (AMT) to Mineral Exploration, Geophysics, 38, 1159-1175

Sasaki, H., (1988): Interpretation of CSAMT Data including Source Effect. Butsuri-Tansa 41(1), 27-34

Uchida, T., Yokokawa, K., Nishikawa, N. and Hanaoka, N. (1989): Attempt of Tensor Audiofrequency Magnetotellurics, Butsuri-tansa, 42(1), 27-39

Yamashita, M. (1984): CSAMT Controlled Source Audio Magnetotellurics, PHOENIX Geophysics Limited.

Yamashita, M. and Hallof, P.G. (1985): FCSAMT case histories with a mult-channel CSAMT system and discussion of near-field data correction, The 55th SEG Annual Meeting, Washington, D.C.

Zonge Engineering & Research Organization, INC. (1982): Interpretation Guide for CSAMT data.

Geophysics: IP Method

Bertin, J. (1976): Experimental & Theoretical Aspect of IP. Vol.1. Presentation and Application of the IP Method Case Histories. Gebruder Borntraeger, Berlin 1976, 250pp

Dey, A. and Morison, H.F. (1973): Electromagnetic Coupling in Frequency and Time domain Induced Polarization Surveys over Multilayered Earth. Geophysics, 38, 380-405.

Hohmann, G.W. (1973): Electromagnetic Coupling between Grounded Wires at the Surface of a Two Layered Earth. Geophysics, 38, 854-863

Keller, G.V. and Frischknecht, F.C. (1966): Electrical Methods in Geophysical Prospecting. Pergamon Press, London, 517pp

Madden, T.R., & T. Cantwell (1967): Induced Polarization. A Review, Mining Geophysics, 2, 373-400, S.E.G. Tulsa, Okla.

Parasnis, D.S. (1972): Principles of Applied Geophysics. Chapman & Hall, London.

Parasnis, D.S. (1973): Mining Geophysics. Elsevier, Amsterdam, 395pp

Pelton, W.H., Ward, S.H., Hallof, P.G., Sill, W.R., and Nelson, P.H. (1978) : Mineral Discrimination and Removal of Inductive Coupling with Multi-frequency IP. Geophysics, 43, 598-609

Sato, M. and Mooney, H.M. (1960): The Electrochemical Mechanism of Sulphide Self-potentials. Geophysics 25 No.1, pp226-249.

Scintrex Limited (1992): IPR-12 Time Domain IP/Resistivity Receiver operator Manual.

Seigel, H.O. (1959): Mathematical Formulation and Type Curves for Induced Polarization. Geophysics 24 547-565.

Seigel, H.O. (1967): The Induced Polarization Method. In L.W. Morley (Editor), Mining and Groundwater Geophysics. Geol. Rep., No.26. Geol. Surv. Can. pp123-137.

REFERENCE OF DATA COMPILE

1. Regional Geology

- (1) Yilmaz, O. & Boztuğ, D. (1986): Kastamonu granitoid belt of northern Turkey First arc plutonism product related to the subduction of the paleo-Tethis, Geology, vol.14 p.179-183

- (2) Aydın, M. ve Diğerleri (1986): Ballıdağ-Çangaldağı (Kastamonu) arasındaki Bölgenin Jeolojisi, Türkiye Jeoloji Kurumu Bülteni, C.29, 1-16
- (3) Kılıç, M. ve Diğerleri (1977): Kastamonu-Küre Bakırlı Pirit Aramaları, Jeoloji Ön Raporu, MTA MEAD Rap No. 1940
- (4) Güner, M. (1980): Küre Civarının Masif Sülfid Yatakları ve Jeolojisi, Pontidler (Kuzey Türkiye), MTA Dergisi 93/94, Sa. 65-109
- (5) Eşen, K. (1989): Küre Bakırlı Pirit İşletmesi Müessesesi AR- 31961 numaralı sahada-Ersizlerdere ve İpsinler Köyü Civarında Yapılan Jeolojik Etüd Hakkında Rapor, Etibank MAD Rapor No. 1359
- (6) Yılmaz, O. (1980): Daday-Devrekani Masifi Kuzeydoğu Kesimi Litostratigrafi Birimleri ve Tektoniği Yerbilimleri Cilt 5-6 Sa. 101-135
- (7) Uzluç, O. (1969): Küre ilçesi Fırıncık (Köseli) Köyleri Civarında Yapılan Jeolojik Etüd Raporu, Etibank MAD Rapor No. 617
- (8) Kamitani, M. ve Çamaşircioğlu, A. (1976): Kastamonu-Küre'nin Batı Kesimlerindeki Cevherleşme ve Jeolojisi, MTA MEAD Rapor No. 1335
- (9) Özgüneyli, A. (1974): Karadeniz Bakır İşletmelerinin Kastamonu E32-dl Paftasına Ait Kepez Köyü Bakır Anomalisinin Detay Jeolojisi, MTA MEAD Rapor No. 209
- (10) Akkuş, T. ve Dirim, M.S. (1991): Kastamonu-Taşköprü-Musabozarmut Sahası Jeoloji ve Jeofizik Etüdüleri Raporu, Etibank MAD Rapor No. 1495
- (11) Ketin, I. (1962): 1/500,000 Ölçekli Jeolojik Harita ve İzahnamesi (Sinop), MTA Enst. Yayını.
- (12) Şengün ve Diğerleri. (1988): Daday, Kastamonu, İnebolu Yöresinin Jeolojisi, MTA Derleme No. 8994

2. Geochemical Prospecting

- (1) Köksoy, M. ve Turan, Y. (1973): Kastamonu-Küre Sahasının Genel Jeoşimik Etüdü, MTA Maden Etüd Dairesi Rapor No. 1400
- (2) Kırıkoğlu, M.S. (1987): Çangal Metaofiyolitinin Jeokimyasal Prospeksiyonu. İTÜ YBYK Uyg. Ar. Merkezi Araştırma Projesi, İTÜ Maden Fakültesi.
- (3) Konya, S. ve Diğerleri. (1988): Kastamonu-Taşköprü-Devrekani yöresi Jeokimya raporu, MTA Derleme No. 8341

3. Geophysical Prospecting

- (1) Haydaroğlu, M. (1964): Küre Self Potansiyel ve Elektromagnetik Etüdü, Etibank MAD Rapor No. 614

- (2) Haydaroglu, M. (1964): Kure Bakirli Pirit Isletmesi Kizilsu Sahasi Jeofizik Etud Raporu, Etibank MAD Rapor No. 613
- (3) Yavuz, E. ve Haydaroglu, M. (1966): Kure Yellicetepesi 1135 Rakim I.P. ve S.P. Etudu, Etibank MAD Rapor No. 610
- (4) Aksoy, A. (1969): Etibank Kure Bakirli Pirit Isletmesi Asikoy-Kizilsu-Karacakaya I.P. Etudu Hakkinda Rapor, Etibank MAD Rapor No. 596
- (5) Kaynak, U. (1969): Kure Bakirli Pirit Isletmesi Imtiyaz Sahalarinda Yapilan Jeofizik I.P. Tahkik Etudune Ait Rapor, Etibank MAD Rapor No. 600
- (6) Kalkan, A. (1973): Kure Rezistivite ve P.S. Etudleri Raporu, Etibank MAD Rapor No. 597
- (7) Nazikoğlu, Z. ve Diğlerleri (1974): Kure Arama Projesi Jeofizik Etudleri Raporu, Etibank MAD Rapor No. 603
- (8) Bolgün, M. ve Akkus, T. (1976): Kure Bakirli Pirit Muessesesi Asikoy-Bakibaba Sahalari Jeofizik Etud Raporu, Etibank MAD Rapor No. 605
- (9) Borağan, H. ve Diğlerleri (1978): 1977 Yılı Kure-Toykondü Mevkii Jeofizik Etud Raporu, Etibank MAD Rapor No. 608
- (10) Dur, İ. ve Aydın, M. (1979): 1978 Yılı Kure-Toykondü Mevkii Jeofizik Etud Raporu, Etibank MAD Rapor No. 1013
- (11) Akkus, T. ve Diğlerleri. (1981): Kure-Inebolu Yolu Üstü 1979-1980 Yılları Jeofizik Etud Raporu, Etibank MAD Rapor No. 481
- (12) Dur, İ. ve Diğlerleri. (1985): Kure Bakirli Pirit Isletmesi Muessesesi Jeofizik Etud Raporu, Etibank Maden Arama Dairesi Rapor No. 1079
- (13) Dur, İ. ve Diğlerleri. (1987): Kure Bakirli Pirit Isletmesi Muessesesi 1986 Yılı Jeofizik Etud Raporu, Etibank MAD Rapor No. 1180
- (14) Dur, İ. ve Diğlerleri. (1988): Kure Bakirli Pirit Isletmesi Muessesesi 1987 Yılı Jeofizik Etud Raporu, Etibank MAD Rapor No. 1275
- (15) Akkus, T. ve Diğlerleri. (1989): Kure Bakirli Pirit Isletmesi Muessesesi 1988 Yılı Jeofizik Etud Raporu, Etibank MAD Rapor No. 1351
- (16) Akkus, T. ve Dirim, M.S. (1991): Kastamonu-Tasköprü-Musabozarmut Sahasi Jeoloji ve Jeofizik Etudleri Raporu, Etibank MAD Rapor

4. Mining Geology

- (1) Kovenko, V. (1944): Kure'deki Eski Bakir Yatađi ile Yeni Keşfedilen Asikoy Yatađının ve Karadeniz orta ve Dođu Kesimleri Sahil Bölgesinin Metallojenisi, MTA, Enstitüsü, 2/32 Sa. 180-211

- (2) Pehlivanođlu, H. (1985): Kastamonu-Küre Piritli Bakır Yatakları (Bakibaba, Aşıköy) ve Çevresinin Jeoloji Raporu, Etibank MAD Rapor No. 1272
- (3) Teknomad(1986): Etibank-Küre Masif Sulfid Yatakları (Aşıköy-Toykondubakibaba) Jeoloji ve Rezerv, Kalite Raporu, Etibank MAD Rapor No. 1444
- (4) Teknomad(1987): Aşıköy-Bakibaba Masif Sulfid Yatakları, Cevherleşmenin Oluşum Model ve Arama Programı Raporu, Etibank MAD Rapor No.
- (5) Dağci, Z. ve Yıldız, T. (1990): Kastamonu-Küre-Bakibaba Maden Yatağı Rezerv Hesapları Raporu, Etibank MAD Rapor

5. Mining Evaluation

- (1) Çağatay, A. ve Diğerleri (1980): Küre Piritleri Bakır Yataklarının Kobalt-Altın Mineralleri ve Yatakların Bu Metaller Açısından Ekonomik Değeri, MTA Dergisi, 93/94 s. 110-117.

MTA: Maden Tetkik ve Arama Genel Müdürlüğü

MAD: Maden Arama Dairesi

MEAD: Maden Etüd ve Arama Dairesi